

REPORT DOCUMENTATION PAGE			Form Approved OMB NO. 0704-0188	
Public reporting burden for this collection of information is estimated to average 1 hour per response, including the time for reviewing instructions, searching existing data sources, gathering and maintaining the data needed, and completing and reviewing the collection of information. Send comment regarding this burden estimate or any other aspect of this collection of information, including suggestions for reducing this burden, to Washington Headquarters Services, Directorate for Information Operations and Reports, 1215 Jefferson Davis Highway, Suite 1204, Arlington, VA 22202-4302, and to the Office of Management and Budget, Paperwork Reduction Project (0704-0188), Washington, DC 20503.				
1. AGENCY USE ONLY (Leave blank)	2. REPORT DATE July 7, 2000	3. REPORT TYPE AND DATES COVERED Final Report 05/01/96 - 04/30/00		
4. TITLE AND SUBTITLE Molecular Mechanisms of Odor Recognition		5. FUNDING NUMBERS DAAH04-96-1-0096		
6. AUTHOR(S) Robert R. H. Anholt, Ph. D.				
7. PERFORMING ORGANIZATION NAMES(S) AND ADDRESS(ES) North Carolina State University Department of Zoology Raleigh, NC 27695		8. PERFORMING ORGANIZATION REPORT NUMBER		
9. SPONSORING / MONITORING AGENCY NAME(S) AND ADDRESS(ES) U.S. Army Research Office P.O. Box 12211 Research Triangle Park, NC 27709-2211		10. SPONSORING / MONITORING AGENCY REPORT NUMBER ARO 34815.7-LS		
11. SUPPLEMENTARY NOTES The views, opinions and/or findings contained in this report are those of the author(s) and should not be construed as an official Department of the Army position, policy or decision, unless so designated by other documentation.				
12a. DISTRIBUTION / AVAILABILITY STATEMENT Approved for public release; distribution unlimited.		12 b. DISTRIBUTION CODE		
13. ABSTRACT (Maximum 200 words) The principal thrust of our work focused on molecular mechanisms of chemoreception in the mammalian vomeronasal organ. We characterized the transduction pathway for the recognition of pheromones in the vomeronasal organ and also characterized subpopulations of olfactory neurons expressing different axonal G proteins in the main and accessory olfactory projections. These studies were extended with a characterization of genetically modified mice deficient in the α subunit of the G-protein, Go, which show profound anosmia. In addition to studies on the mammalian olfactory system, grant DAAH04-96-I-0096 enabled us to expand work on the genomic architecture of olfactory behavior in <i>Drosophila melanogaster</i> . This work led to the discovery of several new gene products that are essential for processing olfactory information, including a sodium channel, a novel dual specificity tyrosine phosphorylation regulated kinase (<i>Dyrk2</i>), a postsynaptic density protein (<i>Scribble</i>), an olfactory receptor, and an odorant binding protein, the latter two interacting with the repellent odorant, benzaldehyde. Finally, we continued work on olfactomedin. We showed that a family of olfactomedin-related proteins is encoded in the human genome with, thus far, at least five members. These olfactomedin-related proteins appear to be members of a diverse family of tissue-specific extracellular matrix components, one of which is associated with the pathogenesis of glaucoma. Our recent discovery of an olfactomedin homologue in <i>Drosophila melanogaster</i> will facilitate studies on the functions of olfactomedin-related proteins and their interactions.				
14. SUBJECT TERMS odorants, smell, chemical signals, olfactory behavior, molecular genetics, chemical detection, olfactomedin, signal transduction, pheromones, quantitative genetics		15. NUMBER OF PAGES 24 (+ appendix)		
		16. PRICE CODE		
17. SECURITY CLASSIFICATION OR REPORT UNCLASSIFIED	18. SECURITY CLASSIFICATION OF THIS PAGE UNCLASSIFIED	19. SECURITY CLASSIFICATION OF ABSTRACT UNCLASSIFIED	20. LIMITATION OF ABSTRACT UL	

TITLE

Molecular Mechanisms of Odor Recognition

TYPE OF REPORT (TECHNICAL, FINAL PROGRESS)

Final

AUTHOR(S)

Robert R. H. Anholt

DATE

June 30, 2000

U.S. ARMY RESEARCH OFFICE CONTRACT/GRANT NUMBER

DAAH04-96-I-0096

INSTITUTION

North Carolina State University

**APPROVED FOR PUBLIC RELEASE;
DISTRIBUTION UNLIMITED.**

THE VIEWS, OPINIONS, AND/OR FINDINGS CONTAINED IN THIS REPORT ARE
THOSE OF THE AUTHOR(S) AND SHOULD NOT BE CONSTRUED AS AN OFFICIAL
DEPARTMENT OF THE ARMY POSITION, POLICY, OR DECISION, UNLESS SO
DESIGNATED BY OTHER DOCUMENTATION.

1. Foreword

This final report describes results obtained with support from ARO grant DAAH04-96-I-0096 between 05/01/96 and 04/30/00. This grant has made considerable impact in that it has enabled us to expand and diversify our research program. The principal thrust of work supported by this grant focused on molecular mechanisms of chemoreception in the mammalian vomeronasal organ. We characterized the transduction pathway for the recognition of pheromones in the vomeronasal organ and also characterized subpopulations of olfactory neurons expressing different axonal G proteins in the main and accessory olfactory projections. These observations bear directly on the formation of chemotopic sensory maps in the brain. These studies were recently extended with a characterization of genetically modified mice deficient in the α subunit of the G-protein, Go, which show profound anosmia. These studies resulted in publications in *Endocrinology* and *Brain Research* and have also been reported in abstract form at several national and international meetings. This work was performed with the involvement of postdoctoral research associate, Dr. Kennedy S. Wekesa, currently an Assistant Professor at Alabama State University, Montgomery, AL. This work is currently being continued with support from the W. M. Keck Foundation.

In addition to studies on the mammalian olfactory system, grant DAAH04-96-I-0096 enabled us to expand work on the genomic architecture of olfactory behavior in *Drosophila melanogaster*, which is currently continued with support from a grant from the National Institute of General Medical Sciences. This work led to the discovery of several new gene products that are essential for processing olfactory information, including a sodium channel, a novel dual specificity tyrosine phosphorylation regulated kinase (*Dyrk2*), a postsynaptic density protein (*Scribble*), an olfactory receptor, and an odorant binding protein, the latter two interacting with the repellent odorant, benzaldehyde. These studies have been published in *Genetics* and documented in abstract form.

Finally, we were able to continue work on olfactomedin. Olfactomedin was originally identified as the major mucus component of the olfactory neuroepithelium. Subsequently, other investigators identified an olfactomedin homologue that is expressed as different splice variants throughout the rat brain. These proteins became especially important when an olfactomedin-related protein was discovered in the anterior segment of the eye and found to be closely associated with the pathogenesis of glaucoma (the trabecular meshwork inducible glucocorticoid response protein, TIGR). Our laboratory has shown that olfactomedin-related proteins occur ubiquitously from *C. elegans* to humans and that they have conserved C-terminal domains with characteristic sequence motifs. Moreover, we showed that a family of olfactomedin-related proteins is encoded in the human genome with, thus far, at least five members. These olfactomedin-related proteins appear to be members of a diverse family of tissue-specific extracellular matrix components. The link between TIGR and ocular hypertension and the expression of several of these proteins in mucus-lined tissues suggest that they play an important role in regulating physical properties of the extracellular environment. Our recent discovery of an olfactomedin homologue in *Drosophila melanogaster* will facilitate studies on the functions of olfactomedin-related proteins and their interactions. Work on olfactomedin was, in part, performed by postdoctoral research associate, Dr. Christa Karavanich, currently a faculty member at Richland College, Dallas, TX. This work has been published in *Molecular Biology and Evolution*, in *Genetical Research* and as several abstracts, and is currently supported by the Glaucoma Research Foundation.

2. Table of Contents

3.	List of Appendices, Illustrations and Tables	4
4.	Body of Report	5
A.	Statement of the Problems Studied	5
(i)	<i>Molecular and cellular mechanisms of chemoreception in the mammalian olfactory system</i>	5
(ii)	<i>Functional genomics of odor-guided behavior</i>	6
(iii)	<i>Characterization of olfactomedin-related proteins</i>	7
B.	Summary of the Most Important Results	8
(i)	<i>Molecular and cellular mechanisms of chemoreception in the mammalian olfactory system</i>	8
(ii)	<i>Functional genomics of odor-guided behavior</i>	9
	1. Behavioral assay	9
	2. Responding to chemosensory information: <i>Odor-guided behavior as a quantitative trait</i>	10
	3. Transposon tagging and the identification of <i>smell impaired genes</i>	11
	4. Epistasis among <i>smi</i> genes	12
	5. Understanding the genetic architecture of behavior: <i>Linking genetic variation to phenotype</i>	13
(iii)	<i>Characterization of olfactomedin-related proteins</i>	15
	1. Identification and characterization of a new family of <i>olfactomedin-related proteins in the human genome.</i>	15
	2. Expression of multiple olfactomedin-related proteins by <i>trabecular meshwork cells.</i>	16
	3. Identification of olfactomedin in <i>Drosophila melanogaster</i>	16
C.	List of All Publications and Technical Reports	17
D.	List of All Participating Scientific Personnel	18
5.	Report of Inventions	18
6.	Bibliography	19
7.	Appendices	25

3. List of Appendices, Illustrations and Tables

Selected reprints:

Wekesa, K. S. and Anholt, R. R. H. (1997) Pheromone-regulated production of inositol-(1,4,5)-trisphosphate in the mammalian vomeronasal organ. Endocrinology **138**: 3497-3504.

Fedorowicz, G. M., Fry, J. D., Anholt, R. R. H. and Mackay, T. F. C. (1998) Epistatic interactions between *smell-impaired* loci in *Drosophila melanogaster*. Genetics **148**: 1885-1891.

Karavanich, C. A. and Anholt, R. R. H. (1998) Molecular evolution of olfactomedin. Mol. Biol. Evol. **15**: 718-726.

Wekesa, K. S. and Anholt, R. R. H. (1999) Differential expression of G proteins in the mouse olfactory system. Brain Research **837**: 117-126.

Figures:

Figure 1: Diagrammatic representation of the “dipstick” assay for measurements of olfactory avoidance responses.

Figure 2: Variation for avoidance response to benzaldehyde among isogenic chromosome 1 and chromosome 3 substitution lines of *Drosophila melanogaster*.

Figure 3: Interaction diagram of *smi* loci.

Figure 4: Unrooted neighbor-joining trees of 18 olfactomedin-related proteins and their olfactomedin homology domains.

Figure 5: Tissue-specific expression of olfactomedin-related gene products.

Tables:

Table 1: Transposon insertion sites and candidate *smi* genes

4. Body of Report

A. Statement of the Problems Studied

(i) *Molecular and cellular mechanisms of chemoreception in the mammalian olfactory system*

Odor recognition is essential for the survival and procreation of most animals. Chemical information transferred via olfactory neurons to the olfactory bulb is transformed into a chemotopic map (Joerges *et al.*, 1997; Friedrich and Korsching, 1997 and 1998; Bozza and Kauer, 1998; Rubin and Katz, 1999). This map is represented by modular neural arrays, glomeruli, which in the mouse number approximately 1,800 (Pomeroy *et al.*, 1990) and each of which represents the convergent projection of neurons of similar chemosensory specificity (reviewed by Hildebrand and Shepherd, 1997).

The olfactory system contains two interacting components: the main olfactory system is dedicated to general odorant discrimination, whereas the accessory olfactory system primarily processes chemical cues that guide social behaviors (reviewed by Meredith, 1998). In the main olfactory system odor recognition is mediated by receptors, which belong to the superfamily of G-protein coupled receptors and are encoded by as many as 1,000 different genes (Buck and Axel, 1991; Levy *et al.*, 1991; Strotmann *et al.*, 1994; Axel, 1995; Buck, 1996; Sullivan *et al.*, 1995 and 1996). Two distinct families of G protein coupled receptors have also been identified as putative pheromone receptors in chemosensory neurons of the vomeronasal organ (VNO), the chemosensory organ of the accessory olfactory system (Dulac and Axel, 1995; Matsunami and Buck, 1997; Herrada and Dulac, 1997; Ryba and Tirindelli, 1997).

In the main olfactory system each olfactory neuron expresses a single odorant receptor from the large repertoire of receptors encoded in the genome (Chess *et al.*, 1994). Thus, binding of an odorant to its receptor translates directly into a distinct pattern of neural activity that encodes its structure. Receptor activation results in stimulation of adenylate cyclase (Pace *et al.*, 1985; Sklar *et al.*, 1986; reviewed by Anholt, 1993), followed by the opening of cyclic nucleotide-gated channels that carry the generator current (Nakamura and Gold, 1987; Firestein *et al.*, 1991). Calcium, entering through these channels (Frings *et al.*, 1995), amplifies the response by opening calcium-gated chloride channels (Kleene and Gesteland, 1991; Kurahashi and Yau, 1993; Reuter *et al.*, 1998) and, after binding to calmodulin, limits the response by lowering the affinity of the cyclic nucleotide-activated channel for cyclic AMP (Chen and Yau, 1994; Kurahashi and Menini, 1997). Although inositol-1,4,5,-triphosphate also has been implicated as second messenger in olfaction (Boekhoff *et al.*, 1990; Ronnett *et al.*, 1993), knock-out mice deficient in the α subunit of the cyclic nucleotide-gated channel were found to be generally anosmic (Brunet *et al.*, 1996) as were mice deficient in G_{olf} (Belluscio *et al.*, 1998), the G protein that links odorant receptor activation to stimulation of adenylate cyclase (Jones and Reed, 1989).

Whereas cyclic AMP appears to be the primary second messenger in olfactory transduction, inositol-1,4,5,-triphosphate has been implicated in signal transduction in the VNO (Jiang *et al.*, 1990; Luo *et al.*, 1994; Taniguchi *et al.*, 1995; Wekesa and Anholt, 1997), although a role for cyclic AMP has also been suggested in this system (Jiang *et al.*, 1990; Luo *et al.*, 1994; Okamoto *et al.*, 1996).

Our laboratory played a major role in elucidating the second messenger pathway that operates in the VNO by obtaining direct measurements of second messengers in membrane preparations from porcine VNO and demonstrating dose-dependent, tissue-specific and sex-dependent generation of inositol-1,4,5,-triphosphate in VNO membranes from prepubertal female pigs in response to seminal fluid and boar urine (Wekesa and Anholt, 1997). This generation of inositol-1,4,5,-triphosphate is GTP-dependent and is thought to be mediated, at least in part, through a $G_{q/11}$ -related G-protein (Wekesa and Anholt, 1997).

The dendritic and axonal compartments of olfactory neurons fulfill distinct functions for the acquisition of chemosensory information. Whereas dendritic specializations mediate odorant recognition and chemosensory transduction, the axonal compartment regulates signal propagation, axon sorting and target innervation. The roles of G proteins in chemosensory transduction at the dendritic compartments of chemosensory neurons have been studied extensively, but the functions of axonal G proteins have not been investigated in detail.

An important role for axonal G proteins in mammalian chemoreception is implicated by the differential distribution of G_{i2} and G_o in the accessory olfactory system. The apical layer of the VNO expresses a distinct family of putative pheromone receptors (VN1 receptors; Dulac and Axel, 1995), whereas VNO neurons in the basal layer express a different family of receptors (VN2 receptors) that resemble metabotropic glutamate receptors (Matsunami and Buck, 1997; Herrada and Dulac, 1997; Ryba and Tirindelli, 1997). *In situ* hybridization studies in the murine VNO (Berghard and Buck, 1996) and immunohistochemical studies in opossum (Halpern *et al.*, 1995) showed that neurons in the apical layer of the VNO express G_{i2} and project to the rostral region of the accessory olfactory bulb (AOB), whereas neurons in the basal layer express G_o and project to the caudal region of the AOB. Our laboratory has demonstrated that differential expression patterns of G_{i2} and G_o are not unique to the AOB, but also occur in the main olfactory bulb (MOB; Wekesa and Anholt, 1999).

(ii) *Functional genomics of odor-guided behavior*

Behavior supports the stage on which the interplay between the environment and the genome guides evolution. Behavioral adaptations to environmental cues determine survival and reproductive success. Among those environmental cues none are more important than chemical signals. Indeed, odor-guided behavior is absolutely essential for most organisms for food localization, avoidance of environmental toxins or predators, oviposition site selection, kin recognition, species recognition and mate selection, and reproduction. The importance of molecular recognition of environmental chemicals is underscored by the discovery that an unusually large percentage of the genome is dedicated to olfaction: in the mammalian genome, odor-recognition alone is mediated by a multigene family of about 1,000 odorant receptors (Buck and Axel, 1991), that has undergone rapid evolution through gene duplication and diversification (Hughes and Hughes, 1993; Ben-Arie *et al.*, 1993; Issel-Tarver and Rine, 1997; Rouquier *et al.*, 1998). Initial chemosensory recognition events, however, are only the first step in a series of complex processes, that involves processing of chemosensory information in the central nervous system, evaluating the nature of the chemosensory perception, and initiating and executing an appropriate behavioral response. It is intuitively evident that this process involves a vast ensemble of genes and that variation in the expression of any of these genes can

generate individual variation in olfactory responsiveness within a natural population. Thus, odor-guided behavior is a quantitative trait and understanding its complex genetic architecture requires quantitative genetic, statistical, and genomic analyses.

We have chosen olfactory avoidance behavior of *Drosophila melanogaster* as a model system for studies on the genetic architecture of odor-guided behavior. *D. melanogaster* is a genetic model system *par excellence*, because its generation time is short, there is no recombination in males, and the availability of balancer chromosomes allows mutations to be stably propagated and enables the manipulation of entire chromosomes to construct “designer genotypes”. Furthermore, highly inbred lines can be readily generated, which eliminates genetic variance and greatly facilitates the analysis of complex traits. In addition, extensive resources are available for genomic studies on *Drosophila*, including deficiency lines and lines that carry transposable element insertions at different defined locations in the genome; these resources are available through large national stock centers. Sequencing of the entire genome has recently been completed (Adams *et al.*, 2000) and a large genomic data base is available (<http://flybase.bio.indiana.edu/>).

There are additional reasons that make *Drosophila* eminently suited for studies on olfactory behavior, as described in more detail below. The functional organization of its olfactory system is similar to that of the vertebrate olfactory system, suggesting similar principles of odor coding, but it is more tractable since it contains about 10,000-100,000 times fewer neurons and 30 times fewer glomeruli (Laissue *et al.*, 1999). Furthermore, *D. melanogaster* is the only insect species to date in which odorant receptors have been identified (Clyne *et al.*, 1999a; Vosshall *et al.*, 1999). Finally - and most importantly - the onset of avoidance responses to repellent odorants can be precisely controlled and a reproducible statistical behavioral assay has been devised to accurately measure small olfactory impairments quantitatively (Anholt *et al.*, 1996).

(iii) Characterization of olfactomedin-related proteins

Olfactomedin was originally identified as the major mucus component of the olfactory neuroepithelium (Snyder *et al.*, 1991; Yokoe and Anholt, 1993). Subsequently, other investigators identified an olfactomedin homologue that is expressed as different splice variants throughout the rat brain (Danielson *et al.*, 1994). These proteins became especially important when an olfactomedin-related protein was discovered in the anterior segment of the eye and found to be closely associated with the pathogenesis of glaucoma (the trabecular meshwork inducible glucocorticoid response protein, TIGR; Stone *et al.*, 1997; Polanski *et al.*, 1997; Kubota *et al.*, 1997). We characterized the family of olfactomedin-related proteins both in the human genome and in *Drosophila* to set the stage for studies aimed at determining their functions. These studies involved a collaboration with Dr. William Atchley from the Department of Genetics and with Dr. Teresa Borrás from the Department of Ophthalmology at Duke University Medical Center.

B. Summary of the Most Important Results

(i) *Molecular and cellular mechanisms of chemoreception in the mammalian olfactory system*

After many years of previous research on signal transduction in the main olfactory system, we turned our attention to pheromonal signal transduction in the vomeronasal organ (VNO), a chemosensory organ specialized for the perception of social chemical signals. We identified the pig as a good model system for biochemical studies because of the large size of its VNOs. We developed a membrane preparation enriched in microvillar membranes from chemosensory vomeronasal neurons. These preparations allowed us to measure for the first time *directly* pheromone-regulated increases in the second messenger, inositol trisphosphate, in the mammalian VNO. We demonstrated in membranes from prepubertal female animals sex-specific, dose-dependent and G-protein mediated increases in inositol trisphosphate in response to boar urine and seminal fluid. Furthermore, our studies implicated $G_{q/11}$ as one of the G-proteins likely to link pheromone receptor activation to stimulation of phospholipase C. These experiments provided for the first time a biochemical assay for the activity of mammalian pheromones and consolidated through direct measurements the notion that the main and accessory olfactory systems use different signal transduction mechanisms to evoke neural activation (Wekesa and Anholt, 1997). Thus, in contrast to the main olfactory system where cyclic AMP is the principal neurotransmitter, inositol trisphosphate is the major neurotransmitter in the VNO, where it most likely mediates influx of calcium via the opening of a recently identified VNO-specific TRP2 ion channel.

Whereas odorant recognition and chemosensory transduction occur at the dendrites of olfactory neurons, signal propagation, axon sorting and target innervation are functions of their axons. Previous studies by other investigators had shown that in the accessory olfactory system vomeronasal neurons, whose cell bodies are located in the superficial layers of the vomeronasal organ, send their axons to the anterior region of the accessory olfactory bulb and express G_{12} , whereas neurons in the basal layer of the vomeronasal neuroepithelium send their axons to the posterior accessory olfactory bulb and express G_o (Halpern *et al.*, 1995; Berghard and Buck, 1996). We showed that differential expression of these G proteins is not unique to the accessory olfactory system, but also occurs in the main olfactory projection. Whereas in the main olfactory projection all neurons express G_o , a subpopulation expresses G_{12} . We showed that the projection of G_{12} -expressing neurons originates from the dorsomedial region of the nasal cavity and fans out across the medial aspect of the main olfactory bulb, sparing the penetration corridor of the vomeronasal nerve and extending sparsely to scattered glomeruli in the lateral olfactory bulb. These results are important in that olfactory neurons expressing the same odorant receptor have been shown to converge on two glomeruli (spherical synaptic neural output modules) in the olfactory bulb, one medial and one lateral. Thus, the olfactory projection forms two chemotopic representations in each olfactory bulb, one lateral map and one medial map. Our results suggest that G_{12} may play a role in signal processing or axonal targeting to the medial chemotopic map. In collaboration with Dr. John Vandenbergh, we are using homologous recombinant mice that lack the α subunit of G_o (Valenzuela *et al.*, 1997) to further explore the functions of these axonal G-proteins in the olfactory projection. The original knock-out mice were generously provided by Dr. Eva Neer from Harvard University.

as C57Bl/129 chimeras. We found that intercrossing heterozygotes of these mice generated few homozygous $G_o^{-/-}$ offspring, presumably due to inbreeding depression. Therefore, we backcrossed these mice into the CD-1 outbred genetic background. This increased the number of homozygous knock-out offspring and their viability. Homozygous knock-outs are slightly smaller in body weight compared to heterozygous littermates at birth, but appear otherwise normal, as reported by Neer and colleagues (Valenzuela *et al.*, 1997). Whereas virtually all of the heterozygotes and wild-type progeny were able to locate a buried food pellet after an overnight starvation period, the $G_o^{-/-}$ mice were less successful in localizing the pellet within the 4 min assay period. Olfactory ability of the $G_o^{-/-}$ mice was further assessed by an olfactory habituation-dishabituation test. When control heterozygous mice are presented with an unfamiliar odor on a cotton wool swab protruding from the cage lid, they rear up to investigate the odor. The number of rearings and total rearing time abates as they habituate to the odor, but can be elicited *de novo* by introducing a different odor. The number of rearings in response to sequential odor exposures was markedly lower or virtually absent in $G_o^{-/-}$ mice, although their mobility was not impaired. Preliminary studies further indicate that absence of G_o may be accompanied by overexpression of G_{i2} . Although upon superficial examination olfactory bulbs in the knock-out animals appear intact, closer examination indicates that the packing and shape of glomeruli in these animals may be altered. Dr. Peter Mombaerts from Rockefeller University has agreed to provide us with his P2-IRES-tau-lacZ knock-in mice, in which the convergent projection of olfactory neurons expressing the P2 odorant receptor can be readily visualized by staining for β -galactosidase (Mombaerts *et al.*, 1996). Introducing the P2-IRES-tau-lacZ knock-in construct into our $G_o^{-/-}$ mice will enable us to assess directly whether the pattern of olfactory projections in these mice has been altered. In the future we will continue to investigate the impact of deletion of G_o on the formation of chemotopic projections and/or compensatory expression of other G-proteins.

(ii) *Functional genomics of odor-guided behavior*

1. *Behavioral assay*

Despite considerable advances in our understanding of the functional organization of the olfactory system of *Drosophila*, the link between odor perception at the molecular and cellular level and odor-guided behavior at the level of the organism remains to be explored. When exposed to a strong repellent odorant, flies will immediately migrate away from the odor source. This ability to avoid odor sources associated with toxic compounds in the environment obviously has important survival value. To investigate the genetic basis for variation in odor-guided behavior, we made use of this natural avoidance response and developed a behavioral paradigm that is rapid, simple and readily quantifiable (Anholt *et al.*, 1996). Moreover, the use of isogenic strains of flies eliminates within-strain genetic variance. All observed variation in measurements between individuals of the same strain is attributable to environmental variation. Controlling the background genotype precisely increases the statistical power to detect differences in behavior between different genotypes.

We have used benzaldehyde, a standard repellent odorant, to measure olfactory responses in flies. We have also used structurally unrelated odorants, such as 2-isobutylthiazole and 2-*n*-propylpyrazine, to test whether olfactory defects of lines with aberrant olfactory behavior are specific to benzaldehyde. Prior to measuring behavioral responses to odorants, single sex groups of five

individuals are placed in test vials without food for 2 hours. The test vials are divided into two compartments by placing a mark on the wall 3 cm from the bottom of the vial. The animals are then exposed to an aqueous solution containing the desired concentration of benzaldehyde. The odorant is introduced into the vial on a cotton swab and the number of flies migrating to a compartment remote from the odor source is measured at 5 second intervals, from 15 seconds to 60 seconds after introduction of the odor source (Fig. 1). Distilled water is used as a control. The "avoidance score" of the replicate is the average of these 10 counts, giving a possible range of avoidance scores between 0 (maximal attraction to the odor source) and 5 (all flies are in the compartment away from the odor source for the entire assay period, i.e. a maximal repellent response). Many replicate assays are done for each line, each consisting of 5 males and 5 females. The elimination of genetic variance through the use of an isogenic genetic background together with our ability to rapidly accumulate large data sets for each line through repeated measurements provides us with the statistical power to reproducibly resolve not only large phenotypic effects, but also small smell impairments (Anholt *et al.*, 1996).

2. Responding to chemosensory information: Odor-guided behavior as a quantitative trait

Can variation in odor-guided behavior in a natural population be resolved and quantified? If so, how much of this variation is due to genetic variance and how much is accounted for by environmental variance? How is genetic variation for olfactory behavior maintained? What is the relationship between variation in odor-guided behavior and variation in fitness? To address these questions, chromosomes were extracted from a natural population and substituted into a common inbred genetic background. The avoidance responses to benzaldehyde were quantified for 43 *X* chromosome substitution lines and 35 third chromosome substitution lines (Mackay *et al.*, 1996). There was significant genetic variation in avoidance scores in this sample of chromosomes. Estimates of quantitative genetic parameters showed that heritabilities of olfactory avoidance behavior were low (averaged for both sexes $h^2 = 0.084$ for the *X* chromosome and $h^2 = 0.134$ for the third chromosome), whereas coefficients of genetic (CV_G) and environmental variance (CV_E) were large, as is characteristic for fitness traits.

Competitive fitness estimates were made for the Chromosome 3 substitution lines, estimating viability and fertility, against a competitor strain using the balancer equilibrium technique described by Sved (1975). There was significant variation in fitness among these lines. However, no significant correlations were observed between odor-guided behavior and fitness estimates. This suggests that the number of loci causing variation in olfactory avoidance behavior may be small relative to the number of loci affecting variation in fitness. Alternatively, the controlled laboratory environment, which does not require flies to make food selection or oviposition site choices or to avoid environmental toxins, may not be suitable for evaluating the relationship between variation in responsiveness to repellent odorants and fitness.

Intriguingly, the genetic correlations between the sexes for olfactory avoidance behavior were extremely low (Fig. 2), suggesting that different genes contribute to variation in avoidance scores in males and females (Mackay *et al.*, 1996). This is intuitively easy to understand, since odor-guided behavior subserves different functions in males and females, e.g. females only must select or reject oviposition sites. The lack of genetic correlation of avoidance scores between the sexes has,

however, profound evolutionary implications. Because the genetic architecture for odor-guided behavior appears sexually dimorphic, it is clear that the olfactory subgenome in males and females may evolve along different evolutionary trajectories, resulting in sexual dimorphism for olfactory behavior. However, the low genetic correlation between the sexes (the sex environment x genotype interaction) may facilitate the maintenance of genetic variation for olfactory behavior. Maintaining variation in the trait ensures survival of at least some members of the species under diverse environmental conditions encountered over evolutionary time. At the same time selection pressure is maintained at each generation, since no single genotype can satisfy optimal fitness requirements for both sexes.

3. Transposon tagging and the identification of smell impaired genes

Early studies on olfaction in *D. melanogaster* led to the identification of several mutants, primarily located on the X-chromosome (Rodrigues and Siddiqi, 1978; Aceves-Piña and Quinn, 1979; Lilly and Carlson, 1989; Helfand and Carlson, 1989; McKenna *et al.*, 1989; Ayer and Carlson, 1992; Woodard *et al.*, 1992; Lilly *et al.*, 1994). These genes were discovered using either larval assays, in which mutant larvae were identified based on their inability to locate an attractant odor source (Aceves-Piña and Quinn, 1979; Rodrigues, 1980; Monte *et al.*, 1989), or using an olfactory jump assay, in which flies of the Canton-S strain failed to jump in response to benzaldehyde (Helfand and Carlson, 1989; McKenna *et al.*, 1989). One of these *acj* (*abnormal chemosensory jump*) mutations, *acj6*, encodes a POU-domain transcription factor, which controls the expression of a subpopulation of putative odorant receptors (Clyne *et al.*, 1999b). The identification of *acj6* (Clyne *et al.*, 1999b), several genes encoding transduction proteins involved in chemosensory transduction (Woodard *et al.*, 1992; Riesgo-Escovar *et al.*, 1995; Talluri *et al.*, 1995; Störtkuhl *et al.*, 1999), genes encoding odorant binding proteins (Pikielny *et al.*, 1994; McKenna *et al.*, 1994; Kim *et al.*, 1998), the *smellblind* (*sbl*) locus, an allele of *paralytic* (*para*) that encodes a voltage gated sodium channel (Lilly and Carlson, 1989; Lilly *et al.*, 1994), an array of genes that mediate olfactory learning (reviewed by DeZazzo and Tully, 1995), and, finally, members of at least one family of putative odorant receptors (Clyne *et al.*, 1999a; Vosshall *et al.*, 1999), all revealed important components that participate in chemosensory pathways in *D. melanogaster*.

A comprehensive understanding of the genetic architecture of odor-guided behavior will, ultimately, require the identification of all the genes that contribute to this trait and characterization of their interactions. One strategy that can, in principle, accomplish this daunting task is the use of *P*-element insertional mutagenesis, which enables phenotypic effects to be linked directly to gene expression (Cooley *et al.*, 1988; Bellen *et al.*, 1989). Introduction of a transposon in the genome of *D. melanogaster* can result in gene disruption at or near the site of insertion of the transposable element. Introduction of a reporter gene in genetically engineered transposable element constructs (e.g. *P*[*lArB*]), which can be driven by promoter/enhancer elements near the insertion site can reveal expression patterns of the affected gene (enhancer trap). Furthermore, the use of a cloning vector, such as pBluescript, in the construct can facilitate cloning of flanking sequences adjacent to the site of *P*-element insertion. An enhancer trap study that surveyed 6,400 lines containing different *P*-element insertion sites showed that about 45% of these lines displayed expression of the *lacZ* reporter gene in the third antennal segment or maxillary palps, and several of these lines showed

specific, non-uniform staining patterns (Riesgo-Escovar *et al.*, 1992). This study, however, did not report whether any of the *P*-element insertions affected odor-guided behavior.

To address this question, we introduced the *P*[*lArB*] construct at random locations into the autosomal genome of a highly inbred line (Anholt *et al.*, 1996). The co-isogenic background of the resulting *P*[*lArB*] insertion lines together with the statistical behavioral assay, described above, provided sufficient resolution to identify not only mutations of large effect, but also smell impairments of smaller effect that might have been missed with conventional mutant screens. We discovered 14 novel olfactory genes by screening a relatively small number (379) of *P*-element insert lines (Anholt *et al.*, 1996). The frequency with which *smell impaired* (*smi*) genes were discovered was about 4%, suggesting that at least 4% of the genome is essential in mediating the simple avoidance response to benzaldehyde. *P*-element insertion sites can be readily determined through *in situ* hybridization to larval salivary gland chromosomes or by cloning of flanking sequences and comparing these sequences to the genomic data base. Candidate genes can then be identified for each of the *P*-element insertion sites (Table 1). Conclusive evidence that a candidate *smi* gene is indeed the locus affected by the transposon and that reduction in the expression of its gene product is causal to observed aberrations in the olfactory avoidance response requires extensive further experimentation. First, the *P*-element can be mobilized and phenotypic revertants generated to demonstrate that the *P*[*lArB*] insertion, rather than an unrelated mutation, is responsible for the *smell-impaired* phenotype. Second, olfactory behavior in flies carrying different alleles in the same candidate gene must be evaluated and complementation tests between the original *P*[*lArB*] insertion line and flies that contain deficiencies or other *P*-element insertions in the region of interest must be performed to provide further genetic evidence that the transposon-tagged candidate gene is associated with the impaired phenotype. Third, the expression of the encoded gene product must be quantified, either by Northern blots, quantitative PCR, or Western blots (if antibodies are available) to show that the *smi* gene message or SMI protein is reduced in mutant flies as compared to wild-type or phenotypic revertants. Fourth, *in situ* hybridization can be used to show that expression patterns in wild-type flies resemble reporter gene expression patterns in the *smi* mutant. Finally, introduction of the wild-type gene into the mutant background is expected to rescue the mutant phenotype if the candidate gene indeed is responsible for the observed deficiency in odor-guided behavior.

4. Epistasis among *smi* genes

The availability of smell impaired lines in a co-isogenic genetic background provides a unique opportunity to investigate epistasis among loci that all affect the same phenotype. Small epistatic effects would not be resolvable in the presence of large genetic variance in diverse genetic backgrounds where such effects would be confounded by segregation of unknown modifiers of the phenotype. However, the absence of genetic variation in our inbred *P*-element host strain and the sensitivity of our behavioral assay provided enough statistical power to identify enhancer and suppressor effects among *smi* loci. Double heterozygous hybrids were constructed among 12 independent *smi* mutations in a classic diallel cross design (Griffing, 1956) and avoidance responses were scored for these transheterozygotes (Fedorowicz *et al.*, 1998). Heterozygous effects and epistasis could be separated by determining the General Combining Ability (GCA) and Specific

Combining Ability (SCA) for each *smi* mutant. The GCA is defined as the average avoidance score of a *smi* mutant as a transheterozygote in combination with all other *smi* mutations. The SCA is defined for each transheterozygous genotype as the difference between the observed avoidance score of each specific genotype from that expected from the sum of the GCAs of each *smi* parent. Statistical analyses of the data revealed significant epistatic interactions for nine transheterozygous genotypes involving 10 of the 12 *smi* loci. An ensemble of eight of these loci could be represented as an epistatic interaction diagram (Fig. 3; Fedorowicz *et al.*, 1998).

The detection of epistasis in this unique set of *smi* mutants which share a common genetic background vividly illustrates the power of quantitative genetic analyses to detect subtle phenotypic effects. These observations also point to an extensive network of epistatic interactions among genes in the olfactory subgenome, of which the set of genes analyzed by Fedorowicz *et al.* (1998) represents only a small fraction. Since the genes that constitute the interaction diagram shown in Fig. 3 are all tagged with the *P[lArB]* transposon they can be characterized at the molecular level, and epistasis at the level of phenotype can then be evaluated within the context of the functions of their gene products.

5. Understanding the genetic architecture of behavior: Linking genetic variation to phenotype

One of the best understood complex traits in terms of its underlying genetic architecture is mechanosensory bristle number in *Drosophila* (reviewed by Mackay, 1996). Although a vast number of genes are involved in determining the number of sternopleural or abdominal bristles, a smaller number accounts for most of the variation in bristle number (Mackay, 1996). These genes include many neurogenic genes, such as *Delta*, *daughterless*, *extramacrochaetae*, *Hairless*, *Enhancer-of-split*, *hairy*, *scabrous* and the *achaete-scute* complex. Variation in bristle number could be correlated with polymorphisms in *Delta* (Long *et al.*, 1998; Lyman and Mackay, 1998), *scabrous* (Lai *et al.*, 1994; Lyman *et al.*, 1999) and *achaete-scute* (Mackay and Langley, 1990; Long *et al.*, 2000) and the extent to which alleles of each of these loci contribute to variation in bristle number in natural populations could be estimated.

Similar to studies on the contributions of bristle genes to variation in bristle number, the extent to which variation in *smi* loci contributes to naturally occurring variation in olfactory behavior can be assessed by linkage disequilibrium mapping (Lander and Schork, 1994; Neimann-Sorensen and Robertson, 1961; Risch and Merikangas, 1996). Linkage disequilibrium between polymorphic loci is expected to diminish over time as recombination occurs between them. Over a long period of time, only very closely linked polymorphisms will remain in linkage disequilibrium. Therefore, if a polymorphic site at a *smi* gene is associated with differences in odor-guided behavior, that site is, or is closely linked to, the causal site. The use of linkage disequilibrium mapping requires (1) identification of a candidate *smi* gene that is associated with naturally occurring variation in odor-guided behavior; (2) identification of molecular polymorphisms in that *smi* gene that are segregating in a natural population (either insertion/deletion or single nucleotide polymorphisms); and, (3) assessment whether alternative molecular variants are associated with variation in odor-guided behavior.

The genetic architecture of behavior is likely to increase in complexity when compared to that of morphological traits. Thus, the number of genes that contribute prominently to variation in

olfactory avoidance behavior is likely to be far greater than the ensemble that contributes to variation in bristle number.

The first layer of complexity is at the developmental level and may involve several of the same proneural and neurogenic genes that regulate bristle number. For example, *lozenge (lz)* mutants fail to generate basiconic sensilla (Stocker and Gendre, 1988). Variation in the number of chemosensory sensilla among individuals in natural populations has not been investigated and could contribute to variation in olfactory discrimination and responsiveness to odorants.

The next level of complexity is the perception of odorants, and involves odorant binding proteins (Pikielny *et al.*, 1994; McKenna *et al.*, 1994; Kim *et al.*, 1998) and odorant receptors (Clyne *et al.*, 1999a; Vosshall *et al.*, 1999). Mutations in the LUSH odorant binding protein resulted in a specific olfactory impairment, responsiveness to ethanol, propanol and butanol (Kim *et al.*, 1998). Deficits in odorant receptors are likely to be odorant-specific and the magnitude of smell impairment will depend on the redundancy of recognition of the odorant by other receptors. The diversity and relatively small size of the *Drosophila* odorant receptor family suggests that this system has less redundancy in odorant recognition than its mammalian counterpart. Nonetheless, variations in the expression of single odorant receptors may contribute less phenotypic variation in natural populations than polymorphisms in genes that encode proteins common to the perception of all odorants. The best documented example of a specific olfactory deficit due to absence of an odorant receptor has been described for *Caenorhabditis elegans*, where a null mutation in the *odr-10* gene, which encodes an odorant receptor for diacetyl, results in impaired chemotaxis of mutant nematodes to diacetyl (Sengupta *et al.*, 1996). To what extent variation in the expression of the odorant receptor repertoire contributes to variation in olfactory behavior in natural populations, however, remains to be investigated.

Genes encoding odorant binding proteins and odorant receptors confer specificity to the behavior. To perform the behavior, however, several additional processes must occur: signal transduction, transfer of the signal from the periphery to the central nervous system, signal integration and the generation of a behavioral response. These processes are mediated via gene products that are not unique to olfaction and phenotypes resulting from defects in these genes are likely to be pleiotropic. For example, mutations in the *retinal degeneration B (rdgB)* gene, which encodes a phosphatidyl inositol transfer protein, and in the *norpA* gene, which encodes a phospholipase C, result in both visual and olfactory impairments (Smith *et al.*, 1991; Vihtelic *et al.*, 1993; Woodard *et al.*, 1992; Riesgo-Escovar *et al.*, 1994 and 1995).

P-element insertional mutagenesis can, in principle, identify genes from all these categories. Candidate genes for previously identified *smi* lines are listed in Table 1. Preliminary characterization of several of these transposon tagged genes implicate genes that mediate signal propagation, including a voltage-gated sodium channel (Kulkarni, Mackay and Anholt, unpublished observations) and a protein containing multiple leucine rich repeats and PDZ domains likely to be involved in postsynaptic organization in the olfactory pathway (I. Ganguly, personal communication). Several novel genes of unknown function have also been implicated, including a novel tyrosine regulated protein kinase (G. Fedorowicz, personal communication). Of greatest interest is our recent realization that the *smi21F* insertion tags a gene encoding a novel putative pheromone binding protein. Previous reporter gene expression showed differential expression in the proximal dorsal region of the antenna as well as specificity in smell impairment to some, but not all odors (Anholt

et al., 1996). In addition, the *smi45E* insertion appears to disrupt the function of a nearby gene encoding an olfactory receptor. Specificity of the smell impairment suggests that this receptor has affinity for benzaldehyde. The characterization of these candidate genes is in progress and will be completed in the near future. The discovery and characterization of novel gene products that have major, hitherto unappreciated effects on olfactory behavior will provide new insights in the generation and regulation of odor-guided behavior. A complete understanding of the genetic architecture of odor-guided behavior, ultimately, requires identification of all the genes involved, characterization of their interactions in shaping the phenotype at the genetic level, and identification of polymorphisms that generate phenotypic variation at the population level. Although this seems a monumental enterprise, ongoing improvements in genomic technologies are bringing the realization of this goal within reach.

(iii) *Characterization of olfactomedin-related proteins*

Studies on the molecular evolution of olfactomedin-related proteins showed that olfactomedin homology domains are highly conserved across species (Karavanich and Anholt, 1998). Olfactomedin homologues were found in many tissues, including the brain (Danielson *et al.*, 1994), and in species ranging from *Caenorhabditis elegans* to *Homo sapiens* (Karavanich and Anholt, 1998). These observations led to the hypothesis that olfactomedin homology domains may mediate homophilic protein-protein interactions. We sought to provide evidence for this hypothesis in the eye, where the glaucoma-associated TIGR/myocilin protein, an olfactomedin-related protein, may interact with other olfactomedin-related proteins. Elucidating such interactions would also contribute to enhancing our understanding of the pathogenesis of glaucoma.

1. Identification and characterization of a new family of olfactomedin-related proteins in the human genome.

The prevalence of olfactomedin-related proteins among species and their identification in different tissues prompted us to investigate whether a gene family exists within a species, specifically *Homo sapiens*. A GenBank search indeed revealed an entire human gene family of olfactomedin-related proteins with at least five members, designated hOlfA through hOlfD, and the TIGR/myocilin protein (Kulkarni *et al.*, 2000). hOlfA corresponds to the previously described rat neuronal AMZ protein (Danielson *et al.*, 1994). Phylogenetic analyses of 18 olfactomedin-related sequences resolved four distinct subfamilies (Fig. 4). Among the human proteins, hOlfA and hOlfC, both expressed in brain, are most closely related. Northern blot analyses of 16 human tissues demonstrated highly specific expression patterns: hOlfA is expressed in brain, hOlfB in pancreas and prostate, hOlfC in cerebellum, hOlfD in colon, small intestine and prostate, and TIGR/myocilin in heart and skeletal muscle (Fig. 5). The link between TIGR/myocilin and ocular hypertension and the expression of several of these proteins in mucus-lined tissues suggest that they play an important role in regulating physical properties of the extracellular environment. These observations led to the obvious question of whether any of these olfactomedin-related proteins are co-expressed with TIGR/myocilin.

2. Expression of multiple olfactomedin-related proteins by trabecular meshwork cells.

The identification of additional olfactomedin-related proteins enabled us to design primers for PCR amplification and to assess whether messages for these proteins are produced in trabecular meshwork cells. Indeed, messages that encode hOlfA and hOlfB, but not hOlfC, could be readily amplified from a cDNA library from trabecular meshwork cells. Sequencing of the amplification products confirmed that they indeed represent hOlfA and hOlfB. Since the expression of TIGR/myocilin is induced by glucocorticoids, we investigated whether glucocorticoids would also upregulate expression of hOlfA and hOlfB. Northern blots of control eyes and eyes exposed to dexamethasone showed dramatic upregulation of TIGR/myocilin, but did not show differences in the constitutive expression levels of hOlfA and hOlfB. These observations suggest a possible novel mode of action for TIGR/myocilin in the pathogenesis of glaucoma. In this model hOlfA and hOlfB form an extracellular matrix in the intraocular environment similar to the way in which olfactomedin polymers constitute the scaffold of the lower mucus layer that covers the olfactory neuroepithelium. Upregulation of TIGR/myocilin would disrupt or expand this matrix through interactions between the olfactomedin domains of TIGR/myocilin and those of hOlfA and hOlfB. It is this alteration in molecular partners between different intraocular olfactomedins, that would alter the flow characteristics of the intraocular fluid and, hence, increase the intraocular pressure. The first step toward verifying that such molecular interactions actually occur is to assess by double immunofluorescence whether or not hOlfA, hOlfB and TIGR/myocilin co-localize in the anterior segment of the eye. The production of antibodies against these three proteins is in progress.

3. Identification of olfactomedin in *Drosophila melanogaster*

We used a signature motif of the olfactomedin homology domain to search the *Drosophila* genome data base for homologues. In contrast to *Caenorhabditis elegans*, which has two olfactomedin-related proteins (Karavanich and Anholt, 1998), *Drosophila melanogaster* contains a single gene that expresses a protein containing an olfactomedin homology domain. This is the CG6867 gene product located on the X-chromosome at cytological location 16F1. It encodes a protein of 935 amino acids that contains a coiled coil region, a collagen-like domain, two immunoglobulin-like c2 domains, and a large, well-defined olfactomedin homology domain at its C-terminus. One of the closest mammalian homologues of the CG6867 gene product is the TIGR/myocilin protein. The CG6867 gene product is clearly an extracellular matrix protein designed to engage in multiple protein-protein interactions, a feature it appears to share with all other members of the family of olfactomedin-related proteins. Identification of olfactomedin in *Drosophila* is likely to facilitate studies on its function.

C. List of All Publications and Technical Reports

(1) *journal articles*

1. Wekesa, K. S. and Anholt, R. R. H. (1997) Pheromone-regulated production of inositol-(1,4,5)-trisphosphate in the mammalian vomeronasal organ. Endocrinology **138**: 3497-3504.
2. Karavanich, C. and Anholt, R. R. H. (1998) Evolution of olfactomedin: Structural constraints and conservation of primary sequence motifs. Ann. NY Acad. Sci. **855**:294-300.
3. Fedorowicz, G. M., Fry, J. D., Anholt, R. R. H. and Mackay, T. F. C. (1998) Epistatic interactions between *smell-impaired* loci in *Drosophila melanogaster*. Genetics **148**: 1885-1891.
4. Karavanich, C. A. and Anholt, R. R. H. (1998) Molecular evolution of olfactomedin. Mol. Biol. Evol. **15**: 718-726.
5. Wekesa, K. S. and Anholt, R. R. H. (1999) Differential expression of G proteins in the mouse olfactory system. Brain Research **837**: 117-126.
6. Kulkarni, N. H., Karavanich, C. A., Atchley, W. R. and Anholt, R. R. H. (2000) Characterization and differential expression of a human gene family of olfactomedin-related proteins. Genet. Res., **76**: 41-50.

(ii) *Abstracts*

1. Anholt, R. R. H. (1997) Evolution of olfactomedin: Structural constraints and conservation of primary sequence motifs. International Symposium on Olfaction and Taste XII (San Diego, CA) p. 33.
2. Wekesa, K. S. and Anholt, R. R. H. (1997) Signal transduction pathway in the mammalian vomeronasal organ: The role of IP3 International Symposium on Olfaction and Taste XII (San Diego, CA) p. 41.
3. Kulkarni, N. H., Buczkowska, G., Mackay, T. F. C. and Anholt, R. R. H. (1997) Molecular cloning of *smell-impaired* genes that affect odor-guided behavior in *Drosophila melanogaster*. International Symposium on Olfaction and Taste XII (San Diego, CA) p. 77.
4. Fedorowicz, G. M., Fry, J. D., Anholt, R. R. H. and Mackay, T. F. C. (1998) Epistatic interactions between *smell-impaired* loci in *Drosophila melanogaster*. Thirty-ninth annual Drosophila Research Conference (Washington, DC).

5. Wekesa, K. S. and Anholt, R. R. H. (1998) Distinct glomerular projection patterns of primary olfactory axons expressing different G-protein α subunits in the mouse olfactory system. Twentieth Annual Meeting of the Association for Chemoreception Sciences, Abst. 22.
6. Fedorowicz, G. M., Kulkarni, N., Roote, J., Ashburner, M., Mackay, T. F. C. and Anholt, R. (1999) Disruption of the gene encoding a Dyrk2 kinase homologue causes olfactory impairment in *Drosophila melanogaster*. Fortieth annual Drosophila Research Conference (Bellevue, WA), Abst. 587A.
7. Fedorowicz, G. M., Kulkarni, N., Roote, J., Ashburner, M., Mackay, T. F. C. and Anholt, R. (1999) Disruption of the gene encoding a Dyrk2 kinase homologue causes olfactory impairment in *Drosophila melanogaster*. XXIst meeting of the Association for Chemoreception Sciences (Sarasota, FL), Abst.61.
8. Anholt, R., Kulkarni, N., Fedorowicz, G., Ganguly, I. and Mackay, T. (2000) Functional genomics of odor-guided behavior in *Drosophila melanogaster*. XXIIInd meeting of the Association for Chemoreception Sciences (Sarasota, FL), Abst. 11.
9. Luo, A. H., Wekesa, K. S., Vandenberg, J. G. and Anholt, R. R. (2000) Olfactory impairment in homologous recombinant mice deficient in the α subunit of Go. XXIIInd meeting of the Association for Chemoreception Sciences (Sarasota, FL), Abst. 269.

D. List of All Participating Scientific Personnel

Dr. Robert R. H. Anholt, Principal Investigator
 Dr. Kennedy S. Wekesa, postdoctoral fellow *
 Dr. Christy A. Karavanich, postdoctoral fellow *
 Ms. Nalini Kulkarni, research technician
 Ms. Indrani Ganguly, graduate research assistant
 Ms. Grazyna Fedorowicz, graduate research assistant
 Ms. Alice Luo, undergraduate research assistant

5. **Report of Inventions**

None.

6. Bibliography

- Aceves-Piña, E. and Quinn, W. (1979) Learning in normal and mutant *Drosophila* larvae. *Science* **206**: 93-96.
- Adams *et al.* (2000) The genome sequence of *Drosophila melanogaster*. *Science* **287**: 2185-2195.
- Anholt, R. R. H. (1993) Molecular neurobiology of olfaction. *Crit. Rev. Neurobiol.* **7**: 1-22.
- Anholt, R. R. H., Lyman, F. L. and Mackay, T. F. C. (1996) Effects of single *P*-element insertions on olfactory behavior in *Drosophila melanogaster*. *Genetics* **143**: 293-301.
- Ashburner, M. *et al.* (1999) An exploration of the sequence of a 2.9-Mb region of the genome of *Drosophila melanogaster*: The *Adh* region. *Genetics* **153**: 179-219.
- Axel, R. (1995) The molecular logic of smell. *Scientific American* **273**: 154-159.
- Ayer, R. K. and Carlson, J. (1992) Olfactory physiology in the *Drosophila* antenna and maxillary palp: *acj6* distinguishes two classes of odorant pathways. *J. Neurobiol.* **23**: 965-982.
- Bellen, H. J., O'Kane, C. J., Wilson, C., Grossniklaus, V., Pearson, R. K. and Gehring W. J. (1989) *P*-element-mediated enhancer detection: A versatile method to study development in *Drosophila*. *Genes Dev.* **3**: 1288-1300.
- Belluscio, L., Gold, G. H., Nemes, A. and Axel, R. (1998) Mice deficient in G_{olf} are anosmic. *Neuron* **20**: 69-81.
- Ben-Arie, N., Lancet, D., Taylor, C., Khen, M., Walker, N., Ledbetter, D. H., Carrozzo, R., Patel, K., Sheer, D., Lehrach, H. and North, M. A. (1994) Olfactory receptor gene cluster on human chromosome 17: possible duplication of an ancestral receptor repertoire. *Hum. Mol. Genet.* **3**: 229-235.
- Berghard, A. and Buck, L. (1996) Sensory transduction in vomeronasal neurons: evidence for G_o , $G\alpha_{i2}$, and adenylyl cyclase II as major components of a pheromone signaling cascade. *J. Neurosci* **16**: 909-918.
- Boekhoff, I., Tareilus, E., Strottman, J. and Breer, H. (1990) Rapid activation of alternative second messenger pathways in olfactory cilia from rats by different odorants. *EMBO J.* **9**: 2453-2458.
- Bozza, T. C. and Kauer, J. S. (1998) Odorant response properties of convergent olfactory receptor neurons. *J. Neurosci.* **18**: 4560-4569.
- Brunet, L. J., Gold, G. H. and Ngai, J. (1996) General anosmia caused by a targeted disruption of the mouse olfactory cyclic nucleotide-gated cation channel. *Neuron* **17**: 681-693.
- Buck, L. and Axel, R. (1991) A novel multigene family may encode odorant receptors: A molecular basis for odor recognition. *Cell* **65**: 175-187.
- Buck, L. B. (1996) Information coding in the olfactory system. *Annu. Rev. Neurosci.* **19**: 517-544.
- Chen, T. Y. and Yau, K. W. (1994) Direct modulation by Ca^{2+} -calmodulin of cyclic nucleotide-activated channel of rat olfactory receptor neurons. *Nature* **368**: 545-548.
- Chess, A., Simon, I., Cedar, H. and Axel, R. (1994) Allelic inactivation regulates olfactory receptor gene expression. *Cell* **78**: 823-834.
- Clyne, P. J., Warr, C. G., Freeman, M. R., Lessing, D., Kim, J. H. and Carlson, J. R. (1999a) A novel family of divergent seven-transmembrane proteins: Candidate odorant receptors in *Drosophila*. *Neuron* **22**: 327-338.

- Clyne, P. J., Certel, S. J., de Bruyne, M., Zaslavsky, L., Johnson, W. A. and Carlson, J. R. (1999b) The odor specificities of a subset of olfactory receptor neurons are governed by Acj6, a POU-domain transcription factor. *Neuron* **22**: 339-347.
- Cooley, L., Kelley, R. and Spradling, A. (1988) Insertional mutagenesis of the *Drosophila* genome with single *P*-elements *Science* **239**: 1121-1128.
- Danielson, P. E., Forss-Petter, S., Battenberg, E. L. F., deLecea, L., Bloom, F. E. and Sutcliffe, J. G. (1994) Four structurally distinct neuron-specific olfactomedin-related glycoproteins produced by differential promoter utilization and alternative mRNA splicing from a single gene. *J. Neurosci. Res.* **38**: 468-478.
- DeZazzo, J. and Tully, T. (1995) Dissection of memory formation: From behavioral pharmacology to molecular genetics. *Trends Neurosci.* **18**: 212-218.
- Dulac, C. and Axel, R. (1995) A novel family of genes encoding putative pheromone receptors in mammals. *Cell* **83**: 195-206.
- Fedorowicz, G. M., Fry, J. D., Anholt, R. R. H., and Mackay, T. F. C. (1998) Epistatic interactions between *smell impaired* loci in *Drosophila melanogaster*. *Genetics* **148**: 1885-1891.
- Firestein, S., Darrow, B. and Shepherd, G. M. (1991) Activation of the sensory current in salamander olfactory receptor neurons depends on a G protein-mediated cAMP second messenger system. *Neuron* **6**: 825-835.
- Friedrich, R. W. and Korsching, S. I. (1997) Combinatorial and chemotopic odorant coding in the zebrafish olfactory bulb visualized by optical imaging. *Neuron* **18**: 737-752.
- Frings, S., Seifert, R., Godde, M. and Kaupp, U. B. (1995) Profoundly different calcium permeation and blockage determine the specific function of distinct cyclic nucleotide-gated channels. *Neuron* **15**: 169-179.
- Griffing, B. (1956) Concept of general and specific combining ability in relation to diallel crossing systems. *Aust. J. Biol. Sci.* **9**: 463-493.
- Halpern, M., Shapiro, L. S. and Jia, C. (1995) Differential localization of G proteins in the opossum vomeronasal system. *Brain Res* **677**: 157-61.
- Helfand, S. L. and Carlson, J. (1989) Isolation and characterization of an olfactory mutant in *Drosophila* with a chemically specific defect. *Proc. Natl. Acad. Sci. U.S.A.* **86**: 2908-2912.
- Herrada, G. and Dulac, C. (1997) A novel family of putative pheromone receptors in mammals with a topographically organized and sexually dimorphic distribution. *Cell* **90**: 763-773.
- Hildebrand, J. G. and Shepherd, G. M. (1997) Mechanisms of olfactory discrimination: Converging evidence for common principles across phyla. *Annu. Rev. Neurosci.* **20**: 595-631.
- Hughes, A. L. and Hughes, M. K. (1993) Adaptive evolution in the rat olfactory receptor gene family. *J. Mol. Evol.* **36**: 249-254.
- Issel-Tarver, L. and Rine, J. (1997) The evolution of mammalian olfactory receptor genes. *Genetics* **145**: 185-195.
- Jiang, X. C., Inouchi, J., Wang, D. and Halpern, M. (1990) Purification and characterization of a chemo-attractant from electric shock-induced earthworm secretion, its receptor binding, and signal transduction through the vomeronasal system of garter snakes. *J. Biol. Chem.* **265**, 8736-8744.
- Joerges, J., Küttner, A., Galizia, C. G., and Menzel, R. (1997) Representations of odours and odour mixtures visualized in the honeybee brain. *Nature* **387**: 285-288.

- Jones, D. T. and Reed, R. R. (1989) G_{olf} : an olfactory neuron specific-G protein involved in odorant signal transduction. *Science* **244**: 790-795.
- Karavanich, C. A. and Anholt, R. R. H. (1998) Molecular evolution of olfactomedin. *Mol. Biol. Evol.* **15**: 718-726.
- Kim, M. S., Repp, A. and Smith, D. P. (1998) LUSH odorant-binding protein mediates chemosensory responses to alcohols in *Drosophila melanogaster*. *Genetics* **150**: 711-721.
- Kleene, S. J. and Gesteland, R. C. (1991) Calcium-activated chloride conductance in frog olfactory cilia. *J. Neurosci.* **11**: 3624-3629.
- Kubota, R., Noda, S., Wang, Y., Minoshima, S., Asakawa, S., Kudoh, J., Mashima, Y., Oguchi, Y. and Shimizu, N. (1997) A novel myosin-like protein (myocilin) expressed in the connecting cilium of the photoreceptor: Molecular cloning, tissue expression, and chromosomal mapping. *Genomics* **41**: 360-369.
- Kulkarni, N. H., Karavanich, C. A., Atchley, W. R. and Anholt, R. R. H. (2000) Characterization and differential expression of a human gene family of olfactomedin-related proteins. *Genet. Res.*, **76**: 41-50.
- Kurahashi, T. and Yau, K. W. (1993) Co-existence of cationic and chloride components in odorant-induced current of vertebrate olfactory receptor cells. *Nature* **363**: 71-74.
- Kurahashi, T. and Menini, A. (1997) Mechanism of odorant adaptation in the olfactory receptor cell. *Nature* **385**: 725-729.
- Lai, C., Lyman, R. F., Long, A. D., Langley, C. H. and Mackay, T. F. C. (1994) Naturally occurring variation in bristle number and DNA polymorphisms at the *scabrous* locus of *Drosophila melanogaster*. *Science* **266**: 1697-1702.
- Laissue, P. P., Reiter, C., Hiesinger, P. R., Halter, S., Fischbach, K. F., and Stocker, R. F. (1999) Three-dimensional reconstruction of the antennal lobe in *Drosophila melanogaster*. *J. Comp. Neurol.* **405**: 543-552.
- Lander, E. S. and Schork, N. J. (1994) Genetic dissection of complex traits. *Science* **265**: 2037-2048.
- Levy, N. S., Bakalyar, H. A. and Reed, R. R. (1991) Signal transduction in olfactory neurons. *J. Steroid Biochem Molec Biol* **39**: 633-637.
- Lilly, M., and Carlson, J. (1989) *Smellblind*: A gene required for *Drosophila* olfaction. *Genetics* **124**: 293-302.
- Lilly, M., Kreber, R., Ganetzky, B. and Carlson, J. (1994) Evidence that the *Drosophila* olfactory mutant *smellblind* defines a novel class of sodium channel mutation. *Genetics* **136**: 1087-1096.
- Long, A. D., Lyman, R. F., Langley, C. H. and Mackay, T. F. C. (1998) Two sites in the *Delta* gene region contribute to naturally occurring variation in bristle number in *Drosophila melanogaster*. *Genetics* **149**: 999-1017.
- Long, A. D., Lyman, R. F., Morgan, A. H., Langley, C. H. and Mackay, T. F. C. (2000) Both naturally occurring insertions of transposable elements and intermediate frequency polymorphisms at the *achaete-scute* complex are associated with variation in bristle number in *Drosophila melanogaster*. *Genetics* **154**: 1255-1269.
- Lyman, R. F., Lai, C. and Mackay, T.F.C. (1999) Linkage disequilibrium mapping of molecular polymorphisms at the *scabrous* locus associated with naturally occurring variation in bristle number in *Drosophila melanogaster*. *Genet. Res.* **74**: 303-311.

- Lyman, R. F. and Mackay, T. F. C. (1998) Candidate quantitative trait loci and naturally occurring variation for bristle number in *Drosophila melanogaster*: The *Delta-Hairless* gene region. *Genetics* **149**: 983-998.
- Luo, Y., Lu, S., Chen, P., Wang, D. and Halpern, M. (1994) Identification of chemoattractant receptors and G proteins in the vomeronasal system of garter snakes. *J. Biol. Chem.* **269**: 16867-16877.
- Mackay, T. F. C. (1996) The nature of quantitative genetic variation revisited: Lessons from *Drosophila* bristles. *BioEssays* **18**: 113-121.
- Mackay, T. F. C. and Langley, C. H. (1990) Molecular and phenotypic variation in the *achaete-scute* region of *Drosophila melanogaster*. *Nature* **348**: 64-66.
- Mackay, T. F. C., Hackett, J. B., Lyman, R. F., Wayne, M. L. and Anholt, R. R. H. (1996) Quantitative genetic variation of odor-guided behavior in a natural population of *Drosophila melanogaster*. *Genetics* **144**: 727-735.
- Matsunami, H. and Buck, L. (1997) A multigene family encoding a diverse array of putative pheromone receptors in mammals. *Cell* **90**: 775-784.
- McKenna, M., Monte, P., Helfand, S. L., Woodward, C. and Carlson, J. (1989) A simple chemosensory response in *Drosophila* and the isolation of *acj* mutants in which it is affected. *Proc. Natl. Acad. Sci. U.S.A.* **86**: 8118-8122.
- McKenna, M. P., Hekmat-Scafe, D. S., Gaines, P. and Carlson, J. (1994) Putative *Drosophila* pheromone-binding proteins expressed in a subregion of the olfactory system. *J. Biol. Chem.* **269**: 16340-16347.
- Meredith, M. (1998) Vomeronasal function. *Chem Senses* **23**: 463-466.
- Mombaerts, P., Wang, F., Dulac, C., Chao, S. K., Nemes, A., Mendelsohn, M., Edmondson, J. and Axel, R. (1996) Visualizing an olfactory sensory map. *Cell* **87**: 675-686.
- Nakamura, T. and Gold, G. H. (1987) A cyclic nucleotide-gated conductance in olfactory receptor cilia. *Nature* **325**: 442-444.
- Neimann-Sorensen, A. and Robertson, A. (1961) The association between blood groups and several production characteristics in three Danish cattle breeds. *Acta Agriculturae Scandinavica* **11**: 163-196.
- Okamoto, K., Tokumitsu, Y. and Kashiwayanagi, M. (1996) Adenylyl cyclase activity in turtle vomeronasal and olfactory epithelium. *Biochem. Biophys. Res. Commun.* **220**: 98-101.
- Pace, U., Hanski, E., Salomon, Y. and Lancet, D. (1985) Odorant-sensitive adenylyl cyclase may mediate olfactory reception. *Nature* **316**: 255-258.
- Pikielny, C. W., Hasan, G., Rouyer, F. and Rosbash, M. (1994) Members of a family of *Drosophila* putative odorant-binding proteins are expressed in different subsets of olfactory hairs. *Neuron* **12**: 35-49.
- Polanski, J. R., Fauss, D. J., Chen, P., Chen, H., Luetjen-Drecoll, E., Johnson, D., Kurtz, R. M., Ma, Z. D., Bloom, E. and Nguyen, T. D. (1997) Cellular pharmacology and molecular biology of the trabecular meshwork inducible glucocorticoid response gene product. *Ophthalmologica* **211**: 126-139.
- Pomeroy, S. L., Lamantia, A. S. and Purves, D. (1990) Postnatal construction of neural circuitry in the mouse olfactory bulb. *J. Neurosci.* **10**: 1952-1966.

- Riesgo-Escovar, J. Woodard, C., Gaines, P. and Carlson, J. (1992) Development and organization of the *Drosophila* olfactory system: An analysis using enhancer traps. *J. Neurobiol.* **23**: 947-964.
- Riesgo-Escovar, J. R. Woodard, C. and Carlson, J. (1994) Olfactory physiology in the maxillary palp requires the visual system gene *rdgB*. *J. Comp. Physiol. (A)* **175**: 687-693.
- Riesgo-Escovar, J., Raha, D. and Carlson, J. R. (1995) Requirement for a phospholipase C in odor response: Overlap between olfaction and vision in *Drosophila*. *Proc. Natl. Acad. Sci. U.S.A.* **92**: 2864-2868.
- Risch, N. and Merikangas, K. (1996) The future of genetic studies of complex human diseases. *Science* **273**: 1516-1517.
- Rodrigues, V. and Siddiqi, O. (1978) Genetic analysis of chemosensory pathway. *Proc. Ind. Acad. Sci.* **87B**: 147-160.
- Ronnett, G. V., Cho, H., Hester, L. D., Wood, S. F. and Snyder, S. H. (1993) Odorants differentially enhance phosphoinositide turnover and adenylyl cyclase in olfactory receptor neuronal cultures. *J. Neurosci.* **13**, 1751-1758.
- Rouquier, S., Taviaux, S., Trask, B. J., Brand-Arpon, V., van den Engh, G., Demaille, J. and Giorgi, D. (1998) Distribution of olfactory receptor genes in the human genome. *Nature Genetics* **18**: 243-250.
- Rubin, B. D. and Katz, L. C. (1999) Optical imaging of odorant representations in the mammalian olfactory bulb. *Neuron* **23**: 499-511.
- Ryba, N. J. P. and Tirindelli, R. (1997) A new multigene family of putative pheromone receptors. *Neuron* **19**: 371-379.
- Sengupta, P., Chou, J. C. and Bargmann, C. I. (1996) *odr-10* encodes a seven transmembrane domain olfactory receptor required for responses to the odorant diacetyl. *Cell* **84**: 899-909.
- Sklar, P. B., Anholt, R. R. H. and Snyder, S. H. (1986) The odorant-sensitive adenylate cyclase of olfactory receptor cells: Differential stimulation by distinct classes of odorants. *J. Biol. Chem.* **261**: 15538-15543.
- Smith, D. P., Stamnes, M. A. and Zucker, C. S. (1991) Signal transduction in the visual system of *Drosophila*. *Annu. Rev. Cell Biol.* **7**: 161-190.
- Snyder, D. A., Rivers, A. M., Yokoe, H., Menco, B. Ph. M. and Anholt, R. R. H. (1991) Olfactomedin: Purification, characterization and localization of a novel olfactory glycoprotein. *Biochemistry* **30**: 9143-9153.
- Stocker, R. F. and Gendre, N. (1988) Peripheral and central nervous effects of *lozenge*³: A *Drosophila* mutant lacking basiconic antennal sensilla. *Dev. Biol.* **127**: 12-24.
- Stone, E. M., Fingert, J. H., Alward, W. L. M., Nguyen, T. D., Polansky, J. R., Sunden, S. L. F., Nishimura, D., Clark, A. F., Nystuen, A., Nichols, B. E., Mackey, D. A., Ritch, R., Kalenak, J. W., Craven, E. R. and Sheffield, V. C. (1997) Identification of a gene that causes primary open angle glaucoma. *Science* **275**: 668-670.
- Störtkuhl, K. F., Hovemann, B. T. and Carlson, J. R. (1999) Olfactory adaptation depends on the Trp Ca²⁺ channel in *Drosophila*. *J. Neurosci.* **19**: 4839-4846.
- Strotmann, J., Wanner, I., Helfrich, T., Beck, A. and Breer, H. (1994) Rostrocaudal patterning of receptor expressing neurons in the rat nasal cavity. *Cell Tissue Res* **278**: 11-20.

- Sullivan, S. L., Bohm, S., Ressler, K. J., Horowitz, L. F. and Buck, L. B. (1995) Target-independent pattern specification in the olfactory epithelium. *Neuron* **15**: 779-789.
- Sullivan, S. L., Adamson, M. C., Ressler, K. J., Kozak, C. A. and Buck, L. B. (1996) The chromosomal distribution of mouse odorant receptor genes. *Proc Natl Acad Sci USA* **93**: 884-888.
- Sved, J. A. (1975) Fitness of third chromosome homozygotes in *Drosophila melanogaster* *Genet. Res.* **25**: 197-200.
- Talluri, S., Bhatt, A. and Smith, D. P. (1995) Identification of a *Drosophila* G protein α subunit (dG $_{\alpha}$ -3) expressed in chemosensory cells and central neurons. *Proc. Natl. Acad. Sci. U.S.A.* **92**: 11475-11479.
- Taniguchi, M., Kashiwayanagi, M. and Kurihara, K. (1995) Intracellular injection of inositol 1,4,5-triphosphate increases a conductance in membranes of turtle vomeronasal receptor neurons in the slice preparation. *Neurosci. Lett.* **188**: 5-8.
- Valenzuela, D., Han, X., Mende, U., Fankhauser, C., Mashimo, H., Huang, P., Pfeffer, J., Neer, E. J. and Fishman, M. C. (1997) G α_o is necessary for muscarinic regulation of Ca²⁺ channels in mouse heart. *Proc Natl Acad Sci USA* **94**: 1727-1732.
- Vihtelic, T. S., Goebel, M., Milligan, S., O'Tousa, J. E. and Hyde, D. R. (1993) Localization of *Drosophila* retinal degeneration B, a membrane-associated phosphatidylinositol transfer protein. *J. Cell Biol.* **122**: 1013-1022.
- Vosshall, L. B., Amrein, H., Morozov, P. S., Rzhetsky, A. and Axel, R. (1999) A spatial map of olfactory receptor expression in the *Drosophila* antenna. *Cell* **96**: 725-736.
- Wekesa, K. S. and Anholt, R. R. H. (1997) Pheromone regulated production of inositol-(1,4,5)-trisphosphate in the mammalian vomeronasal organ. *Endocrinology* **138**: 3497-3504.
- Wekesa, K. S. and Anholt, R. R. H. (1999) Differential expression of G proteins in the mouse olfactory system. *Brain Research* **837**: 117-126.
- Woodard, C., Alcorta, E. and Carlson, J. (1992.) The *rdgB* gene in *Drosophila*: A link between vision and olfaction. *J. Neurogenetics* **8**: 17-32.
- Yokoe, H. and Anholt, R. R. H. (1993) Molecular cloning of olfactomedin, an extracellular matrix protein specific to olfactory neuroepithelium. *Proc. Natl. Acad. Sci. U.S.A.* **90**: 4655-4659.

Pheromone Regulated Production of Inositol-(1, 4, 5)-Trisphosphate in the Mammalian Vomeronasal Organ*

KENNEDY S. WEKESA AND ROBERT R. H. ANHOLT

Department of Zoology, North Carolina State University, Raleigh, North Carolina 27695

ABSTRACT

Social behaviors of most mammals are profoundly affected by chemical signals, pheromones, exchanged between conspecifics. Pheromones interact with dendritic microvilli of bipolar neurons in the vomeronasal organ (VNO). To investigate vomeronasal signal transduction pathways, microvillar membranes from porcine VNO were prepared. Incubation of such membranes from prepubertal females with boar seminal fluid or urine results in an increase in production of inositol-(1, 4, 5)-trisphosphate (IP_3). The dose response for IP_3 production is biphasic with a GTP-dependent component at low stimulus concentrations and a nonspecific increase in IP_3 at higher stimulus concentrations. The GTP-dependent stimulation is mimicked by

GTP γ S and blocked by GDP β S. Furthermore, the GTP-dependent component of the stimulation of IP_3 production is sex specific and tissue dependent. Studies with monospecific antibodies reveal a $G\alpha_{q/11}$ -related protein in vomeronasal neurons, concentrated at their microvilli. Our observations indicate that pheromones in boar secretions act on vomeronasal neurons in the female VNO via a receptor mediated, G protein-dependent increase in IP_3 . These observations set the stage for further investigations on the regulation of stimulus-excitation coupling in vomeronasal neurons. The pheromone-induced IP_3 response also provides an assay for future purification of mammalian reproductive pheromones. (*Endocrinology* 138: 3497–3504, 1997)

MOST MAMMALS use pheromones to coordinate reproduction (1). These chemical signals can be classified into two categories: those with short-term effects on the behavior of the recipient (signaling pheromones), and those with long term effects on the physiology of the recipient (priming pheromones) (1). For example, signaling pheromones in urine or glandular secretions play a role in the initiation of copulatory behavior (2), whereas priming pheromones are responsible for puberty acceleration (3–8) and reproductive activation (9, 10). Although the majority of studies on reproductive pheromones have been done on rodents, pheromone-dependent effects on reproduction have been documented also for sheep (11), cattle (12), and pigs (5, 13, 14).

One of the most extensively studied pheromonal effects is the acceleration of puberty in the female house mouse (3, 4, 6, 7). The presence of an adult male, or his urine, accelerates the onset of puberty in prepubertal female mice as evident from a rapid and dramatic increase in uterine weight (3, 4, 6, 7). The induction of the puberty accelerating pheromone is androgen dependent because urine from prepubertal males, castrated adult males, or adult females fails to accelerate puberty (4). Pheromone-dependent puberty acceleration is not unique to rodents but occurs also in pigs (5, 13), sheep (11), and cows (12).

Whereas the perception of signaling pheromones may be mediated by the main olfactory system, the physiological effects of most priming pheromones are initiated in the

vomeronasal organ (VNO; 1, 15–17). The VNOs are paired, cartilage-encased elongated organs associated with the vomer bone in the rostral nasal cavity. The VNO contains a lumen that communicates via a duct with the oral (most mammals, including pigs) or nasal (e.g. horses) cavity (15, 16). Chemical stimuli in urine and glandular secretions of conspecifics act upon the dendritic microvilli of bipolar chemosensory neurons in the VNO. The VNO is the chemoreceptive organ of the accessory olfactory system, which is functionally and anatomically distinct from the main olfactory system (16, 18, 19). The main olfactory bulb sends projections to the primary olfactory cortex, the nucleus of the lateral olfactory tract, the olfactory tubercle, and the periamygdaloid region, while afferent neurons from the VNO project to the accessory olfactory bulb, from which secondary neurons extend into the bed nucleus of the stria terminalis, the medial amygdala, and the hypothalamus, enabling pheromones to influence reproductive physiology and behavior (16, 18). Removal of the VNO or the accessory olfactory bulb impairs reproductive behavior, whereas lesions of the main olfactory epithelium or main olfactory bulb that result in anosmia do not impair pheromonal effects (17, 19, 20). Thus, whereas the main olfactory bulb analyses odors in the environment, the accessory olfactory bulb is specialized to detect conspecific chemical signals that activate stereotypic instinctive behaviors via the neuroendocrine system.

In the main olfactory system, odorants bind to heptahelical, G protein-coupled receptors on the ciliated dendrites of olfactory neurons (21). These odorant receptors are encoded by a diverse array of about 1,000 genes (21, 22). Binding of an odorant to its receptor activates a heterotrimeric G protein ($G\alpha_{olf}$; 23), which leads to activation of adenylyl cyclase (22, 24). The resulting increase in cAMP elicits the generator potential by directly opening cyclic nucleotide-gated channels in the ciliary plasma membrane (22, 24–26).

Received March 17, 1997.

Address all correspondence and requests for reprints to: Dr. Robert R. H. Anholt, Department of Zoology, Box 7617, North Carolina State University, Raleigh, North Carolina 27695.

* This work was supported by a grant from the North Carolina Biotechnology Center (9605-ARG-0015) and partially by grants from the National Institutes of Health (DC-02485) and the U.S. Army Research Office (DAAH04-96-1-0096).

The VNO and olfactory epithelium both derive from the olfactory placode. Both the VNO and main olfactory epithelium possess bipolar neurons that are functionally replaced from neurogenic precursor cells throughout life (27). In addition, in both systems primary chemosensory neurons form convergent projections onto the main olfactory bulb or accessory olfactory bulb. Similarities in embryonic development, anatomical organization, and chemosensory function initially suggested that transduction mechanisms in the VNO would resemble those in the olfactory epithelium. However, screens of complementary DNA (cDNA) libraries from murine VNO failed to yield cDNAs encoding $G_{\alpha_{olf}}$, adenylate cyclase type III, and the α -subunit of the olfactory cyclic nucleotide-gated channel (28, 29). Studies in rat also indicate that the olfactory epithelium and VNO differ in signal transduction pathways (30). Electrophysiological characterization of chemosensory neurons from the murine VNO failed to detect functional cyclic nucleotide-gated channels in vomeronasal neurons (31, 32). Finally, a family of putative pheromone receptors has been identified in the VNO (33). Although these belong to the superfamily of heptahelical receptors, they do not share motifs characteristic of the family of odorant receptors (21). These studies all support the notion that chemosensory neurons of the main olfactory system and the accessory olfactory system use different signal recognition and transduction pathways (32).

Functional biochemical studies on the VNO that would complement molecular biological approaches have been hampered by the small size of the VNO in most common laboratory animals. To eliminate this problem, we selected the domestic pig (*Sus scrofa*) as our model system. Pigs have large VNOs that are well separated from the main olfactory system, and their reproductive physiology and behavior, like that of rodents, is regulated by pheromones (5, 13, 14). We have developed a procedure for the preparation of a VNO membrane fraction enriched in dendritic microvillar membranes that allows routine measurements of second messengers. Here we report that pheromones contained in seminal fluid and boar urine stimulate the production of inositol-(1, 4, 5)-trisphosphate (IP_3) when applied to microvillar VNO membranes from female juvenile pigs (gilts). This stimulation is dose dependent, GTP dependent, sex dependent, and tissue specific. We show further that this microvillar membrane preparation contains a G protein of the G_{α_q} class, which commonly mediates receptor-activated increases in IP_3 (34). Finally, immunohistochemical studies show prominent $G_{\alpha_{q/11}}$ immunoreactivity concentrated at the microvilli of vomeronasal neurons, supporting the notion that pheromones in seminal fluid and boar urine stimulate vomeronasal neurons of female pigs via a receptor mediated $G_{\alpha_{q/11}}$ coupled IP_3 pathway.

Materials and Methods

Membrane preparations

Freshly collected boar urine, gilt urine, and seminal fluid were provided by Dr. W. L. Flowers from the Animal Science Department at North Carolina State University. The seminal fluid was centrifuged to remove cells. The seminal fluid, boar urine and gilt urine were stored as

aliquots under argon at -80°C until used. Pigs were made available immediately following euthanasia by Drs. R. A. Argenzio, N. A. Monteiro-Riviere, and R. A. Abdullahi, from the College of Veterinary Medicine at North Carolina State University. VNOs from gilts, up to six months old, were dissected from their crevices in the nasal cavity, removed from the cartilaginous capsule, and frozen on dry ice. The tissues were then minced and crushed with a razor blade and subjected to sonication for 2–5 min in ice-cold PBS in a Bransonic bath sonicator. The resulting suspension was layered on a 45% (wt/wt) sucrose cushion and centrifuged at 4°C for 30 min at 40,000 rpm in a Beckman SW55Ti rotor. The membrane fraction on top of the sucrose was collected and centrifuged as before for 15 min to pellet the membranes. The membranes were resuspended in 100 μl of ice-cold PBS. Protein was then determined according to the method of Lowry *et al.* (35), using BSA as standard. Membranes from olfactory tissue were prepared according to the same procedure. Membranes from liver, brain, kidney, and lung were prepared by homogenizing the tissue in PBS with a Teflon homogenizer. Membranes were collected by centrifugation, washed once, and resuspended in PBS.

Second messenger assays

Forskolin and nucleotides were purchased from Boehringer Mannheim (Indianapolis, IN). [^3H] cAMP and [^{32}P]- α -ATP were from Amersham Radiochemical Corporation (Arlington Heights, IL). Adenylate cyclase activity was measured according to the method of Salomon *et al.* (36), in the presence of 10 μM forskolin, boar urine or 10 μM guanosine 5'-0-(3-thiotriphosphate (GTP γ S)). For IP_3 assays, reactions were incubated for 1 min at 37°C in 25 mM Tris-acetate buffer, pH 7.2, 5 mM Mg-acetate, 1 mM dithiothreitol, 0.5 mM ATP, 0.1 mM CaCl_2 , 0.1 mg/ml BSA, 10 μM GTP, and 20 μg VNO membrane protein. Reactions were terminated by adding 1 M trichloroacetic acid. IP_3 was measured with a kit from New England Nuclear, Inc. (Boston, MA) according to the manufacturer's instructions and is based on displacement of [^3H] IP_3 from a specific IP_3 binding protein. Differences between experimental and control animals were analyzed using the Student's *t* test.

Western Blotting

VNO membrane samples were subjected to electrophoresis on a 10% SDS-polyacrylamide gel, followed by electrophoretic transfer onto a nitrocellulose membrane. Strips of the membrane, containing approximately 10 μg protein were probed with a 1,000-fold dilution of normal rabbit serum or 1,000-fold dilutions of rabbit antisera against specific G protein subunits (Calbiochem, La Jolla, CA). Bound antibody was visualized via a biotinylated goat-antirabbit secondary antibody complexed with avidin and biotinylated horseradish peroxidase, using Amersham's chemiluminescent ECL detection system. Migration distances were calibrated with biotinylated low range molecular weight markers (Bio-Rad, Richmond, CA).

Immunohistochemistry

Formalin-fixed and paraffin-embedded, 5- μm thick, coronal sections through the VNO were deparaffinized in xylene and rehydrated through graded alcohols. Sections were blocked with 0.5% casein for 1 h at room temperature. They were then incubated with a 200-fold dilution of either normal rabbit serum or anti- $G_{\alpha_{q/11}}$ antiserum in PBS, 0.05% Triton X-100. This was followed by several washes and incubation for 1 h at room temperature with biotinylated goat antirabbit IgG in PBS supplemented with 0.05% Triton X-100 and 1% normal rabbit serum. At this stage, endogenous peroxidase activity was abolished by exposing the sections for 10 min to 0.3% hydrogen peroxide. After addition of streptavidin-biotinylated horseradish peroxidase complex (Zymed Laboratories, Inc., San Francisco, CA), bound antibody was visualized as brown immunoprecipitates using 3,3'-diaminobenzidine as chromogenic substrate. Sections were then counterstained with hematoxylin, and viewed and photographed under a Zeiss Axioplan microscope.

Results

Dose-dependent and GTP-dependent increases in IP_3 levels induced by boar seminal fluid and urine in VNO membranes from gilts

To study transduction pathways activated by pheromonal stimuli from the male, we developed a preparation enriched in microvillar membranes from VNOs of gilts. The tissue is subjected to sonication to detach microvilli from the vomeronasal neuroepithelial surface, and the resulting membranes are then collected by centrifugation on a sucrose cushion. The yield of these membranes is $141 \pm 9 \mu\text{g}$ protein/VNO ($n = 11$) and this membrane fraction is approximately 3-fold, enriched in both the specific activities of adenylate cyclase and phospholipase C. The basal activity of adenylate cyclase ($68 \pm 12 \text{ pmol/min-mg}$ $n = 5$) can be readily activated by the nonhydrolyzable GTP analogue, GTP γ S, and forskolin (117 ± 13 and $228 \pm 38 \text{ pmol/min-mg}$, respectively, $n = 5$), but we could not detect stimulation with pheromonal stimuli from either seminal fluid, boar urine, or the known boar pheromone, 5 α -androst-16-en-3-one (Sigma Chemical Company, St. Louis, MO). Vomeronasal adenylate cyclase activity is approximately 50-fold lower than activities observed in olfactory cilia preparations (37, 38) and is not affected by calcium/calmodulin (38). This is in line with observations by Berghard and Buck which indicate that the vomeronasal adenylate cyclase is the calmodulin-insensitive type II isoform rather than the adenylate cyclase type III found in olfactory receptor cells (29).

In contrast to the vomeronasal adenylate cyclase, incubation of microvillar membranes from gilts with seminal fluid results in a robust, dose-dependent increase in IP_3 (Fig. 1). The dose-response curve is biphasic. At lower stimulus con-

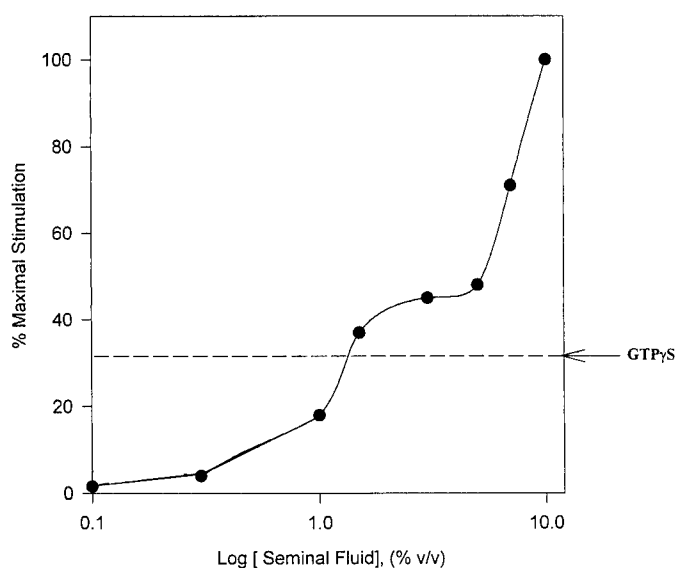


FIG. 1. Dose dependence of the production of IP_3 by seminal fluid in female VNO membranes. The dose-response curve for activation of IP_3 is biphasic with a specific GTP-dependent component at lower concentrations of seminal fluid and a nonspecific GTP-independent component at higher concentrations. Each data point represents the mean of four to six independent experiments, each consisting of duplicate measurements. SEs are within 18% of the mean for all measurements.

centrations a component of the response saturates at the level of stimulation observed with GTP γ S. At higher stimulus, concentrations an additional nonsaturable, nonspecific increase in IP_3 is observed. The response seen at low concentrations of seminal fluid (up to 1.5% vol/vol) is mimicked by GTP γ S and blocked by GDP β S (Fig. 2). Similar responses are elicited with urine from the boar, but here higher stimulus concentrations (up to 3% vol/vol) are required to resolve the GTP-dependent component of the IP_3 response. No increases in IP_3 were observed in response to 5 α -androst-16-en-3-one up to concentrations of 100 mM. This is consistent with previous studies that suggest that androstenone is a signaling pheromone which mediates its effects via the main olfactory rather than the accessory olfactory system (39). We conclude from these observations that female VNO membranes respond to stimuli in boar seminal fluid and urine with an increase in IP_3 via a G protein coupled pathway.

Sex specificity and tissue specificity of the IP_3 response

Relatively little information is available about the chemical nature of mammalian pheromones. Because the active components in boar seminal fluid and urine have not been identified, we deemed it important to establish whether the observed IP_3 responses were physiologically relevant. Previous studies on rodents have shown that production of reproductive pheromones by the male is androgen dependent (4). We reasoned, therefore, that only boar urine, but not urine from prepubertal females, should elicit an increase in IP_3 in VNO membranes from gilts. The results presented in Fig. 3 demonstrate that this prediction is correct. Whereas boar urine elicits a robust increase in IP_3 , experiments using urine samples from gilts failed to activate IP_3 production above the basal level. To further document specificity of the observed IP_3 response, we investigated the tissue specificity of seminal fluid-induced increases in IP_3 by testing the effect of 1.5% seminal fluid side-by-side on microvillar VNO membranes and membranes obtained from olfactory tissue, brain, lung, liver, and kidney. Basal activity of phospholipase C was detected in all samples and was particularly high in membranes from olfactory tissue (Fig. 4). However, whereas seminal fluid caused a 2-fold increase in IP_3 production in VNO

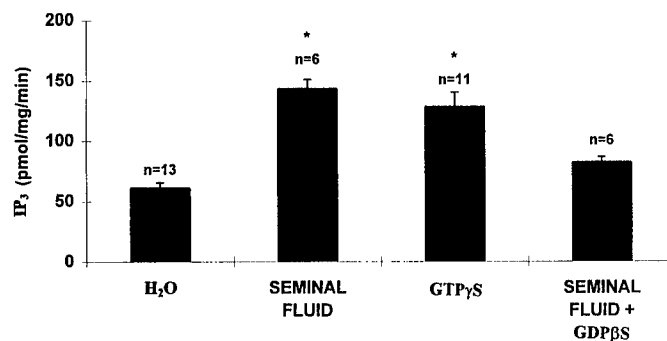


FIG. 2. GTP dependence of the production of IP_3 by seminal fluid in female VNO membranes. Reactions were performed without stimulus, in the presence of 1.5% seminal fluid (vol/vol), $10 \mu\text{M}$ GTP γ S, or 1.5% seminal fluid together with $100 \mu\text{M}$ GDP β S. Significant stimulation compared with basal activity is observed in the presence of seminal fluid and GTP γ S (*, $P < 0.05$) and not in the presence of seminal fluid together with GDP β S.

FIG. 3. Sex dependence of the production of IP_3 in female VNO membranes. Reactions were performed without stimulus, in the presence of 3% (vol/vol) gilt urine, 3% (vol/vol) boar urine, 1.5% (vol/vol) seminal fluid, and 10 μM GTP γ S. All assays were done in the presence of 10 μM GTP. Significant stimulation compared with basal activity is observed in the presence of boar urine, seminal fluid, and GTP γ S (*, $P < 0.05$). Levels of IP_3 production by boar urine, seminal fluid, and GTP γ S are not statistically different. There is also no significant difference between the baseline control and stimulation by gilt urine.

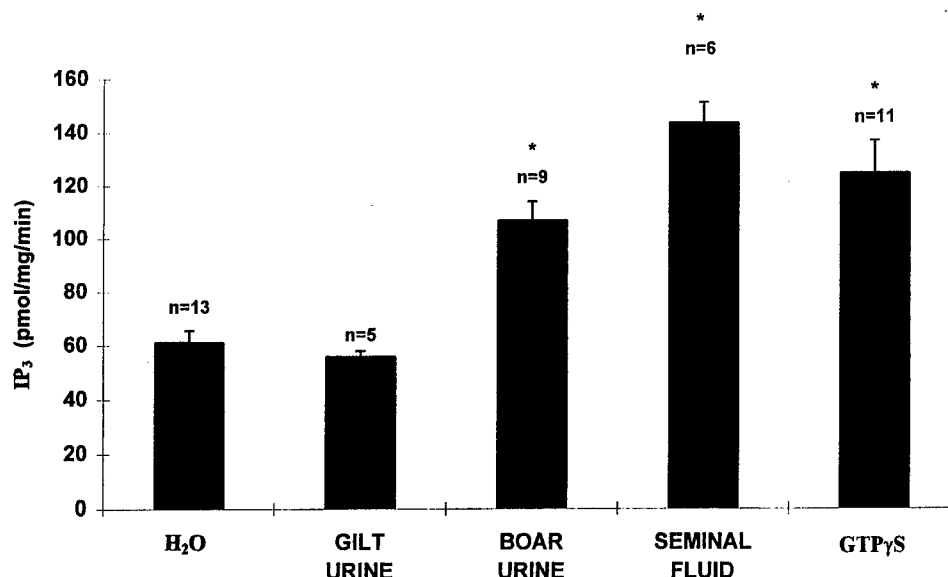
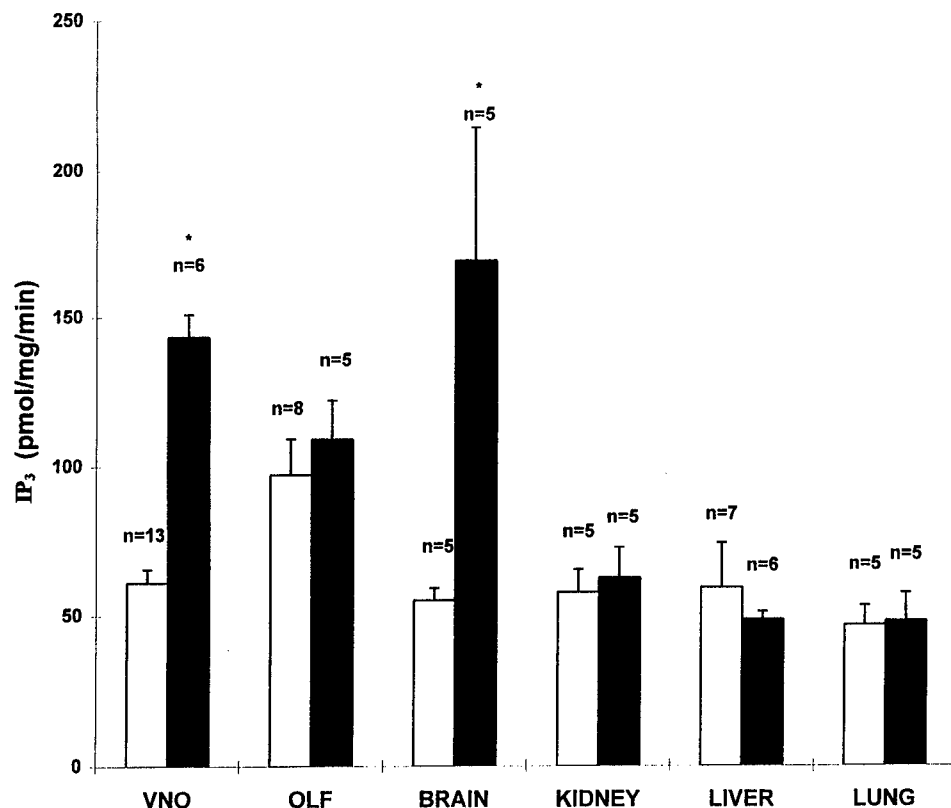


FIG. 4. Tissue specificity of the production of IP_3 by seminal fluid in female VNO membranes. Reactions were performed using 20 μg of membrane protein and 1.5% seminal fluid (vol/vol) as the stimulus. There were no significant differences between the basal level of IP_3 (open bars) and its level in the presence of seminal fluid (closed bars) with membranes from olfactory tissue (OLF), kidney, liver, or lung. Significant differences between control and stimulated IP_3 levels are observed in VNO membranes and brain membranes (*, $P < 0.05$).



membranes, no significant stimulation above the basal level was observed in membranes from olfactory tissue, liver, lung, and kidney. Besides the VNO, significant increases in the level of IP_3 upon exposure to seminal fluid were observed only in membranes from brain. We attribute this stimulation to the presence of neuroactive substances in seminal fluid.

The experiments described above demonstrate a GTP-dependent and dose-dependent increase in the formation of IP_3 , but not cAMP, in female VNO membranes upon exposure to boar seminal fluid or urine. This stimulation shows tissue

specificity and sex dependence. Together, these observations indicate that pheromones from the male activate the production of IP_3 in the female VNO via specific G protein-coupled receptors.

Identification of a $G\alpha_{q/11}$ related G protein on the microvillar surface of the VNO

Previously, immunohistochemical studies identified α -subunits of G_{i2} and G_o in distinct subpopulations of vome-

ronasal neurons. Although we cannot exclude that either of these two G proteins could mediate the observed stimulation of phospholipase C, we decided to investigate whether our VNO membrane preparation contains a G protein of the $G\alpha_q$ class, known to cause activation of at least the $\beta 1$ -isoform of phospholipase C (34). Using subunit-specific rabbit antisera against unique peptide sequences of $G\alpha_s$, $G\alpha_{i1}/G\alpha_{i2}$, $G\alpha_{i1}$, $G\alpha_{i3}/G\alpha_o$, $G\alpha_{i3}$, $G\alpha_{q/11}$, and $G\beta$, we confirmed in our microvillar membrane preparation the presence of $G\alpha_{i2}$ and $G\alpha_o$, as reported previously (29, 40; Fig. 5). In addition, we observe $G\alpha_s$, and a single β -subunit at 35 kDa. A $G\alpha_{i3}/G\alpha_o$ specific antiserum sometimes reveals a doublet of immunoreactive bands, suggesting the presence of both $G\alpha_{i3}$ and $G\alpha_o$. Of greatest interest, however, is the observation of a prominent, previously unreported, immunoreactivity revealed by an antiserum against the $G\alpha_{q/11}$ protein (Fig. 5).

We investigated whether the $G\alpha_{q/11}$ protein is localized to the microvillar surface of the VNO. The apical region of porcine vomeronasal neurons contains a dense group of microvilli in contrast to supporting cells that carry smaller groups of microvilli (41). Immunohistochemical staining of coronal sections through the VNO with the $G\alpha_{q/11}$ antiserum reveals intense staining of microvillar tufts at the surface of the vomeronasal lumen (Fig. 6A). Cell bodies of vomeronasal neurons and dendritic processes are also stained, but the staining here is lighter, and it is obvious that immunoreactivity is concentrated primarily at the microvillar surface. To verify the specificity of this staining, adjacent sections were incubated either without the primary antibody or with normal rabbit serum at the same concentration. Under these conditions, no staining was detected (Fig. 6B). Thus, $G\alpha_{q/11}$,

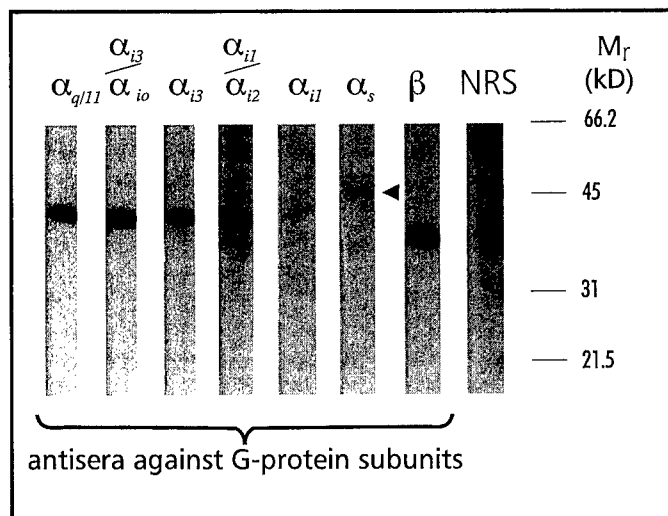


FIG. 5. Identification of G protein subunits in vomeronasal membranes. Each strip contained 10 μ g of VNO membrane protein and was probed either with 1,000-fold dilution of normal rabbit serum (NRS) or monospecific rabbit antisera against subunits of G proteins, as indicated. The arrow indicates the 45-kDa $G\alpha_s$ subunit, identified by the $G\alpha_s$ -antiserum. A single β -subunit is detected which migrates at 35 kDa. The immunoreactive bands identified by antisera against $G\alpha_{i3}$ and $G\alpha_{i3}/G\alpha_o$ can sometimes be resolved as doublets, suggesting the presence of both $G\alpha_{i3}$ and $G\alpha_o$. Note also the presence of $G\alpha_{i2}$ and the prominent presence of a polypeptide immunoreactive with anti- $G\alpha_{q/11}$.

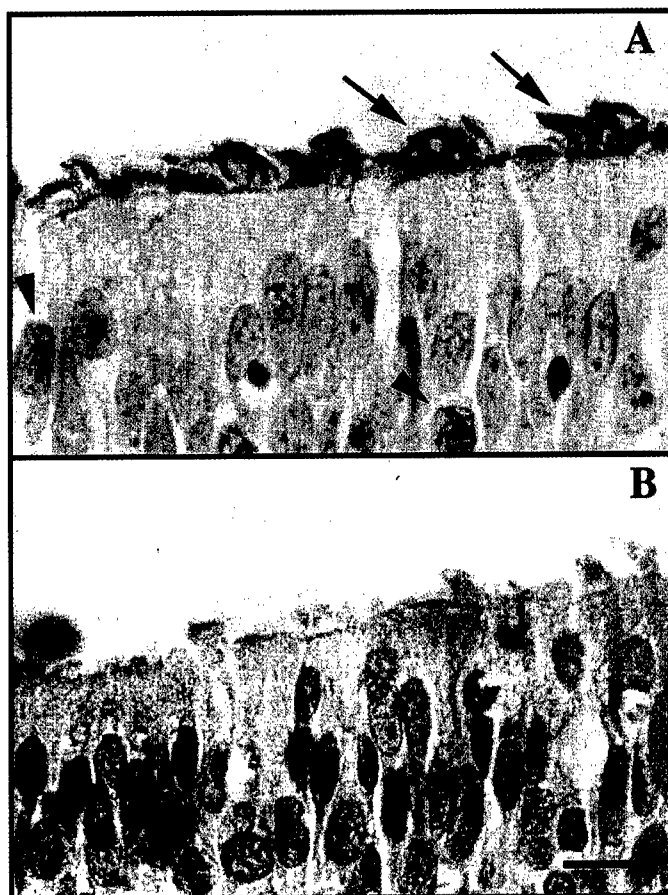


FIG. 6. Immunohistochemical localization of $G\alpha_{q/11}$ to the microvillar surface of the VNO. A, Section stained with a 200-fold dilution of antiserum against $G\alpha_{q/11}$. Note the deposition of brown reaction product on microvillar tufts along the microvillar surface of the neuroepithelium (arrows) and in the cell bodies of the vomeronasal neurons (arrowheads). B, Adjacent section incubated with normal rabbit serum. Scale bar, 100 μ m.

which links receptor mediated responses to activation of phospholipase C, is expressed by vomeronasal neurons and concentrated at the microvillar surface, where the pheromone first encounters the chemosensory neurons.

Discussion

Our results suggest that in the porcine VNO IP_3 is the principal second messenger that mediates pheromonal signal transduction. This is in contrast to the main olfactory system, where cAMP appears to be the dominant second messenger that regulates olfactory transduction (22, 24–26). Although we cannot exclude a role for cAMP in vomeronasal signal transduction, we were unable to detect effects of either boar urine or boar seminal fluid on vomeronasal adenylate cyclase. Failure to detect message for $G\alpha_{olf}$ adenylate cyclase type III and the α -subunit of the olfactory cyclic nucleotide gated channel in cDNA libraries from VNO (29, 30) further accentuates the differences between chemosensory transduction in olfactory and vomeronasal neurons.

Involvement of IP_3 has also been implicated in signal transduction in the reptilian VNO. In garter snakes, a polypeptide purified from secretions of earthworms, the snake's prey,

induces a G protein-dependent increase in IP_3 and a decrease in cAMP, suggesting interactions between both signal transduction pathways (42, 43). Furthermore, patch-clamp studies on vomeronasal neurons from the turtle have shown that intracellular injection of IP_3 elicits a membrane conductance (44), although effects of cAMP have also been reported in this system (45). Thus, the role of IP_3 in vomeronasal signal transduction may be universal among vertebrates, whereas the influence of cAMP in vomeronasal signaling remains to be evaluated further.

Despite behavioral, electrophysiological, and molecular biological studies on the mammalian VNO, no direct measurements of dose-dependent, GTP-dependent increases in second messengers upon exposure to pheromones have been reported until now. Evaluation of the dose dependence of vomeronasal stimulation is especially important in light of the large nonspecific component we observed. In light of the previously observed diversity of putative pheromone receptors (33), it may seem puzzling that in our case specific G protein-dependent production of IP_3 in response to boar seminal fluid approaches the level of IP_3 production observed with GTP γ S. However, this observation can be explained, if we assume that boar seminal fluid contains a cocktail of pheromones and that the high stimulus concentrations used in our study activate the vast majority of pheromone receptors, coupled to the IP_3 pathway. Although the chemical nature of the pheromonal stimuli in boar urine and boar seminal fluid are not known, we believe that the IP_3 responses we report reflect the physiological response of the vomeronasal neuron to pheromones because: 1) the response shows a saturable dose-dependent component; 2) this component is GTP dependent, indicating the involvement of a G protein, and by inference, G protein-coupled receptors (33); 3) the response is sex dependent, as expected from pheromones produced only by the male and intended to affect the female; 4) the response shows tissue-specificity, in agreement with the notion that it is mediated via receptors expressed selectively in the VNO; and 5) a $G_{\alpha_{q/11}}$ type G protein, classically involved with receptor-mediated activation of phospholipase C (34), is expressed in vomeronasal neurons and concentrated on their chemosensory microvilli.

The procedure used for the preparation of microvillar membranes is modeled after well established methods for harvesting olfactory cilia from olfactory neuroepithelium (46, 47). Sonication of olfactory membranes results not only in the detachment of olfactory cilia but also in the detachment of microvilli from sustentacular cells and plasma membrane fragments from other components of the neuroepithelium (46, 47). Electron microscopic examination of these preparations revealed membrane vesicles, axonemal structures devoid of a plasma membrane, and axonemal structures associated with membrane fragments (47). The membrane preparation we refer to as "microvillar membranes" is, therefore, likely to contain contaminants derived from other components of the VNO, including microvillar membranes from supporting cells, and it is difficult to estimate the purity of this preparation precisely. However, our preparation appears to be sufficiently enriched in chemosensory mem-

branes for the purpose of our studies. This assessment is based on the fact that the observed pheromone induced responses are tissue specific, sex dependent, and G protein mediated. It is further supported by the notion that the prominent expression of $G_{\alpha_{q/11}}$ immunoreactivity at the microvillar surface of the neuroepithelium (Fig. 6) mirrors the prominent visualization of $G_{\alpha_{q/11}}$ immunoreactivity observed in the microvillar membrane preparation on Western blots (Fig. 5).

Immunohistochemical studies on opossum (40) and *in situ* hybridization studies in mouse (29) revealed that a population of neurons in the apical layer of the vomeronasal neuroepithelium expresses $G_{\alpha_{i2}}$. These neurons project to the anterior region of the accessory olfactory bulb (40). In contrast, a population of neurons located in the base of the vomeronasal neuroepithelium expresses G_{α_o} (29) and projects to the posterior region of the accessory olfactory bulb (40). Both α -subunits of these G proteins are also detected in the VNO of the pig. It remains to be determined whether these G proteins play roles directly in pheromonal transduction or in signaling processes that coordinate the growth and differentiation of vomeronasal neurons. In an extensive screen of a rat VNO cDNA library, Berghard and Buck (29) detected several cDNAs encoding $G_{\alpha_{11}}$. It seems, therefore, reasonable to presume that the $G_{\alpha_{q/11}}$ immunoreactivity we detect most likely represents $G_{\alpha_{11}}$. Because the frequency of clones encoding $G_{\alpha_{11}}$ in the library screened by Berghard and Buck (29) was low relative to cDNAs encoding $G_{\alpha_{i2}}$ and G_{α_o} , it appears that low levels of message are produced for the $G_{\alpha_{11}}$ protein, which may reflect a slower turnover than $G_{\alpha_{i2}}$ and G_{α_o} . Although a direct link between pheromone detection and activation of $G_{\alpha_{11}}$ must still be documented, the uniform presence of this G protein on all microvillar tufts suggests a role for this G protein in pheromonal signaling in all mature vomeronasal neurons. Localization of $G_{\alpha_{q/11}}$ to the neuronal compartment of the VNO is supported by the observation that neuronal cell bodies of the vomeronasal epithelium also stain and is in agreement with immunohistochemical observations at the electron microscopic level by Menco *et al.* (48), who reported presence of G_{α_q} immunoreactivity on axons of vomeronasal neurons.

Pheromone-induced increases in IP_3 imply a role for calcium in vomeronasal signal transduction (49). Although the mechanisms that underlie transduction-excitation coupling in the VNO remain to be elucidated, several lines of circumstantial evidence support a role for calcium in this process. High levels of three calcium binding proteins, calretinin, calbindin-D28k, and parvalbumin are found in vomeronasal neurons (50, 51). In addition, patch-clamp studies identified both an L-type and T-type calcium current in rat vomeronasal neurons, indicating a role for calcium in neuronal excitation (31). Electron microscopic studies show that, in all species thus far examined, including pigs, the apical dendritic domes of vomeronasal neurons are densely populated with intracellular vesicles (41). It is tempting to speculate that these vesicles may serve as calcium storage depots, from where calcium can be released by IP_3 . It will be of interest to determine in future studies whether IP_3 receptors are located

on these vesicular membranes. In addition, we have observed that incubation of microvillar membranes with phorbol esters results in protein phosphorylation (data not shown). Thus diacylglycerol formed together with IP_3 may also play a role in pheromonal signaling through activation of protein kinase C.

Although behavioral and physiological effects of pheromones have been well documented, mostly in rodents (1–4, 6–10), but also in pigs (5, 13, 14), unambiguous identification of pheromones from urine has been problematic. Several laboratories have reported the identification of putative pheromones (6, 7), but independent confirmation of these claims has been notoriously lacking. Hitherto, identification of pheromones has depended on laborious and time-consuming bioassays that involve many animals maintained under controlled environmental conditions to limit individual variation. This renders systematic isolation of pheromones extremely difficult and virtually impossible if the biological response depends on a blend of pheromones, of which individual components may separate during fractionation. In addition to setting the stage for further biochemical studies on regulation of pheromonal signal transduction pathways and transduction-excitation coupling in the VNO, our experiments provide a biochemical assay, *i.e.* a robust GTP-dependent increase in IP_3 , for the future identification of mammalian pheromones.

Acknowledgments

We thank Marjory Gray, Martha Armstrong, Drs. R. A. Argenzio, N. A. Monteiro-Riviere, and R. A. Abdullahi, from the College of Veterinary Medicine at North Carolina State University for enabling us to obtain fresh porcine vomeronasal organs and Dr. W. L. Flowers from the Department of Animal Science at North Carolina State University for providing us with gilt urine, boar urine, and seminal fluid. We thank Yee-Lut Kwok and Sundip Patel for technical assistance. We would also like to thank Dr. John G. Vandenbergh for valuable discussions and critical reading of the manuscript.

References

- Vandenbergh JG 1994 Pheromones and mammalian reproduction. In: Knobil E, Neill D (eds) *Physiology of Reproduction*. Vol. 2, Raven Press, New York, pp 343–359
- Murphy MR 1980 Sexual preferences of male hamsters: importance of preweaning and adult experience, vaginal secretion and olfactory or vomeronasal sensation. *Behav Neurol Biol* 30:323–340
- Vandenbergh JG 1969 Male odor accelerates female sexual maturation in mice. *Endocrinology* 81:345–349
- Drickamer LC, Murphy RX 1978 Female mouse maturation: effects of excreted and bladder urine from juvenile and adult males. *Dev Psychobiol* 11:63–72
- Pearce GP, Hughes PE 1987 The influence of boar component stimuli on puberty attainment in the gilt. *Anim Prod* 44:293–302
- Mucignat-Caretta C, Caretta A, Cavaggoni A 1995 Acceleration of puberty onset in female mice by male urinary proteins. *J Physiol* 482:517–522
- Jemiolo B, Andreolini F, Xie T, Wiesler D, Novotny M 1989 Puberty-affecting synthetic analogs of urinary chemosignals in the house mouse, *Mus domesticus*. *Physiol Behav* 46:293–298
- Hasler JF, Banks EM 1975 The influence of mature males on sexual maturation in female collared lemmings (*Dicrostonyx groenlandicus*). *J Reprod Fertil* 42:583–586
- Lepri JJ, Vandenbergh JG 1986 Puberty in pine voles, *Microtus pinetorum*, and the influence of chemosignals on female reproduction. *Biol Reprod* 34:370–377
- Carter CS, Getz LL, Gavish L, McDermott JL, Arnold P 1980 Male related pheromones and the activation of female reproduction in the prairie vole *Microtus ochrogaster*. *Biol Reprod* 23:1038–1045
- Signoret JP 1991 Sexual pheromones in the domestic sheep: importance and limits in the regulation of reproductive physiology. *J Steroid Biochem Mol Biol* 39:639–645
- Izard MK, Vandenbergh JG 1982 The effects of bull urine on puberty and calving date in crossbred beef heifers. *J Anim Sci* 55:1160–1168
- Signoret JP, Baldwin BA, Fraser D, Hafez ESE 1975 The behavior of swine. In: Hafez ESE (ed) *The Behavior of Domestic Animals*. Williams & Wilkins, Baltimore, pp 295–329
- Dorries KM 1992 Sex differences in olfaction in mammals. In: Serby MJ, Chobor, KL (eds) *Science of Olfaction*. Springer-Verlag, New York, pp 245–275
- Meredith M 1983 Sensory physiology of pheromone communication. In: Vandenbergh JG (ed) *Pheromones and Reproduction in Mammals*. Academic Press, New York, pp 95–112
- Wysocki CJ, Meredith M 1991 The vomeronasal system. In: Finger TE, Silver WL (eds) *Neurobiology of Taste and Smell*. John Wiley & Sons, New York, pp 125–150
- Kaneko N, Debski EA, Wilson MC, Whitten WK 1980 Puberty acceleration in mice. II. Evidence that the vomeronasal organ is a receptor for the primer pheromone in male mouse urine. *Biol Reprod* 22:873–878
- Winans SS, Scalia F 1970 Amygdaloid nucleus: new afferent input from the vomeronasal organ. *Science* 170:330–332
- Powers JB, Winans SS 1975 Vomeronasal organ: critical role in mediating sexual behavior of the male hamster. *Science* 187:961–963
- Wysocki CJ, Lepri JJ 1991 Consequences of removing the vomeronasal organ. *J Steroid Biochem Mol Biol* 39:661–669
- Buck L, Axel R 1991 A novel multigene family may encode odorant receptors: a molecular basis for odor recognition. *Cell* 65:175–187
- Buck LB 1996 Information coding in the olfactory system. *Annu Rev Neurosci* 19:517–544
- Jones DT, Reed RR 1989 Golf: an olfactory neuron specific G-protein involved in odorant signal transduction. *Science* 244:790–795
- Anholt RRH 1993 Molecular neurobiology of olfaction. *Crit Rev Neurobiol* 7:1–22
- Firestein S, Darrow B, Shepherd GM 1992 Activation of the sensory current in salamander olfactory receptor neurons depends on a G protein-mediated cAMP second messenger system. *Neuron* 6:825–835
- Nakamura T, Gold GH 1987 A cyclic nucleotide-gated conductance in olfactory receptor cilia. *Nature* 325:442–444
- Cushieri A, Bannister LH 1975 The development of the olfactory mucosa in the mouse: light microscopy. *J Anat* 119:277–286
- Berghard A, Buck LB, Liman ER 1996 Evidence for distinct signaling mechanisms in two mammalian olfactory sense organs. *Proc Natl Acad Sci USA* 93:2365–2369
- Berghard A, Buck L 1996 Sensory transduction in vomeronasal neurons: evidence for G_{α_s} , $G_{\alpha_{12}}$, and adenylyl cyclase II as major components of a pheromone signaling cascade. *J Neurosci* 16:909–918
- Wu Y, Tirindelli R, Ryba NJ 1996 Evidence for different chemosensory signal transduction pathways in olfactory and vomeronasal neurons. *Biochem Biophys Res Commun* 220:900–904
- Liman ER, Corey DP 1996 Electrophysiological characterization of chemosensory neurons from the mouse vomeronasal organ. *J Neurosci* 16:4625–4637
- Liman ER 1996 Pheromone transduction in the vomeronasal organ. *Curr Opin Neurobiol* 6:487–493
- Dulac C, Axel R 1995 A novel family of genes encoding putative pheromone receptors in mammals. *Cell* 83:195–206
- Taylor SJ, Chae HZ, Rhee SG, Exton JH 1991 Activation of the β_1 isozyme of phospholipase C by α subunits of the G_q class of G proteins. *Nature* 350:516–518
- Lowry OH, Rosebrough NJ, Farr AL, Randall RJ 1951 Protein measurement with the Folin phenol reagent. *J Biol Chem* 193:265–275
- Salomon Y, Londos C, Rodbell M 1974 A highly sensitive adenylyl cyclase assay. *Anal Biochem* 58:541–548
- Sklar PB, Anholt RRH, Snyder SH 1986 The odorant-sensitive adenylyl cyclase of olfactory receptor cells: Differential stimulation by distinct classes of odorants. *J Biol Chem* 261:15538–15543
- Anholt RRH, Rivers AM 1990 Olfactory transduction: crosstalk between second messenger systems. *Biochemistry* 29:4049–4054
- Dorries KM, Adkins-Reagan E, Halpern BP 1996 Sensitivity and behavioral responses to the pheromone androstenedione are not mediated by the vomeronasal organ in domestic pigs. *Brain Behav Evol* 49:53–62
- Halpern M, Shapiro LS, Jia C 1995 Differential localization of G proteins in the opossum vomeronasal system. *Brain Res* 677:157–61
- Adams DR 1992 Fine structure of the vomeronasal and septal olfactory epithelia and of glandular structures. *Microsc Res Tech* 23:86–97
- Luo Y, Lu S, Chen P, Wang D, Halpern M 1994 Identification of chemoattractant receptors and G proteins in the vomeronasal system of garter snakes. *J Biol Chem* 269:16867–16877
- Jiang XC, Inouchi J, Wang D, Halpern M 1990 Purification and characterization of a chemo-attractant from electric shock-induced earthworm secretion, its receptor binding, and signal transduction through the vomeronasal system of garter snakes. *J Biol Chem* 265:8736–8744
- Taniguchi M, Kashiwayanagi M, Kurihara K 1995 Intracellular injection of inositol-(1, 4, 5)-trisphosphate increases a conductance in membranes of turtle vomeronasal receptor neurons in the slice preparation. *Neurosci Lett* 188:5–8

45. **Okamoto K, Tokumitsu Y, Kashiwayanagi M** 1996 Adenylyl cyclase activity in turtle vomeronasal and olfactory epithelium. *Biochem Biophys Res Commun* 220:98-101
46. **Anholt RRH** 1995 Preparation of olfactory cilia. In: Spielman AI, Brand JG (eds) *Experimental Cell Biology of Taste and Olfaction, Current Techniques and Protocols*. CRC Press, New York, pp 163-168
47. **Anholt RRH, Aebi U, Snyder SH** 1986 A partially purified preparation of isolated chemosensory cilia from the olfactory epithelium of the bull frog, *Rana catesbeiana*. *J Neurosci* 6:1962-1969
48. **Menco BPhM, Tekula FD, Farbman AI, Danho W** 1994 Developmental expression of G-proteins and adenylyl cyclase in peripheral olfactory systems. Light microscopic and freeze-substitution electron microscopic immunocytochemistry. *J Neurocytol* 23:708-727
49. **Berridge MJ** 1993 Inositol trisphosphate and calcium signaling. *Nature* 316:315-325
50. **Johnson EW, Eller PM, Jafek BW, Norman AW** 1992 Calbindin-like immunoreactivity in two peripheral chemosensory tissues of the rat: taste buds and the vomeronasal organ. *Brain Res* 572:319-324
51. **Kishimoto J, Keverne EB, Emson PC** 1992 Calretinin, calbindin-D28k and parvalbumin-like immunoreactivity in mouse chemoreceptor neurons. *Brain Res* 610:325-329

Epistatic Interactions Between *smell-impaired* Loci in *Drosophila melanogaster*

Grażyna M. Fedorowicz,^{*,†} James D. Fry,^{†,1} Robert R. H. Anholt^{*} and Trudy F. C. Mackay[†]

Departments of ^{*}Zoology and [†]Genetics, North Carolina State University, Raleigh, North Carolina 27695-7614

Manuscript received July 14, 1997

Accepted for publication January 5, 1998

ABSTRACT

Odor-guided behavior is a polygenic trait determined by the concerted expression of multiple loci. Previously, *P*-element mutagenesis was used to identify single *P*[*lArB*] insertions, in a common isogenic background, with homozygous effects on olfactory behavior. Here, we have crossed 12 lines with these *smell impaired* (*smi*) mutations in a half-diallel design (excluding homozygous parental genotypes and reciprocal crosses) to produce all possible 66 doubly heterozygous hybrids with *P*[*lArB*] insertions at two distinct locations. The olfactory behavior of the transheterozygous progeny was measured using an assay that quantified the avoidance response to the repellent odorant benzaldehyde. There was significant variation in general combining abilities of avoidance scores among the *smi* mutants, indicating variation in heterozygous effects. Further, there was significant variation among specific combining abilities of each cross, indicating dependencies of heterozygous effects on the *smi* locus genotypes, *i.e.*, epistasis. Significant epistatic interactions were identified for nine transheterozygote genotypes, involving 10 of the 12 *smi* loci. Eight of these loci form an interacting ensemble of genes that modulate expression of the behavioral phenotype. These observations illustrate the power of quantitative genetic analyses to detect subtle phenotypic effects and point to an extensive network of epistatic interactions among genes in the olfactory subgenome.

THE fundamental goal of quantitative genetics is to understand how complex traits are shaped through the interactions of multiple genes in different genetic backgrounds and under varying environmental conditions. Perhaps the most complex category of polygenic traits is represented by various forms of animal behavior. *Drosophila melanogaster* presents an ideal model system to study the genetic basis of behavioral quantitative traits, because mutations in highly inbred strains can be easily generated, allowing control over the segregation of many individual loci that contribute to the trait and enabling the effect of each locus to be studied independently. We have used odor-guided behavior in *D. melanogaster* as a model system to study the quantitative genetics of behavior.

Odor-guided behavior is of special interest, because the ability of an organism to respond to chemical signals from its environment is essential for its survival and, often, its procreation. Thus, olfactory behavior contributes to individual fitness (MACKAY *et al.* 1996). In recent years, considerable progress has been made in elucidating the molecular mechanisms that underlie odor recognition, olfactory transduction, and neural coding of olfactory information both in vertebrates (reviewed by

ANHOLT 1993; AXEL 1995; BUCK 1996) and in invertebrate model systems, such as *Caenorhabditis elegans* (TROMEL *et al.* 1996; SENGUPTA *et al.* 1996) and lobster (FADOOL and ACHE 1992). However, the genetic basis of variation in olfactory responsiveness and the genetic mechanisms that shape behavioral responses to odorants are still poorly understood.

Chemical mutagenesis has been used to induce mutations affecting olfactory behavior in *D. melanogaster*, mostly on the X chromosome (RODRIGUES and SIDDIQI 1978; ACEVES-PIÑA and QUINN 1979; HELFAND and CARLSON 1989; LILLY and CARLSON 1989; MCKENNA *et al.* 1989; AYER and CARLSON 1992; WOODARD *et al.* 1992; LILLY *et al.* 1994a,b). This resulted in the characterization of a number of genes that encode proteins likely to participate in olfactory signal transduction in *Drosophila*, such as *smellblind* (an allele of *paralytic*), which encodes a voltage-gated sodium channel (RODRIGUES and SIDDIQI 1978; ACEVES-PIÑA and QUINN 1979; LILLY and CARLSON 1989; LILLY *et al.* 1994a,b), *norpA*, which encodes a phospholipase C (WOODARD *et al.* 1992; RIESGO-ESCOVAR *et al.* 1995), and *rdgB*, which encodes a phosphatidyl inositol transfer protein (VIHTELIC *et al.* 1993). Although mutations in any of these genes cause extensive impairment of olfactory behavior, it is not clear how these genes contribute quantitatively to variation in olfactory responsiveness and how they function in the context of the genetic background, *i.e.*, the entire olfactory subgenome. Recently, we have identified 14 loci that contribute to olfactory behavior by *P*-element insertional mutagenesis

Corresponding author: Trudy F. C. Mackay, Department of Genetics, Box 7614, North Carolina State University, Raleigh, NC 27695-7614. E-mail: trudy_mackay@ncsu.edu

[†] Present address: Department of Biology, Utah State University, Logan, UT 84332-5305.

in an isogenic strain (ANHOLT *et al.* 1996). Identification of these loci, designated *smell impaired* (*smi*), was achieved using statistical and quantitative genetic analysis of measurements of olfactory behavior. These analyses are capable of detecting small phenotypic effects with a resolution limited only by sample size.

As the *smi* loci have similar phenotypes, they are likely to be functionally related and participate in common physiological and/or developmental pathways that shape olfactory responsiveness. One genetic method for identifying and ordering genes in functionally interacting groups is to screen for mutations at unlinked loci that enhance or suppress the mutant effects of a known member of the pathway (GARCÍA-BELLIDO 1981). Epistatic interactions between such genes can be deduced by examining the phenotypes of the one- and two-locus genotypes. For independent loci, the phenotypes of the two-locus genotypes are the sum of the single-locus phenotypes; *i.e.*, the loci act additively. Departures from strict additivity indicate epistatic, or interacting, loci. A simple test for interaction that can be used for recessive mutations with large, qualitative effects that have similar loss-of-function phenotypes and that therefore affect a common process, is to examine the phenotypes of double mutant heterozygotes. Epistasis is evident when the double heterozygote has the same loss-of-function phenotype as the single homozygous mutations as a result of combined haploinsufficiency of function. This approach and variants of it have been used to identify epistatic interactions and to identify new loci that modify mutant phenotypes of other loci (BOTAS *et al.* 1982; BELOTE *et al.* 1985; KENNISON and RUSSELL 1987; HOMYK and EMERSON 1988; TRICOIRE 1988; DAMBLY-CHAUDIÈRE *et al.* 1988).

Detecting interactions between mutations with quantitative effects is more difficult, because the mutations are not usually completely recessive (MACKAY *et al.* 1992; LYMAN *et al.* 1996). Further, the background genotype needs to be controlled to enable small phenotypic effects to be perceived and to ensure any interactions are due to epistasis between the mutations of interest, and are not confounding nonadditive interactions among alleles segregating between the background genotypes in which the mutations were induced. The *smi* mutations are in a common isogenic background and therefore can be used to detect epistasis. We have generated all possible double heterozygous hybrids among 12 independent *smi* mutations that appear amenable to molecular characterization in a diallel cross design (GRIFFING 1956), which is the quantitative genetic analogue of the transheterozygote test for epistasis. This approach is based on the assumption that reduced expression of two independent *P[ArB]*-tagged *smi* genes in double heterozygotic offspring may result in quantitative failure to complement (MACKAY and FRY 1996; LONG *et al.* 1996) if these genes interact.

Significant epistatic interactions were identified for nine transheterozygote genotypes, involving 10 of the

12 *smi* loci. Interactions between eight of these loci show evidence of a web of mutually interactive genes, the coordinated expression of which modulates the behavioral phenotype. These findings illustrate the power of quantitative genetic analyses to detect subtle phenotypic effects and indicate that phenotypic determination of odor-guided behavior in *D. melanogaster* depends quantitatively on an extensive network of genetic interactions.

MATERIALS AND METHODS

Generation of transheterozygous *P[ArB]* insert lines: The parental lines used to generate double mutant heterozygotes were 12 homozygous *smi* lines obtained by *P*-element mutagenesis of the isogenic Samarkand; *ry*⁵⁰⁶ strain: *smi21F*, *smi26D*, *smi27E*, *smi28E*, *smi35A*, *smi45E*, *smi51A*, *smi60E*, *smi61A*, *smi65A*, *smi97B*, and *smi98B* (ANHOLT *et al.* 1996). The mutations were named according to the cytological insertion sites of the *P* elements. The 12 *smi* lines were crossed in a half-diallel design (excluding homozygous parental lines and reciprocal crosses) to produce all 66 possible combinations of F₁ transheterozygous offspring with two *P* elements at different loci. Crosses were initiated at a density of five females of *smi* line *i* and five males of *smi* line *j* (*i* ≠ *j*) in plastic culture vials. All animals were reared at 25° on agar-yeast-molasses medium.

Behavioral assay: To quantify odor-guided behavior we used the simple, rapid, and highly reproducible "dipstick" assay, described previously (ANHOLT *et al.* 1996). This assay was chosen because it has several advantages over other commonly used assays. The Y-maze assay, developed by RODRIGUES and SIDDIQI (1978), is better suited for measurements of attraction and odor discrimination than repulsion and is laborious for large behavioral screens. The olfactory jump assay, described by McKENNA *et al.* (1989), was in our hands unreliable, because in contrast to Canton-S flies for which this assay was developed, flies of both our inbred Samarkand strain and of substitution lines containing chromosomes from natural populations (MACKAY *et al.* 1996) seldom jumped in response to repellent odorants. The "dipstick assay" used in this study and in previous studies (ANHOLT *et al.* 1996; MACKAY *et al.* 1996) is a simple, rapid, and highly reproducible statistical sampling assay that quantifies odor-guided behavior with a resolution limited only by sample size and, hence, can detect subtle olfactory impairments (ANHOLT *et al.* 1996). Previously, this assay has led to the identification of 14 novel *smi* loci. In addition, known mutants, such as *smellblind* (RODRIGUES and SIDDIQI 1978; ACEVES-PIÑA and QUINN 1979; LILLY and CARLSON 1989; LILLY *et al.* 1994a,b), are immediately apparent and readily quantifiable in this assay (ANHOLT *et al.* 1996).

After 2–4 hr of starvation, 2–10-day post-eclosion transheterozygous progeny were tested for responsiveness to benzaldehyde, a repellent odorant, exactly as described by ANHOLT *et al.* (1996). Briefly, one replicate assay consisted of a single-sex group of five individuals in a test vial. The animals were exposed to 1% benzaldehyde (v/v) introduced on a cotton wool swab, and the number of flies migrating to a compartment remote from the odor source was measured at 5-sec intervals, from 15 to 60 sec after introduction of the odor source. The "avoidance score" of the replicate is the average of these 10 counts, giving a possible range of avoidance scores between 0 (all flies in the compartment near the odor source for the entire assay period) and 5 (all flies in the compartment away from the odor source for the entire assay period). For each of the 66 crosses, 10 replicate avoidance score estimates were obtained for each sex, for a total of 20 replicates (100

individual flies) per double heterozygote genotype, and a total sample size of 6600 animals.

Statistical analyses: The avoidance scores of transheterozygous genotypes were analyzed by two-way analysis of variance (ANOVA), with Genotype and Sex the fixed cross-classified main effects. Sums of squares were partitioned into sources (degrees of freedom) attributable to Genotype (65), Sex (1), Genotype \times Sex interaction (65), and Error (1188). As this is a fixed effects model, the error mean square was used as the denominator for all *F*-ratio tests of significance. To analyze epistatic effects between *smi* loci, we could not simply compare the responses of double heterozygotes with the single heterozygotes of *smi* lines with *Sam*, because the effect of *P*[*lArB*] insert copy number (2 *vs.* 1) could be confounding. Rather, the correct control for this analysis is measurement of the deviation from the average of all other transheterozygotes with the two single inserts being compared. Thus, the general combining ability (*GCA*) of a mutation is its average avoidance score as a transheterozygote with all other mutations, expressed as the deviation from the overall mean (SPRAGUE and TATUM 1942), and is an estimate of the average heterozygous effect of the mutation relative to the heterozygous effects of the other mutations. The specific combining ability (*SCA*) of a transheterozygous genotype is the difference between the observed avoidance score of the genotype, x_{ij} (where *i* and *j* denote two different *smi* mutations), and the score expected from the sum of the corresponding *GCA*s of mutants *i* and *j*. The sums of squares due to Genotype and Genotype \times Sex were further partitioned into sources of variation (degrees of freedom) attributable to *GCA* (11), *SCA* (54), *GCA* \times Sex (11), and *SCA* \times Sex (54). *SCA* effects are due to variation in heterozygous effects that depend on the genetic background with respect to other *smi* mutations and can only be caused by epistatic interactions.

This fixed effects half-diallel corresponds to Method 4, Model I of GRIFFING (1956). Consequently, the *GCA* for each *smi* mutant was estimated as

$$GCA_i = T_i / (n - 2) - \sum T_j / (n - 2) \quad (1)$$

where T_i is the sum of mean avoidance score values (averaged over all replicates) of heterozygotes with the *i*th mutation, $\sum T$ is twice the sum of mean avoidance score values of all heterozygotes, and *n* is the number of mutant lines (see also FALCONER and MACKAY 1996). The *SCA* effects were computed using the method of GRIFFING (1956) for each heterozygous genotype as

$$SCA_{ij} = x_{ij} - (T_i + T_j) / (n - 2) + \sum T / (n - 1)(n - 2). \quad (2)$$

The significance of the overall *GCA*, *SCA*, *GCA* \times Sex, and *SCA* \times Sex effects was tested using an *F* variance ratio test statistic with the error mean square as the denominator. Standard errors of individual *GCA* and *SCA* effects were computed according to the formulae given by GRIFFING (1956). Analyses of variance and tests of significance were calculated using SAS procedures (SAS INSTITUTE, INC. 1988), and *GCA* and *SCA* sums of squares were computed using the diallel cross analysis program of SCHAFER and USANIS (1969).

RESULTS AND DISCUSSION

The effects of 12 *P*-element insertional mutations with homozygous effects on olfactory behavior were evaluated in all possible double heterozygote combinations, in a half-diallel design. The mean avoidance responses to benzaldehyde, averaged over sexes, are shown for each of the 66 transheterozygote genotypes in Table 1.

TABLE 1
Diallel cross of the *smi* lines

	<i>smi</i> 97B	26D	51A	27E	60E	35A	45E	61A	65A	28E	21F	T_i	<i>GCA</i>	<i>HOM</i>
98B	3.640	3.365	3.800	3.870	3.600	4.020	4.085	4.435	3.985	4.160	4.145	43.105	-0.083 ^{ns}	2.870
97B		3.510	3.960	3.805	3.810	4.060	4.250	4.330	3.925	3.800	3.520	42.610	-0.133 ^{**}	1.975
26D			3.355	3.935	3.655	3.710	3.790	4.010	3.655	3.690	4.055	40.730	-0.321 ^{***}	2.600
51A				3.825	3.720	4.020	4.070	4.320	3.510	3.890	3.700	42.170	-0.177 ^{***}	3.220
27E					3.890	4.105	4.025	4.340	3.920	3.695	4.300	43.710	-0.023 ^{ns}	2.230
60E						4.385	4.355	3.810	3.945	4.190	3.980	43.340	-0.060 ^{ns}	2.270
35A							4.515	4.680	4.390	4.375	4.290	46.550	0.261 ^{***}	3.190
45E								4.480	4.240	4.130	3.720	45.660	0.172 ^{***}	3.155
61A									4.145	4.260	4.170	46.980	0.304 ^{***}	3.210
65A										3.970	4.135	43.820	-0.012 ^{ns}	2.930
28E											4.200	44.360	0.042 ^{ns}	2.540
21F												44.215	0.028 ^{ns}	3.135

Flies of each of 12 *smi* lines, with mean homozygous avoidance scores as given in the last column (ANHOLT *et al.* 1996), were crossed to flies of the remaining 11 lines. The parental *smi* lines are listed in the top row and first column. The arithmetic means of avoidance scores from 20 measurements are given for each hybrid cross. T_i is the sum of avoidance scores used to compute the *GCA* for each line. *GCA* is defined in the text. Avoidance scores of the parental homozygous *smi* lines (*HOM*) are given for comparison (ANHOLT *et al.* 1996). Avoidance scores for males and females of sexually dimorphic *smi* lines (*smi*21F, *smi*45E, *smi*51A, and *smi*97B; ANHOLT *et al.* 1996) are averaged, because no statistically significant sex-specific epistatic effects were observed for the transheterozygotes derived from these lines. ^{ns}*P* > 0.05, not significant; ^{**}0.001 < *P* < 0.01; ^{***}*P* < 0.0001.

TABLE 2

Analysis of variance of avoidance responses to benzaldehyde of transheterozygous *smi* lines

Source	d.f.	SS	F	P
Genotype	65	110.917	3.82	0.0001
Sex	1	4.983	11.15	0.0009
Genotype \times Sex	65	32.493	1.12	0.2457
Error	1188	530.695		

The analysis of variance of these data is given in Table 2. The differences in mean avoidance responses among the heterozygous genotypes were highly significant ($P = 0.0001$). There was also significant sexual dimorphism in avoidance response to benzaldehyde, averaged over all genotypes ($P = 0.0009$), with a mean male avoidance score of 4.1 and a mean female score of 3.9. Sexual dimorphism for olfactory avoidance response has been observed previously for homozygous *P*-element insertional mutations (ANHOLT *et al.* 1996) and among a sample of isogenic *X* and third chromosomes extracted from a natural population and substituted into the same inbred strain used for *P*-element mutagenesis (MACKAY *et al.* 1996). Interestingly, both the homozygous *P*-element insertions and the naturally occurring alleles affecting olfactory behavior had very large genotype \times sex interaction effects, indicating that there was variation in the magnitude of the sex dimorphism of effects among the homozygous genotypes. However, the genotype \times sex interaction was not significant for the double heterozygote genotypes; therefore, the sex-specific effects observed previously are on average recessive.

Variation among the transheterozygous genotypes can arise from two sources: variation in mean heterozygous effects of the different mutations, and variation from epistatic interactions. Because all *P*-element insertions are in the same inbred strain, all genetic variation among the genotypes is attributable to one of these two sources, with no confounding effects contributed by the background genotype. Classical diallel cross analysis enables us to separate heterozygous from epistatic effects by partitioning the variation among double heterozygous genotypes into their general (*GCA*) and specific (*SCA*) combining abilities. As mentioned above, the *GCA* of a mutation is an estimate of its mean heterozygous effect in the background of each of the other mutations. Estimates of the *GCA* of each *smi* mutation, expressed as deviations from the overall mean of the population of heterozygous genotypes, are given in Table 1. For comparison, also given in Table 1 are the mean avoidance scores of each *smi* mutation, at the same concentration of odorant used to assess transheterozygote olfactory behavior (HOM; ANHOLT *et al.* 1996). All homozygous *smi* mutations have reduced avoidance scores relative to the transheterozygotes.

TABLE 3

Analysis of variance of general and specific combining abilities of transheterozygous *smi* lines

Source	d.f.	SS	F	P
Sex	1	4.983	11.15	0.0009
<i>GCA</i>	11	71.189	14.49	<0.0001
<i>SCA</i>	54	39.728	1.65	0.0025
<i>GCA</i> \times Sex	11	2.711	0.55	0.87
<i>SCA</i> \times Sex	54	29.782	1.23	0.13
Error	1188	530.695		

Therefore, negative *GCA* effects reflect lower mean heterozygous avoidance scores and a more mutant heterozygous phenotype; conversely, positive *GCA* effects reflect higher than average mean heterozygous scores and a more wild-type phenotype. This variation in *GCA* among the *smi* mutations is highly significant ($P < 0.0001$, Table 3), and from this we can infer that all the *smi* mutations are not completely recessive.

The overall mean avoidance score of the transheterozygous genotypes, 3.99 ± 0.08 (Table 1), is significantly higher than that of the *Sam*; γ^{506} strain, 3.65 ± 0.08 (ANHOLT *et al.* 1996). Technically, this could be interpreted as overdominance for olfactory behavior. However, the selectable visible marker used in this system of *P*-element mutagenesis is γ^+ , and there is a concern that this marker has a direct effect on fitness and other quantitative traits relative to the γ^- mutant background of the control strain (LYMAN *et al.* 1996). For this reason, we cannot use these data to estimate *d*, the value of the heterozygote expressed as a deviation from the mean mutant and control strain value (FALCONER and MACKAY 1996) for each *smi* mutation. However, we can estimate the average degree of dominance of the *smi* mutations from the slope of the regression *b* of *GCA* on homozygous avoidance score of *smi* mutations, where each homozygous score is expressed as a deviation from the overall homozygous mutant mean. The estimate of the average degree of dominance *k* is $2(b - 0.5)$ (MACKAY *et al.* 1992; LYMAN *et al.* 1996), where *k* ranges from -1 (completely recessive mutations) through 0 (strict additivity) to 1 (completely dominant mutations). For these data, $b = 0.197$ ($0.01 < P < 0.05$) and $k = -0.605$. On average, the *smi* mutations are partially recessive.

The *SCA* of a pair of mutations reflects the extent to which the mean avoidance score of the double heterozygote, expressed as a deviation from the mean of the total population of heterozygous genotypes, departs from that expected given the sum of the *GCA*s of the two mutant parents. Typically, diallel crosses are made among inbred lines that each vary at a number of loci affecting the measured trait, and significant *SCA* effects can only be attributed to nonadditive interactions in general, including dominance and epistasis (FALCONER

TABLE 4
Estimates of specific combining abilities of
transheterozygous *smi* lines

Parent 1	Parent 2	SCA	P
<i>smi21F</i>	<i>smi26D</i>	0.354	0.009
<i>smi21F</i>	<i>smi27E</i>	0.301	0.026
<i>smi21F</i>	<i>smi45E</i>	-0.474	0.001
<i>smi21F</i>	<i>smi97B</i>	-0.369	0.006
<i>smi27E</i>	<i>smi26D</i>	0.284	0.036
<i>smi28E</i>	<i>smi27E</i>	-0.319	0.018
<i>smi51A</i>	<i>smi97B</i>	0.275	0.042
<i>smi61A</i>	<i>smi60E</i>	-0.429	0.002
<i>smi65A</i>	<i>smi51A</i>	-0.296	0.029

and MACKAY 1996). However, in this experimental design the genetic background has been standardized, and SCA interactions can only result from epistasis, *i.e.*, variation in heterozygous effects of a *smi* mutation depending on the genetic background with respect to other *smi* mutations.

We observed highly significant SCA effects ($P = 0.0025$, Table 3) for olfactory avoidance among the transheterozygote genotypes. This observation is not a scale effect. The effect of SCA was also highly significant if log, square root, and square transformations are applied to the data (data not shown). This suggests that epistatic interactions among loci affecting olfactory behavior are very common, because we have sampled only a small fraction of the total number of possible genotypes at 12 loci, each with two alleles ($66/1728 = 3.8\%$). To determine which interacting mutations contributed to the overall variation in SCA, we determined for which transheterozygote lines SCA effects are significantly different from zero. The results are given in Table 4. Nine transheterozygous crosses reveal statistically significant epistatic interactions between *smi* loci. In addition, the *smi98B/smi60E* transheterozygote has an SCA value (-0.251) that is nearly formally significant ($P = 0.063$). In five of the nine statistically significant cases, the difference between the observed and expected avoidance scores (SCA) is negative; *i.e.*, the avoidance response of the double heterozygote is more mutant than would be expected given the average degrees of dominance of both parents. In four cases, the SCA estimates were positive, indicating better olfactory responses of the hybrid offspring than expected from the average heterozygous effects of parental mutations. It should be noted that all of the transheterozygotes show avoidance scores within wild-type range, *i.e.*, complementation, but it is the quantitative analysis of the degree of complementation that reveals epistatic effects. The negative and positive interactions are quantitative genetic analogues of mutations that enhance or suppress, respectively, the effects of other mutations affecting the same phenotype.

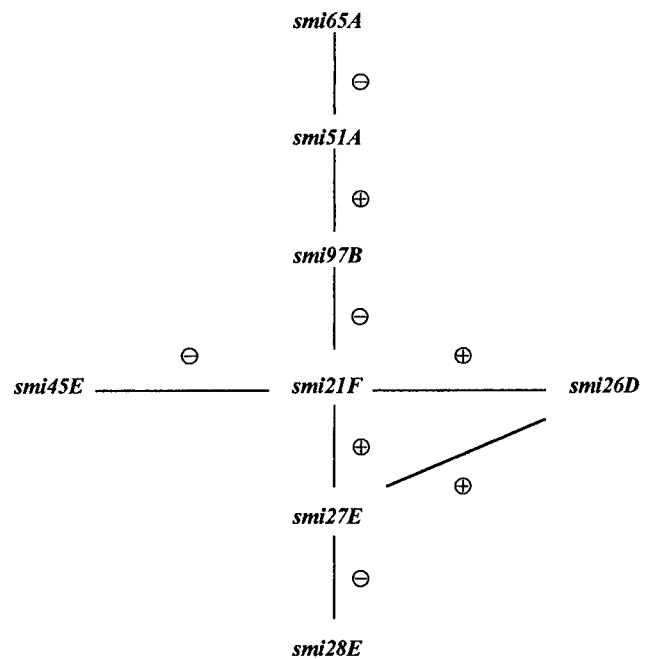


FIGURE 1.—Interaction diagram of *smi* loci. The ⊕ and ⊖ symbols indicate epistatic effects that suppress and enhance the homozygous mutant phenotype, respectively. Two loci, *smi60E* and *smi61A*, form an independent pair with a positive epistatic effect (not shown).

The observed epistatic effects are quite large; the mean of the absolute values of significant SCA effects is 0.34. This value is of the same magnitude as the mean of the absolute values of significant GCA effects (0.23), and is one-half of the environmental standard deviation. However, it is clear that these "large" quantitative effects are very subtle in absolute terms and cannot be discerned without quantitative genetic analysis of the phenotypes, or in variable genetic backgrounds. The magnitude of the epistatic effects are not necessarily correlated with the size of the homozygous mutant effects. *smi* loci with relatively small effects on olfactory behavior of homozygotes, *e.g.*, *smi21F* and *smi45E* (ANHOLT *et al.* 1996), produce large effects in double heterozygous progeny. We cannot, however, determine to what extent each locus of an interacting pair of loci contributes to the observed epistatic effect. Furthermore, we do not know to what extent the *P[ArB]* insertion limits the expression of the gene it affects. We predict, therefore, that epistatic effects will be stronger in double heterozygotes that contain null mutations, such as deletions, at the *smi* loci.

The pattern of interactions observed is interesting. Of the 12 *smi* loci, 10 interact with at least one other. Epistatic interactions between eight *smi* loci can be represented in a simple interaction diagram (Figure 1). *smi60E* and *smi61A* interact, but are independent of the others. It is possible that *smi98B* interacts with *smi60E* (the *P* value of the SCA is on the borderline of formal statistical significance), which would place 11 of the

12 *smi* genes in two interacting groups. It is somewhat surprising that the mutation that interacts most extensively with other *smi* mutants, *smi21F*, has itself very weak homozygous effects. The mutant phenotype of this gene is only apparent at a low concentration of benzaldehyde and is strongly sexually dimorphic (only females display aberrant olfactory responses; males are not significantly different from wild type) (ANHOLT *et al.* 1996). Yet it elicits strong interactions in transheterozygotes with four of the *smi* mutations, and in both sexes.

These loci represent only a small sample of the genes that affect olfactory behavior. The frequency with which *smi* lines were detected in our previous *P*-element mutagenesis screen indicated that ~4% of the *Drosophila* genome participates in shaping odor-guided behavior (ANHOLT *et al.* 1996), which corresponds to a conservative estimate of about 400 genes. Most likely, the ensemble of genes illustrated in Figure 1 is integrated into a more extensive network of interactions within the olfactory subgenome. Thus, loci that appear noninteractive, *i.e.*, *smi35A* and (possibly) *smi98B*, and loci that interact independently of the larger ensemble, *i.e.*, *smi60E* and *smi61A*, may prove to be part of a wider network of interacting genes once more olfactory genes are identified. Such extensive epistatic interactions between *smi* loci indicate that they form a complex network of genes that together shape odor-guided behavior.

In recent years, other investigators have identified olfactory mutants in *D. melanogaster*, mostly with mutations located on the X chromosome (VIHTELIC *et al.* 1993; WOODARD *et al.* 1992; RIESGO-ESCOVAR *et al.* 1995; LILLY and CARLSON 1989; LILLY *et al.* 1994a,b), but epistatic interactions among them and their effects on phenotypic variation have not been assessed. Our observations suggest that olfactory genes identified on the X chromosome might also interact within functional genetic networks and these possible interactions could also include the *smi* loci described here. However, different genetic backgrounds may render the detection of such epistatic effects more difficult than detection of epistasis among *smi* genes in a coisogenic background.

Because each of the *smi* genes used in this study is tagged by a *P*-element, it will, in principle, be possible in future studies to characterize their expression products and to obtain an understanding of the molecular basis for the observed genetic interactions. Moreover, our ability to use coisogenic *P*[*ArB*]-insertion lines for the characterization of networks of interacting genes in the olfactory subgenome will enable the future identification of new olfactory genes by virtue of epistatic interactions with known *smi* genes. Thus, these experiments pave the road for the use of quantitative genetic analysis of subtle phenotypes as a tool for targeted gene discovery.

We thank DR. RICHARD F. LYMAN for assistance in analyzing the data and J. BRANT HACKETT for technical assistance. This work was

supported by grants from the National Institutes of Health (DC-02485, GM-45344, and GM-45146) and the U.S. Army Research Office (DAAH04-96-1-0096).

LITERATURE CITED

- ACEVES-PIÑA, E., and W. QUINN, 1979 Learning in normal and mutant *Drosophila* larvae. *Science* **206**: 93–96.
- ANHOLT, R. R. H., 1993 Molecular neurobiology of olfaction. *Crit. Rev. Neurobiol.* **7**: 1–22.
- ANHOLT, R. R. H., R. F. LYMAN and T. F. C. MACKAY, 1996 Effects of single *P*-element insertions on olfactory behavior in *Drosophila melanogaster*. *Genetics* **143**: 293–301.
- AXEL, R., 1995 The molecular logic of smell. *Sci. Amer.* **273**: 154–159.
- AYER, R. K., and J. CARLSON, 1992 Olfactory physiology in the *Drosophila* antenna and maxillary palp: *acj6* distinguishes two classes of odorant pathways. *J. Neurobiol.* **23**: 965–982.
- BELOTE, J. M., M. B. MCKEOWN, D. J. ANDREW, T. N. SCOTT and B. S. BAKER, 1985 Control of sexual differentiation in *Drosophila melanogaster*. Cold Spring Harbor Symp. Quant. Biol. **50**: 605–614.
- BOTAS, J., J. M. DEL PRADO and A. GARCIA-BELLIDO, 1982 Gene-dose titration analysis in the search of trans-regulatory genes in *Drosophila*. *EMBO J.* **1**: 307–310.
- BUCK, L. B., 1996 Information coding in the olfactory system. *Annu. Rev. Neurosci.* **19**: 517–544.
- DAMBLY-CHAUDIERE, C., A. GHYSEN, L. Y. JAN and Y. N. JAN, 1988 The determination of sense organs in *Drosophila*: interaction of *scute* with *daughterless*. *Roux's Arch. Dev. Biol.* **197**: 419–423.
- FADOOL, D. A., and B. W. ACHE, 1992 Plasma membrane inositol-1,4,5-triphosphate-activated channels mediate signal transduction in lobster olfactory receptor neurons. *Neuron* **9**: 907–918.
- FALCONER, D. S., and T. F. C. MACKAY, 1996 *Introduction to Quantitative Genetics*, Ed. 4, Addison-Wesley Longman, Harlow, UK.
- GARCIA-BELLIDO, A., 1981 The bithorax syntagma, pp. 135–148 in *Advances in Genetics, Development and Evolution of Drosophila*, edited by S. LAKOVAARA. Plenum Press, NY.
- GRIFFING, B., 1956 Concept of general and specific combining ability in relation to diallel crossing systems. *Aust. J. Biol. Sci.* **9**: 463–493.
- HELFAND, S. L., and J. CARLSON, 1989 Isolation and characterization of an olfactory mutant in *Drosophila* with a chemically specific defect. *Proc. Natl. Acad. Sci. USA* **86**: 2908–2912.
- HOMYK, T., and C. P. EMERSON, 1988 Functional interactions between unlinked muscle genes within haploinsufficient regions of the *Drosophila* genome. *Genetics* **119**: 105–121.
- KENNISON, J. A., and M. A. RUSSELL, 1987 Dosage-dependent modifiers of homeotic mutations in *Drosophila melanogaster*. *Genetics* **116**: 75–86.
- LILLY, M., and J. CARLSON, 1989 *Smellblind*: a gene required for *Drosophila* olfaction. *Genetics* **124**: 293–302.
- LILLY, M., R. KREBER, B. GANETZKY and J. R. CARLSON, 1994a Evidence that the *Drosophila* olfactory mutant *smellblind* defines a novel class of sodium channel mutation. *Genetics* **136**: 1087–1096.
- LILLY, M., J. RIESGO-ESCOVAR and J. CARLSON, 1994b Developmental analysis of the *smellblind* mutants: evidence for the role of sodium channels in *Drosophila* development. *Dev. Biol.* **162**: 1–8.
- LONG, A. D., S. L. MULLANEY, T. F. C. MACKAY and C. H. LANGLEY, 1996 Genetic interactions between naturally occurring alleles at quantitative trait loci and mutant alleles at candidate loci affecting bristle number in *Drosophila melanogaster*. *Genetics* **144**: 1497–1518.
- LYMAN, R. F., F. LAWRENCE, S. NUZDZHIN and T. F. C. MACKAY, 1996 Effects of single *P*-element insertions on bristle number and viability in *Drosophila melanogaster*. *Genetics* **143**: 277–292.
- MACKAY, T. F. C., and J. D. FRY, 1996 Polygenic mutation in *Drosophila melanogaster*: genetic interactions between selection lines and candidate quantitative trait loci. *Genetics* **144**: 671–688.
- MACKAY, T. F. C., R. F. LYMAN and M. S. JACKSON, 1992 Effects of *P*-element insertions on quantitative traits in *Drosophila melanogaster*. *Genetics* **130**: 315–332.
- MACKAY, T. F. C., J. B. HACKETT, R. F. LYMAN, M. L. WAYNE and R. R. H. ANHOLT, 1996 Quantitative genetic variation of odor-guided behavior in a natural population of *Drosophila melanogaster*. *Genetics* **144**: 727–735.

- McKENNA, M., P. MONTE, S. HELFAND, C. WOODARD and J. CARLSON, 1989 A simple chemosensory response in *Drosophila* and the isolation of *acj* mutants in which it is affected. *Proc. Natl. Acad. Sci. USA* **86**: 8118–8122.
- RIESGO-ESCOVAR, J., D. RAHA and J. R. CARLSON, 1995 Requirement for a phospholipase C in odor response: overlap between olfaction and vision in *Drosophila*. *Proc. Natl. Acad. Sci. USA* **92**: 2864–2868.
- RODRIGUES, V., and O. SIDDIQI, 1978 Genetic analysis of chemosensory pathway. *Proc. Ind. Acad. Sci.* **87B**: 147–160.
- SAS INSTITUTE, INC., 1988 SAS/STAT User's Guide, Release 6.03 Edition, SAS Institute, Inc., Cary, NC.
- SCHAFER, H. E., and R. A. USANIS, 1969 *General least squares analysis of diallel experiments: a computer program—DIALL*. Genetics Department, North Carolina State University.
- SENGUPTA, P., J. C. CHOU and C. I. BARGMANN, 1996 *odr-10* encodes a seven transmembrane domain olfactory receptor required for responses to the odorant diacetyl. *Cell* **84**: 899–909.
- SPRAGUE, G. F., and L. A. TATUM, 1942 General *vs.* specific combining ability in single crosses of corn. *J. Amer. Soc. Agron.* **34**: 923–932.
- TRICOIRE, H., 1988 Dominant maternal interactions with *Drosophila* segmentation genes. *Roux's Arch. Dev. Biol.* **197**: 115–123.
- TROEMEL, E. R., J. H. CHOU, N. D. DWYER, H. A. COLBERT and C. I. BARGMANN, 1996 Divergent seven transmembrane receptors are candidate chemosensory receptors in *C. elegans*. *Cell* **83**: 207–218.
- VIHTELIC, TH. S., M. GOEBL, S. MILLIGAN, J. E. O'TOUSA and D. R. HYDE, 1993 Localization of *Drosophila retinal degeneration B*, a membrane-associated phosphatidylinositol transfer protein. *J. Cell Biol.* **122**: 1013–1022.
- WOODARD, C., E. ALCORTA and J. CARLSON, 1992 The *rdgB* gene in *Drosophila*: a link between vision and olfaction. *J. Neurogenetics* **8**: 17–32.

Communicating editor: L. PARTRIDGE

Molecular Evolution of Olfactomedin

Christa A. Karavanich and Robert R. H. Anholt

Department of Zoology, North Carolina State University

Olfactomedin is a secreted polymeric glycoprotein of unknown function, originally discovered at the mucociliary surface of the amphibian olfactory neuroepithelium and subsequently found throughout the mammalian brain. As a first step toward elucidating the function of olfactomedin, its phylogenetic history was examined to identify conserved structural motifs. Such conserved motifs may have functional significance and provide targets for future mutagenesis studies aimed at establishing the function of this protein. Previous studies revealed 33% amino acid sequence identity between rat and frog olfactomedins in their carboxyl terminal segments. Further analysis, however, reveals more extensive homologies throughout the molecule. Despite significant sequence divergence, cysteines essential for homopolymer formation such as the CXC motif near the amino terminus are conserved, as is the characteristic glycosylation pattern, suggesting that these posttranslational modifications are essential for function. Furthermore, evolutionary analysis of a region of 53 amino acids of fish, frog, rat, mouse, and human olfactomedins indicates that an ancestral olfactomedin gene arose before the evolution of terrestrial vertebrates and evolved independently in teleost, amphibian, and mammalian lineages. Indeed, a distant olfactomedin homolog was identified in *Caenorhabditis elegans*. Although the amino acid sequence of this invertebrate protein is longer and highly divergent compared with its vertebrate homologs, the protein from *C. elegans* shows remarkable similarities in terms of conserved motifs and posttranslational modification sites. Six universally conserved motifs were identified, and five of these are clustered in the carboxyl terminal half of the protein. Sequence comparisons indicate that evolution of the N-terminal half of the molecule involved extensive insertions and deletions; the C-terminal segment evolved mostly through point mutations, at least during vertebrate evolution. The widespread occurrence of olfactomedin among vertebrates and invertebrates underscores the notion that this protein has a function of universal importance. Furthermore, extensive modification of its N-terminal half and the acquisition of a C-terminal SDEL endoplasmic-reticulum-targeting sequence may have enabled olfactomedin to adopt new functions in the mammalian central nervous system.

Introduction

As genome-sequencing projects proceed at an unprecedented rate, increasing numbers of genes that encode proteins of unknown function are being discovered. These include a host of orphan receptors, transcription factors and proteins of which the functions are open to conjecture. Uncovering the functions of many of these novel gene products would increase our understanding and may change our current views of many cellular and intercellular processes. Evolutionary analysis is of value in this endeavor, since it can reveal conserved motifs throughout the phylogenetic history of a protein, thereby providing insights into its potential function or, at the very least, identifying domains as targets for future molecular studies, such as site-directed mutagenesis studies, to evaluate structure–function relationships. Here, we report a study on the molecular evolution of olfactomedin, an extracellular matrix protein of yet unknown function, thought to play an important role in olfaction, neurosecretion, and neural development.

The discovery of olfactomedin resulted from studies aimed at the identification of novel proteins involved in olfaction. A library of monoclonal antibodies was raised against chemosensory cilia from the frog (*Rana catesbeiana*) to find antigens uniquely associated with olfactory membranes (Anholt, Petro, and Rivers 1990). A group of polypeptides that met this criterion appeared

to consist of monomeric, dimeric, and polymeric forms of the same protein, which was named “olfactomedin” (Snyder et al. 1991). Immunohistochemical studies showed that olfactomedin is synthesized in Bowman’s glands and sustentacular cells of the olfactory epithelium and is secreted into the viscous lower mucus layer that surrounds the apical dendrites of olfactory neurons (Snyder et al. 1991; Bal and Anholt 1993). In the frog, olfactomedin immunoreactivity was not detected in olfactory nerve membranes, nonchemosensory cilia from respiratory epithelium, or membranes from brain, heart, kidney, or lung (Anholt, Petro, and Rivers 1990). Subsequently, molecular cloning of olfactomedin showed its amino acid sequence to have no homologies to any other known protein (Yokoe and Anholt 1993).

Based on the sequence of the mature polypeptide (448 amino acids), together with previous biochemical and immunohistochemical observations, a structural model was proposed in which cysteines at positions 160, 177, 283, and 290 form intramolecular disulfide bonds dividing the molecule into central “head” and “neck” loops and two “legs” of similar length. The N-terminal leg contains two nearby cysteines, each forming disulfide bonds with an adjacent olfactomedin molecule. An additional disulfide bond is made by cysteine 377 on the C-terminal leg, creating large polymers that constitute the architecture of the extracellular matrix of the chemosensory interface of the olfactory epithelium (Yokoe and Anholt 1993). Olfactomedin contains six potential N-linked glycosylation sites scattered throughout its sequence, and all of them carry carbohydrate moieties (Bal and Anholt 1993).

Despite a wealth of structural information, the function of olfactomedin remains unknown. By analogy

Key words: olfactomedin, molecular evolution, olfaction, neurogenesis, neural development, extracellular matrix.

Address for correspondence and reprints: Robert R. H. Anholt, Department of Zoology, Box 7617, North Carolina State University, Raleigh, North Carolina 27695-7617. E-mail: anholt@ncsu.edu.

Mol. Biol. Evol. 15(6):718–726. 1998

© 1998 by the Society for Molecular Biology and Evolution. ISSN: 0737-4038

to functions of other extracellular matrix proteins of the nervous system, it was proposed that olfactomedin might play a neurotropic role during development of the apical olfactory dendrite (Yokoe and Anholt 1993). Adult olfactory neurons undergo continuous replacement from a population of neurogenic stem cells (Graziadei and Monti-Graziadei 1978, 1979; Farbman 1990; Calof et al. 1996). Whereas questions about axon sorting during formation of the primary olfactory projection have received considerable interest (Ngai et al. 1993; Vassar et al. 1994; Mombaerts et al. 1996), little attention has been paid to neurotropic signals that induce differentiation of the apical dendrite to form a knob with chemosensory cilia that mediate odor recognition and olfactory transduction (reviewed by Firestein 1991; Anholt 1993; Axel 1995; Buck 1996). The existence of such signals is inferred from the necessity of a nascent dendrite in vivo to sense its arrival at the mucociliary surface and the failure of isolated olfactory neurons in long-term cell cultures to develop ciliated dendritic knobs (Calof and Chikaraishi 1989; Ronnett, Hester, and Snyder 1991; Calof et al., 1996). It has been estimated that olfactomedin makes up 5% of the total tissue protein in membrane homogenates from frog olfactory tissue (Bal and Anholt 1993). As a prominent component of the extracellular mucus matrix, olfactomedin would be in an ideal position to deliver such a dendritic differentiation signal.

The hypothesis that olfactomedin might play a role in neuronal growth and differentiation received support from the subsequent discovery of an olfactomedin homolog in the mammalian brain. In the rat central nervous system, Danielson et al. (1994) discovered four glycoproteins, splice variants encoded by a single gene, that are expressed throughout the brain and in neuroendocrine tissues such as the anterior pituitary and adrenal glands. Based on in situ hybridization patterns, they concluded that these glycoproteins are produced by neurons. They further observed that the longest of these glycoproteins (the AMZ protein) shares 33% sequence identity at its carboxyl terminal end with the carboxyl terminal half of frog olfactomedin. Using the rat AMZ protein as a probe, we identified an olfactomedin homolog from a mouse olfactory cDNA library. Examination of the GenBank database revealed additional homologs: an open reading frame from a cosmid (Wilson et al. 1994) of *Caenorhabditis elegans*, as well as partial cDNA sequences from fish pituitary and human brain libraries. To set the stage for studies aimed at elucidating the function of olfactomedin, sequences of all known olfactomedin homologs were examined to identify conserved motifs.

This paper reports that sequence homologies between the amphibian protein and its rodent counterparts are far more extensive than previously appreciated (Danielson et al. 1994) and not only cover the C-terminal region, but extend throughout the entire molecule. Furthermore, identification of a distant olfactomedin relative in *C. elegans* and sequence comparisons among vertebrate olfactomedins indicate one highly conserved motif near the amino terminus and five conserved domains

in the carboxyl terminal half of the protein. Evolution of the N-terminal half of olfactomedin is characterized by large insertions of amino acids, in sharp contrast to the C-terminal half, which shows greater sequence conservation, suggesting that this extracellular protein may have acquired new functions during its evolution.

Methods

The following olfactomedin amino acid sequences were analyzed (GenBank accession numbers appear in parentheses): the sequence of frog (*Rana catesbeiana*) olfactomedin obtained from an olfactory cDNA clone (L13595; Yokoe and Anholt 1993); the sequence of the rat (*Rattus norvegicus*) AMZ protein, an olfactomedin homolog identified from brain cDNA (U03416; Danielson et al. 1994); the translated partial sequence of an olfactomedin homolog from halibut (*Hippoglossus hippoglossus*) pituitary (T23140, unpublished sequence, Zhiyuan Gong, National University of Singapore, 1994); the translated partial sequence of a human (*Homo sapiens*) olfactomedin homolog from an infant brain cDNA library (H10467; unpublished sequence, Hillier et al., the Washington University Merck EST Project, 1995); and the sequence of an olfactomedin homolog from *C. elegans* (Z81499; coding sequence in cosmid F11C3, Nematode Sequencing Project; Wilson et al. 1994).

A probe corresponding to the carboxyl terminal region of the rat AMZ protein, kindly donated by Dr. Patria Danielson (The Scripps Research Institute, La Jolla, Calif.), was used to screen a mouse olfactory cDNA library constructed in Lambda ZAPII (Stratagene, La Jolla, Calif.). Standard molecular biological procedures were performed as described by Sambrook, Fritsch, and Maniatis (1989). A clone with a full-length open reading frame was isolated and sequenced at the DNA Sequencing Facility of Iowa State University (Ames, Iowa).

Carboxyl terminal sequence homologies between amphibian and rodent olfactomedins were identified with the BLAST program (Altschul et al. 1990), and their alignment was verified by eye. To enable a comparison between vertebrate olfactomedins and a longer, distant homolog from *C. elegans*, sequences were scaled to 100% of their lengths. The relative positions of conserved sequence motifs and posttranslational modification sites were then placed along linear maps of the scaled sequences. Consensus glycosylation sites and leader sequences were verified with the PC/Gene program from IntelliGenetics, Inc. (Mountain View, Calif.). Aligned sequences were analyzed with the Molecular Evolutionary Genetics Analysis program, version 1.02 (Kumar, Tamura, and Nei 1993).

Results

Figure 1 shows the alignment of the complete amino acid sequences of frog olfactomedin and its rat homolog. Previously, Danielson et al. (1994) observed 33% sequence identity between the carboxyl terminal regions of frog olfactomedin and the rat AMZ protein. Reexamination of sequence homologies between these sequences indicates that homology between these pro-

motif near the amino terminus are conserved. These cysteines form neighboring disulfides with an adjacent olfactomedin molecule creating a stable homodimer (Snyder et al. 1991; Yokoe and Anholt 1993). A cysteine on the opposite carboxyl terminal leg is also conserved and is responsible for linking the homodimers together as polymers (Snyder et al. 1991; Yokoe and Anholt 1993). The glycosylation pattern also appears to be highly conserved. Carbohydrate moieties 2, 3, 5, and 6 of frog olfactomedin (fig. 2A) are found in the same or similar locations in the rodent homolog, corresponding to I, II, III, and V, respectively (fig. 2B). Moreover, folding of

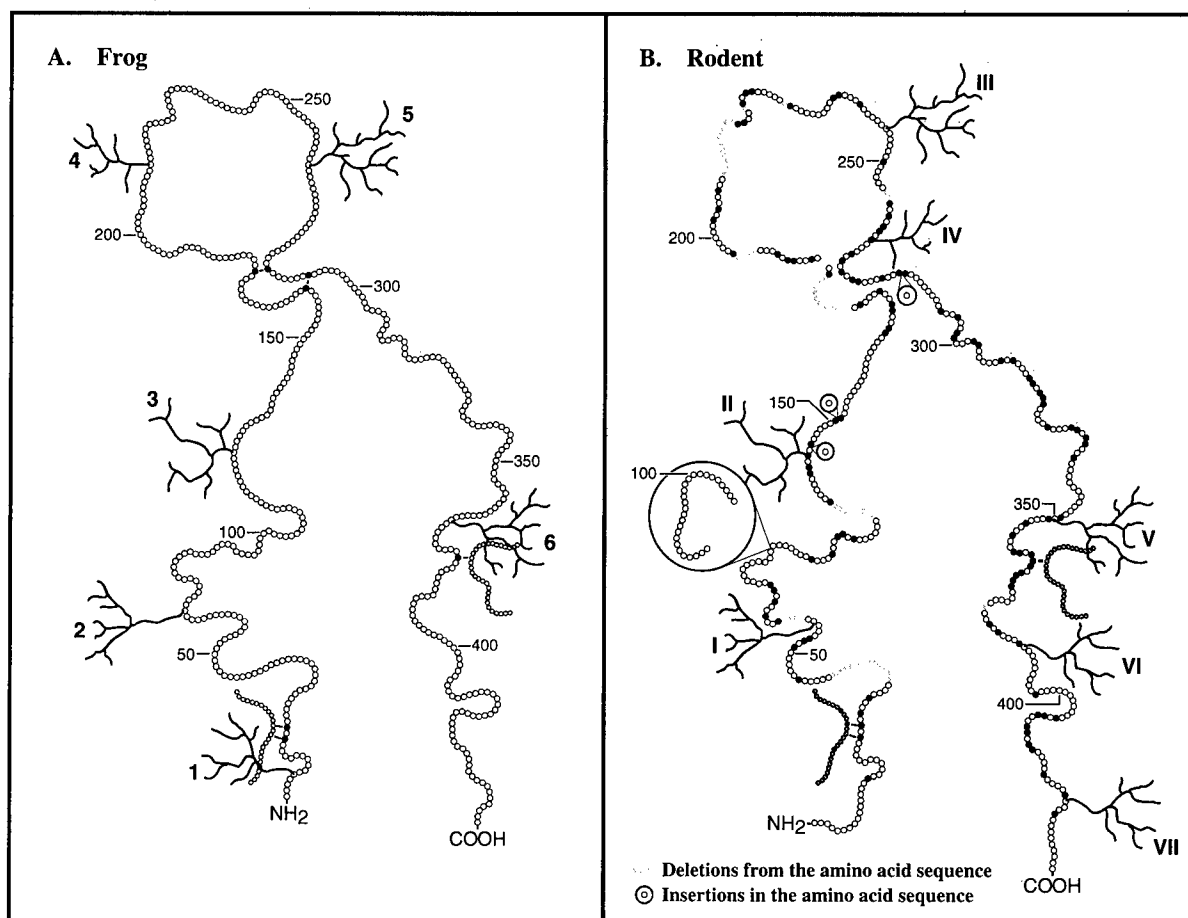


FIG. 2.—Diagrammatic representation of frog olfactomedin (A) and its rodent homolog (B). Amino acids are represented as circles. Closed circles in B indicate amino acid identities with corresponding residues in panel A. Carbohydrate moieties are numbered with Arabic numerals in A and with Roman numerals in B. Optimal alignment was achieved by the introduction of gaps in the sequences, which are illustrated as sequence deletions and insertions in B.

the head region of olfactomedin back on itself across the central axis of the molecule would superimpose carbohydrate moiety 4 in figure 2A on moiety IV in figure 2B. Similarly, intertwining of the amino terminal and carboxyl terminal legs would make the positions of carbohydrate moieties 1 (fig. 1A) and VI and/or VII (fig. 1B) comparable. Thus, despite considerable sequence divergence between frog and rodent olfactomedins, post-translational modifications that enable the formation of disulfide-linked polymers with distinct glycosylation patterns are accurately preserved. In contrast, intramolecular disulfides of frog olfactomedin that generate the head and neck domains are absent from the mammalian homolog, suggesting that these disulfides are not essential, although they may help stabilize the conformation of amphibian olfactomedin.

To verify that olfactomedin in the rodent, as in the frog, is also expressed in olfactory tissue, a cDNA clone encoding olfactomedin was isolated from a mouse olfactory cDNA library. Sequence analysis of this clone revealed that it is closely related to the rat AMZ protein, showing 99.1% amino acid sequence identity. Of 40 nucleotide substitutions between rat and mouse, 36 are in silent third codon positions. Only four amino acids were

different between rat and mouse olfactomedin, at positions 106, 183, 302, and 402 (using the numbering for the rat sequence shown in fig. 1). At these positions, the mouse sequence has threonine, serine, methionine, and arginine, respectively.

To extend our analysis of the evolution of olfactomedin, partial sequences from fish, human, rat, and frog olfactomedin were aligned. Sequence information about the region corresponding to residues 293 and 343 of frog olfactomedin (Yokoe and Anholt 1993) is available for all five species. Sequence alignments of this region are shown in figure 3, and the percentages of sequence identities between these sequences are presented in table 1. Within this region, seven invariant amino acid residues are evident, including hydrophobic residues leu²⁹⁵, leu³⁰⁶, and ala³⁰⁹ and a cluster of negatively charged residues between positions 324 and 331 forming the motif DXDXXXDE, in which X is apolar (numbering is according to the frog olfactomedin sequence). The occurrence of this invariant cluster of negatively charged residues in all four vertebrate species suggests that it may play an important structural and/or functional role.

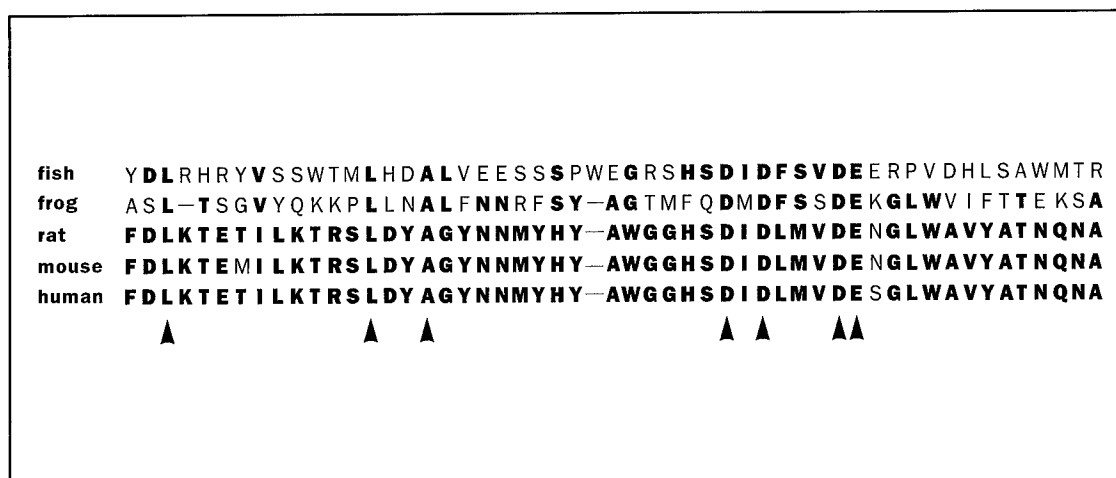


FIG. 3.—Amino acid sequence alignments of overlapping segments from partial sequences of fish, frog, rat, mouse, and human olfactomedins. The sequences were aligned by eye to maximize amino acid identities. Identical amino acids are highlighted in bold print. Percentages of amino acid identities for these sequences are listed in table 1. Invariant amino acid residues are placed against a shaded background and indicated by arrowheads.

Amino acid conservation between frog and fish is no greater than that between frog and rat, showing 24.5% and 32.7% sequence identities, respectively (table 1). In contrast, human and rat olfactomedins are closely related, showing 98.1% identity over this region and 96.8% identity when compared over a longer sequence including an additional 71 amino acids toward the carboxyl terminus. When nucleotide differences between rat and human olfactomedin cDNAs are analyzed, 51 base substitutions are found within a sequence of 373 nucleotides. Of these substitutions, 82% occur in third codon positions and do not alter the amino acid sequence.

Evolutionary distances at the DNA level were estimated for the sequences in figure 3 based on the two-parameter maximum-likelihood model of Kimura (1980), removing gap sites only in pairwise comparisons. Poisson-corrected amino acid substitutions were used to estimate evolutionary distances at the protein level. Rates of evolution calculated as nonsynonymous amino acid substitutions per site per 10^9 years are presented in table 2. At the amino acid level, there are no statistically significant differences between evolutionary rates between teleosts and amphibia or between teleosts and mammals. From Table 2, we calculate that the evolutionary rate between fish and frog is 0.004%/Myr,

compared to 0.0015%/Myr for the evolutionary rate between rat and human. This suggests that evolution of the protein within the mammalian lineage has slowed during the last 80 Myr. However, it is not clear whether these differences in evolutionary rates are significant, since we are not able, at present, to distinguish between orthologous and paralogous relationships among olfactomedins.

Our data suggest that vertebrate olfactomedins evolved from an ancestral gene that predates the evolution of terrestrial vertebrates about 400 MYA (table 1). The analysis presented in table 1 led us to hypothesize that olfactomedin homologs may also occur in invertebrates. Indeed, a search through the GenBank database revealed a coding sequence of *C. elegans* that encodes a distant homolog of the vertebrate olfactomedins. This gene encodes a protein of 654 amino acids, 30% longer than the vertebrate olfactomedins. To identify conserved features between vertebrate olfactomedins and their nematode homolog, amino acid sequences of each species were scaled to 100%, and conserved motifs, sulfhydryls, and glycosylation sites were

Table 1
Sequence Identities Among Teleost, Amphibian, and Mammalian Olfactomedins

	Fish	Frog	Rat	Mouse	Human
Fish.....	—	24.5	22.6	22.6	22.6
Frog.....	412	—	32.7	32.7	32.7
Rat.....	412	345	—	99.1	98.1
Mouse....	412	345	10	—	98.1
Human...	412	345	80	80	—

NOTE.—Numbers in the table in the upper right matrix indicate the percentage of amino acid sequence identity calculated for the partial sequences shown in figure 3. Numbers in the lower left matrix indicate estimated times since divergence (MYA; Graybeal 1994).

Table 2
Rates of Nonsynonymous Substitutions During the Evolution of Olfactomedin

Species Compared	Time Since Divergence (MYA)	Kimura Two-Parameter Model	Poisson-Corrected Amino Acid Substitutions
Fish and frog.....	412	0.46 ± 0.08	1.66 ± 0.29
Fish and rat.....	412	1.07 ± 0.18	1.78 ± 0.31
Rat and Human...	80	0.64 ± 0.17	0.12 ± 0.12

NOTE.—Evolutionary rates are calculated in units of substitutions/site per 10^9 years. Data presented are based on a comparison of 53 codons and are arithmetic means ± standard errors. Nonsynonymous nucleotide substitution rates were estimated using the model of Kimura (1980).

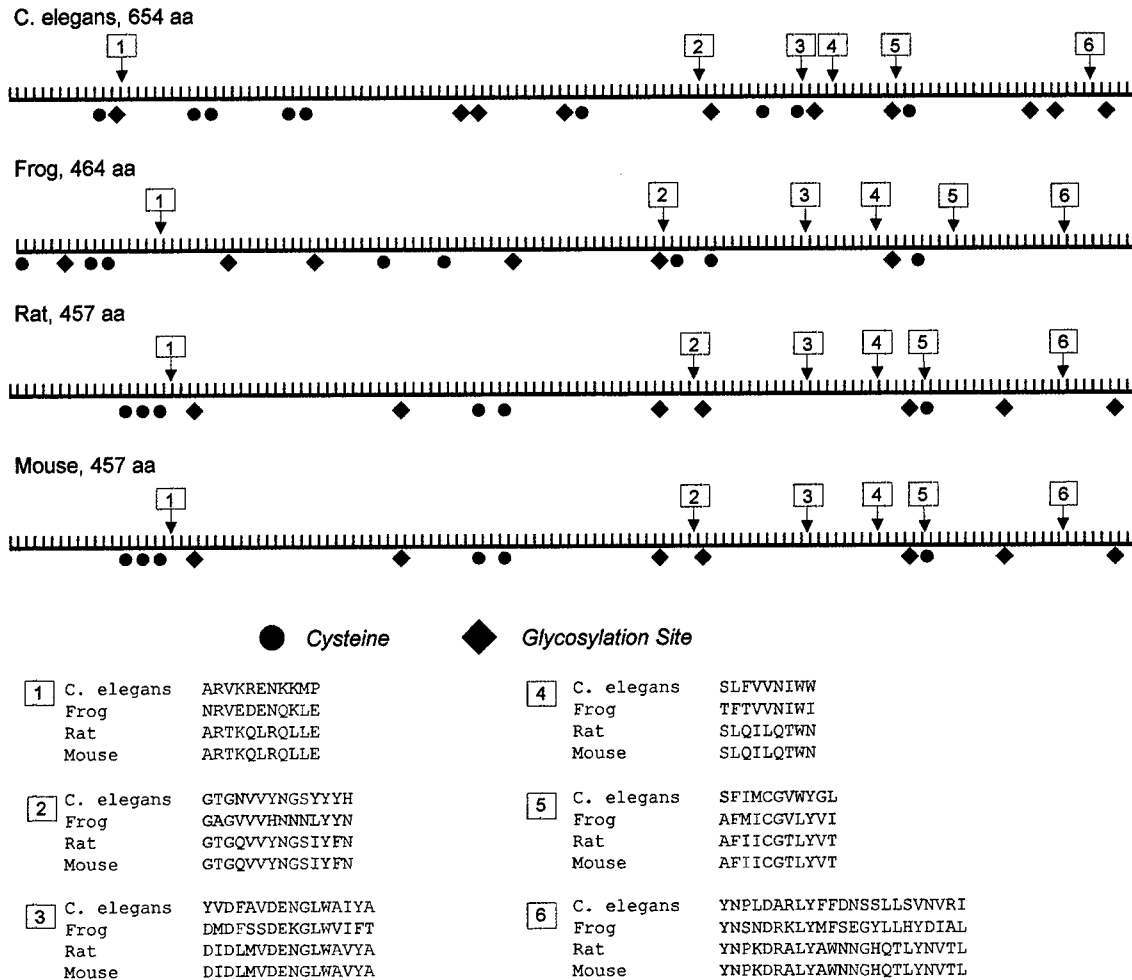


FIG. 4.—Relative alignments of the amino acid sequences of *Caenorhabditis elegans*, frog, rat, and mouse olfactomedins. To accommodate the varying lengths of the amino acid sequences, they were standardized to a scale of 100% of their lengths for each species. Relative locations of cysteines are shown as red circles, and glycosylation sites are shown as blue diamonds. Markers 1–6 indicate areas of highly conserved sequences which are identified below the diagrams. Rat and mouse sequences are identical for all of these conserved motifs. Amino acids shown in green are identical for all four species. Amino acids shown in magenta are the same among three of the four species examined.

mapped to the scaled sequences (fig. 4). Six highly conserved sequence motifs were identified at similar relative locations. One conserved motif occurs near the N-terminus, and the other five are clustered in the C-terminal half of the protein. The DXDXXXDE motif described above is contained in conserved motif 3 and is also present in *C. elegans*. The *C. elegans* protein has 10 potential N-linked glycosylation sites, evenly spaced throughout the molecule as is the case for vertebrate olfactomedins. Glycosylation sites near motifs 2, 5, and 6 occur at similar relative locations in mammalian olfactomedins and the protein from *C. elegans* (fig. 4). Similarly, a single N-terminal CXC motif is apparent for the *C. elegans* homolog, as is a highly conserved sulfhydryl in conserved motif 5, proposed to participate in the formation of homopolymers (Yokoe and Anholt 1993). Thus, despite considerable sequence diversity and difference in polypeptide length, the structural organization of this invertebrate olfactomedin shows remarkable similarities to those of its vertebrate homologs.

Discussion

We investigated evolutionary relationships among vertebrate olfactomedins by comparing the sequences of fish, frog, rat, mouse, and human olfactomedins. Despite considerable amino acid sequence divergence between frog and rat, we identified several invariant motifs, including the CXC motif on the amino terminal leg and a cysteine on the C-terminal leg for the formation of homopolymers, and NX(T/S) consensus glycosylation sites that preserve a distinct pattern of glycosylation (figs. 1 and 2; Bal and Anholt 1993; Yokoe and Anholt 1993). The evolution of olfactomedin within the mammalian lineage appears to be subject to a strong evolutionary pressure toward conservation of primary structure. Since we cannot, at present, discriminate paralogous genes from orthologous genes, it is difficult to draw solid conclusions regarding evolutionary constraints from calculations of evolutionary rates. Nonetheless, a constant rate of substitutions would predict approximately 14% amino acid sequence divergence between human and ro-

dent olfactomedins. Instead, only 2% divergence is observed, with the vast majority of nucleotide substitutions occurring in silent third codon positions. Invariant structural motifs, such as the six motifs identified in figure 4, the CXC sequence, the conserved sulfhydryl in the carboxyl terminal leg, and the glycosylation pattern, are likely to be functionally important and can serve as foci for future studies exploring structure/function relationships.

Evolutionary analysis indicated that an ancestral olfactomedin gene arose before the evolution of terrestrial vertebrates and proceeded to evolve independently in teleost, amphibian, and mammalian lineages. Indeed, a distant homolog of olfactomedin was identified in *C. elegans*. The overall amino acid sequence of this invertebrate protein was longer and highly divergent compared with its vertebrate homologs. Conserved motifs, however, could be identified and mapped relative to the length of the polypeptide (fig. 4). This analysis revealed that the protein from *C. elegans* shows remarkable similarities in terms of conserved motifs and posttranslational modification sites. Most of the conserved motifs occur in the carboxyl terminal half of the protein, in line with the strong homology observed in this region between frog and rat olfactomedins (Danielson et al. 1994). Thus, it appears that the N-terminal half of the molecule has undergone more rapid evolution, characterized by insertions and deletions, than the C-terminal region, which evolved slower, mostly through point mutations, at least during vertebrate evolution. As discussed below, it is conceivable that evolution of the N-terminal half of olfactomedin may have enabled the acquisition of new functions. The identification of an olfactomedin homolog in *C. elegans* predicts that a similar protein may also exist in *Drosophila melanogaster*. The identification of olfactomedin in model organisms that can be readily manipulated genetically can accelerate investigations of its function.

In addition to structural similarities, amphibian and mammalian olfactomedins also show differences. Cysteines at positions 283 and 290 of frog olfactomedin, which form intramolecular disulfides to create the proposed head and neck regions (Yokoe and Anholt 1993), are missing in its mammalian homolog. This indicates either that the proposed positions of intramolecular disulfides in the frog molecule have to be reevaluated or that these intramolecular disulfide bonds are not a priori essential for the functional conformation of olfactomedin. Furthermore, the endoplasmic reticulum targeting sequence SDEL at the carboxyl terminus of rat olfactomedin does not occur in the protein from frog. This suggests either that secretion of amphibian olfactomedin is controlled by different, as yet unidentified, targeting sequences within the molecule, or simply that the polypeptide is secreted via a default pathway which does not need to be specified by an intracellular trafficking signal.

Previous studies have shown that mammalian olfactomedin occurs throughout the central nervous system (CNS) and in neuroendocrine glands, such as the anterior pituitary and adrenal glands (Danielson et al. 1994). Sustentacular cells of the olfactory neuroepithel-

ium and Bowman's glands, which are the source of frog olfactomedin (Snyder et al. 1991; Bal and Anholt 1993), are also derived from neural ectoderm. The close association of olfactomedin with chemosensory dendritic endings of olfactory neurons (Snyder et al. 1991; Bal and Anholt 1993), as mentioned earlier, suggests that olfactomedin exerts a neurotrophic or neurotropic effect on these neurons. It is of interest to note that, thus far, olfactomedin homologs have been found in CNS neurons only in mammalian species (Danielson et al. 1994). The fish homolog was identified from halibut pituitary cDNA, and frog olfactomedin has been found only in olfactory tissue (Anholt, Petro, and Rivers 1990; Snyder et al. 1991; Yokoe and Anholt 1993). The expression pattern of the olfactomedin homolog in *C. elegans* remains to be determined.

Recently, the trabecular-meshwork-inducible glucocorticoid response gene (TIGR) in the eye was shown to contain olfactomedin homology domains. Mutations in these olfactomedin-related domains of TIGR correlate closely with a large fraction of cases of primary open-angle glaucoma, a leading cause of blindness and a disease that strikes 1 out of every 100 individuals over the age of 40 years (Adam et al. 1997; Polanski et al. 1997; Stone et al. 1997). Like olfactomedin, this protein is associated with ciliary structures, i.e., the ciliary rootlet in the rod photoreceptor cell (Kubota et al. 1997). It is therefore possible that the conserved motifs which we identified (fig. 4) may occur in families of related proteins. A complete characterization of the many proteins that contain olfactomedin homology domains in the species examined in this paper will be needed to construct a more accurate phylogenetic history and to determine unambiguously whether the olfactomedins we analyzed are encoded by orthologous or, possibly, paralogous genes.

Failure of immunochemical studies to detect olfactomedin in frog brain tissue may be due to tissue-specific glycosylation and the fact that unique carbohydrate moieties dominate the immunogenicity of olfactomedin (Anholt, Petro, and Rivers 1990; Snyder et al. 1991). Olfactomedin is produced in vast quantities in frog olfactory tissue, representing approximately 5% of total tissue protein (Snyder et al. 1991). Thus, it is possible, although unlikely, that the failure to detect olfactomedin mRNA in frog brain previously by northern blotting (Yokoe and Anholt 1993) may have been due to insufficient exposure of the blots because of the great abundance and easy detection of olfactomedin message in olfactory tissue. A more plausible possibility, however, is that in teleosts and amphibia, olfactomedin might fulfill a function restricted only to neurosecretory tissues, but that during evolution of the mammalian brain, olfactomedin acquired a broader function, utilized also by the nervous system. The expression of olfactomedin in neurons would necessitate the acquisition of the SDEL intracellular trafficking signal, and consolidation of a new neural function would constrain its mutation rate. Preservation of the characteristic carbohydrate groups and the sulfhydryls that are essential for polymerization indicates that these posttranslational modifications are

essential for functional integrity. The functions of the six conserved motifs remain unknown. One possibility is that they may be necessary for protein-protein interactions either with other proteins or with adjacent olfactomedin molecules of the homooligomeric array.

The hypothesis that olfactomedin could perform multiple functions in neural and neuroendocrine tissues gains some support from the existence of splice variants (Danielson et al. 1994). In the rat brain, olfactomedin can be expressed as either a full-length (Z) or a truncated (Y) form. Whereas each of these forms share the same core region (M), they can be coupled to either one of two different amino termini, mostly encoding leader peptide sequences (A and B). Thus, differential splicing gives rise to four splice variants (Danielson et al. 1994). Two different leader peptides have also been observed for frog olfactomedin (Yokoe and Anholt 1993). The significance of differences in leader peptide is not clear, but may bear on translational control or intracellular trafficking. Interestingly, in the rat pituitary gland, only the A form has been observed, whereas in the adrenal gland, only the B form is found (Danielson et al. 1994). The truncated forms of olfactomedin are especially intriguing in that they contain the CXC motif essential for the formation of olfactomedin dimers but lack several of the conserved motifs in the carboxyl terminal region of the molecule, including the sulfhydryl group that mediates the formation of oligomers. The coexpression of truncated and full-length forms of olfactomedin in the mammalian brain lends credence to the notion that different functions could be associated with the amino terminal and carboxyl terminal segments of the protein.

First identified in frog olfactory mucus, it is now clear that olfactomedin occurs universally and is widely expressed in the mammalian brain. The evolutionary analysis presented in this paper has delineated several conserved motifs as targets for future functional studies on this intriguing newly discovered extracellular matrix protein.

Acknowledgments

The authors would like to thank Dr. Patria Danielson for providing probes corresponding to the carboxyl terminal segment of the rat AMZ protein and Nalini Kulkarni for isolating an olfactomedin-encoding cDNA from a mouse olfactory cDNA library. Dr. Trudy F. C. Mackay and members of the North Carolina State University Molecular Evolution Group, including Drs. Jeffrey L. Thorne, Marta L. Wayne, Michael Purugganan, and Brian M. Wiegmann, are gratefully acknowledged for their critical reading of the manuscript and their many helpful discussions and suggestions. The authors would also like to thank two anonymous reviewers for providing valuable critiques of this paper and, in particular, for directing the authors toward the sequence of olfactomedin in *C. elegans*. This work was supported by grants from the National Institutes of Health (DC-02485), the U.S. Army Research Office (DAAH04-96-I-0096), and the North Carolina Biotechnology Center (9605-ARG-0015).

LITERATURE CITED

- ADAM, M. F., A. BELMOUDEN, P. BINISTI et al. (12 co-authors). 1997. Recurrent mutations in a single exon encoding the evolutionary conserved olfactomedin-homology domain of TIGR in familial open-angle glaucoma. *Hum. Mol. Genet.* **6**:2091-2097.
- ALTSCHUL, S. F., W. MILLER, E. W. MYERS, and D. J. LIPMAN. 1990. Basic local alignment search tool. *J. Mol. Biol.* **215**: 403-410.
- ANHOLT, R. R. H. 1993. Molecular neurobiology of olfaction. *Crit. Rev. Neurobiol.* **7**:1-22.
- ANHOLT, R. R. H., A. E. PETRO, and A. M. RIVERS. 1990. Identification of a group of novel membrane proteins unique to chemosensory cilia of olfactory receptor cells. *Biochemistry* **29**:3366-3373.
- AXEL, R. 1995. The molecular logic of smell. *Sci. Am.* **273**: 154-159.
- BAL, R. S., and R. R. H. ANHOLT. 1993. Formation of the extracellular mucous matrix of olfactory neuroepithelium: identification of partially and non-glycosylated precursors of olfactomedin. *Biochemistry* **32**:1047-1053.
- BUCK, L. B. 1996. Information coding in the olfactory system. *Annu. Rev. Neurosci.* **19**:517-544.
- CALOF, A. L., and D. M. CHIKARAISHI. 1989. Analysis of neurogenesis in a mammalian neuroepithelium: proliferation and differentiation of an olfactory neuron precursor in vitro. *Neuron* **3**:115-127.
- CALOF, A. L., N. HAGIWARA, J. D. HOLCOMB, J. S. MUMM, and J. SHOU. 1996. Neurogenesis and cell death in olfactory epithelium. *J. Neurobiol.* **30**:67-81.
- DANIELSON, P. E., S. FORSS-PETTER, E. L. F. BATTENBERG, L. DELECEA, F. E. BLOOM, and J. G. SUTCLIFFE. 1994. Four structurally distinct neuron-specific olfactomedin-related glycoproteins produced by differential promoter utilization and alternative mRNA splicing from a single gene. *J. Neurosci. Res.* **38**:468-478.
- FARBMAN, A. I. 1990. Olfactory neurogenesis: genetic or environmental controls? *Trends Neurosci.* **13**:362-365.
- FIRESTEIN, S. 1991. A noseful of odor receptors. *Trends Neurosci.* **14**:270-272.
- GRAYBEAL, A. 1994. Evaluating the phylogenetic utility of genes: a search for genes informative about deep divergences among vertebrates. *Syst. Biol.* **43**:174-191.
- GRAZIADEI, P. P. C., and G. A. MONTI-GRAZIADEI. 1978. Continuous nerve cell renewal in the olfactory system. Pp. 55-58 in M. JACOBSON, ed. *Handbook of sensory physiology*, Vol. IX. Development of sensory systems. Springer-Verlag, New York.
- . 1979. Neurogenesis and neuron regeneration in the olfactory system of mammals. I. Morphological aspects of differentiation and structural organization of the olfactory sensory neurons. *J. Neurocytol.* **8**:1-18.
- KIMURA, M. 1980. A simple method for estimating evolutionary rates of base substitutions through comparative studies of nucleotide sequences. *J. Mol. Evol.* **16**:111-120.
- KUBOTA, R., S. NODA, Y. WANG, S. MINOSHIMA, S. ASAKAWA, J. KUDOH, Y. MASIMA, Y. OGUCHI, and N. SHIMIZU. 1997. A novel myosin-like protein (myocilin) expressed in the connecting cilium of the photoreceptor: molecular cloning, tissue expression and chromosomal mapping. *Genomics* **41**: 360-369.
- KUMAR, S., K. TAMURA, and M. NEI. 1993. MEGA: molecular evolutionary genetic analysis. Version 1.0. The Pennsylvania State University, University Park.

- MOMBAERTS, P., F. WANG, C. DULAC, S. K. CHAO, A. NEMES, M. MENDELSON, J. EMONDSON, and R. AXEL. 1996. Visualizing an olfactory sensory map. *Cell* **87**:675–686.
- NGAI, J., A. CHESSE, M. M. DOWLING, N. NECLES, E. R. MACAGNO, and R. AXEL. 1993. Coding of olfactory information: topography of odorant receptor expression in the catfish olfactory epithelium. *Cell* **72**:667–680.
- POLANSKI, J. R., D. J. FAUSS, P. CHEN, H. CHEN, E. LUETJENDRECOLL, D. JOHNSON, D. KURTZ, D. Z. MA, E. BLOOM, and T. D. NGUYEN. 1997. Cellular pharmacology and molecular biology of the trabecular meshwork inducible glucocorticoid response gene product. *Ophthalmologica* **211**: 126–139.
- RONNETT, G. V., L. D. HESTER, and S. H. SNYDER. 1991. Primary culture of neonatal rat olfactory neurons. *J. Neurosci.* **11**:1243–1255.
- SAMBROOK, J., E. FRITSCH, and T. MANIATIS. 1989. Molecular cloning: a laboratory manual. Cold Spring Harbor Laboratory Press, Cold Spring Harbor, N.Y.
- SNYDER, D. A., A. M. RIVERS, H. YOKOE, B. PH. M. MENDO, and R. R. H. ANHOLT. 1991. Olfactomedin: purification, characterization and localization of a novel olfactory glycoprotein. *Biochemistry* **30**:9143–9153.
- STONE, E. M., J. H. FINGERT, W. L. M. ALWARD et al. (15 co-authors). 1997. Identification of a gene that causes primary open angle glaucoma. *Science* **275**:668–670.
- VASSAR, R., S. K. CHAO, R. SITCHERAN, J. M. NUÑEZ, L. B. VOSSHALL, and R. AXEL. 1994. Topographic organization of sensory projections to the olfactory bulb. *Cell* **79**:981–991.
- VON HEIJNE, G. 1986. A new method for predicting signal sequence cleavage sites. *Nucleic Acids Res.* **14**:4683–4690.
- WILSON, R., R. AINSCROUGH, K. ANDERSON et al. (55 co-authors) 1994. 2.2 Mb of contiguous nucleotide sequence from chromosome III of *C. elegans*. *Nature* **368**:32–38.
- YOKOE, H., and R. R. H. ANHOLT. 1993. Molecular cloning of olfactomedin, an extracellular matrix protein specific to olfactory neuroepithelium. *Proc. Natl. Acad. Sci. USA* **90**: 4655–4659.

CHARLES F. AQUADRO, reviewing editor

Accepted February 17, 1998

Reprinted from

BRAIN RESEARCH

Brain Research 837 (1999) 117–126

Research report

Differential expression of G proteins in the mouse olfactory system

Kennedy S. Wekesa, Robert R.H. Anholt *

Department of Zoology, Box 7617, North Carolina State University, Raleigh, NC 27695-7617, USA



ELSEVIER

BRAIN RESEARCH

SCOPE AND PURPOSE

BRAIN RESEARCH provides a medium for the prompt publication of articles in the fields of neuroanatomy, neurochemistry, neurophysiology, neuroendocrinology, neuropharmacology, neurotoxicology, neurocommunications, behavioural sciences, molecular neurology and biocybernetics. Clinical studies that are of fundamental importance and have a direct bearing on the knowledge of the structure and function of the brain, the spinal cord, and the peripheral nerves will also be published.

TYPES OF PAPERS

1. **Interactive Reports** are papers describing original, high quality, fundamental research in any area of Neuroscience. These will first appear electronically on the WWW (<http://www.elsevier.com/locate/bres> or <http://www.elsevier.nl/locate/bres>) and published soon after in the relevant section of *Brain Research*. The on-line version may include additional data sets, 3-D/confocal images, animations, etc., and be linked to relevant on-line databases. Comments from readers may be appended later in a linked *Discussion Forum* at the discretion of an appointed Moderator.
2. **Research Reports** reporting results of original fundamental research in any branch in the brain sciences. It is expected that these papers will be published about three months after acceptance.
3. **Short Communications** reporting on research which has progressed to the stage when it is considered that the results should be made known quickly to other workers in the field. The maximum length allowed will be 1500 words or equivalent space in tables and illustrations. It is expected that Short Communications will be published about two months after acceptance.
4. **Protocols**: full-length protocols in any area of Neuroscience, to be published in the journal section *Brain Research Protocols*. Updates on published protocols submitted by the authors thereof, describing new developments which are of sufficient interest to the neuroscience community, but which do not warrant a completely new submission, will be published as **Protocol Updates**. The maximum length allowed will be 1500 words or equivalent space in tables and illustrations. Comments on published Protocols describing useful hints and "tricks" related to any aspect of the Protocol, such as timing, equipment, chemicals, troubleshooting, etc., will be published in the on-line version of the journal as linked **Technical Tips** at the discretion of the Editor.

SUBMISSION OF MANUSCRIPTS

Submission of a paper to *Brain Research* is understood to imply that it deals with original material not previously published (except in abstract form), and that it is not being considered for publication elsewhere. Manuscripts submitted under multiple authorship are reviewed on the assumption that all listed authors concur with the submission and that a copy of the final manuscript has been approved by all authors and tacitly or explicitly by the responsible authorities in the laboratories where the work was carried out. If accepted, the article shall not be published elsewhere in the same form, in either the same or another language, without the consent of the Editors and Publisher. The Publisher and Editor regret that they are unable to return copies of submitted articles except in the case of rejected articles, where only one set of manuscript plus figures will be returned to the author.

Manuscripts in English should be organised according to the *Brain Research Guidelines for the Submission of Manuscripts* and sent to the appropriate address shown below. Authors should state clearly the section of the journal for which the article/Interactive Report should be considered.

Research Reports & Short Communications:

Professor D.P. Purpura
Brain Research, Office of the Dean
Albert Einstein College of Medicine
Jack and Pearl Resnick Campus
1300 Morris Park Avenue
Bronx, NY 10461, USA
Tel.: (1) (718) 430-2387
Fax: (1) (718) 430-8980
E-mail: brain@aecom.yu.edu

Interactive Reports:

Professor F.E. Bloom
Brain Research Interactive
Dept. of Neuropharmacology
The Scripps Research Institute
10666 N. Torrey Pines Road
La Jolla, CA 92037, USA
Fax: (1) (619) 784-8851
E-mail: smart@scripps.edu
Website: <http://smart.scripps.edu>

Protocols & Protocol Updates:

Dr. Floris G. Wouterlood
Department of Anatomy
Faculty of Medicine
Free University
van der Boechorststraat 7
1081 BT Amsterdam
The Netherlands
Fax: (31) (20) 444-8054
E-mail: fg.wouterlood.anat@med.vu.nl

Correspondence regarding accepted manuscripts relating to proofs, publication and reprints should be sent to:

Brain Research, Elsevier Science B.V., P.O. Box 2759, 1000 CT Amsterdam, The Netherlands. Tel.: (31) (20) 485-3415; Fax: (31) (20) 485-2431; E-mail: a.brakel@elsevier.nl

EDITORIAL BOARD

Editor-in-Chief: Dominick P. Purpura (Bronx, NY, USA)

G.K. Aghajanian (New Haven, CT, USA)
B.W. Agranoff (Ann Arbor, MI, USA)
A.J. Aguayo (Montreal, Que., Canada)
P. Andersen (Oslo, Norway)
E.C. Azmitia (New York, NY, USA)
M.V.L. Bennett (Bronx, NY, USA)
L.I. Benowitz (Boston, MA, USA)
J.M. Besson (Paris, France)
A. Björklund (Lund, Sweden)
F.E. Bloom (La Jolla, CA, USA)
D. Choi (St. Louis, MO, USA)
R.E. Coggeshall (Galveston, TX, USA)
H. Collewijn (Rotterdam, The Netherlands)
W.M. Cowan (Bethesda, MD, USA)
A.C. Cuello (Montreal, Que., Canada)
M.S. Cynader (Vancouver, BC, Canada)
J.E. Dowling (Cambridge, MA, USA)
J.J. Dreifuss (Geneva, Switzerland)
R. Dubner (Baltimore, MD, USA)
S.B. Dunnett (Cambridge, UK)
P.C. Emson (Cambridge, UK)
S.J. Enna (Kansas City, KS, USA)
J. Feldman (Los Angeles, CA, USA)
H.L. Fields (San Francisco, CA, USA)
F.H. Gage (San Diego, CA, USA)
J. Glowinski (Paris, France)
P.S. Goldman-Rakic (New Haven, CT, USA)

S. Grillner (Stockholm, Sweden)
B. Gustafsson (Göteborg, Sweden)
A. Hamberger (Göteborg, Sweden)
U. Heinemann (Köln, Germany)
K.-P. Hoffmann (Bochum, Germany)
T.G.M. Hökfelt (Stockholm, Sweden)
R.L. Isaacson (Binghamton, NY, USA)
M. Ito (Saitama, Japan)
B.L. Jacobs (Princeton, NJ, USA)
E.G. Jones (Irvine, CA, USA)
P. Kalivas (Pullman, WA, USA)
K. Kogure (Saitama, Japan)
G.F. Koob (La Jolla, CA, USA)
L. Kruger (Los Angeles, CA, USA)
J. LaVail (San Francisco, CA, USA)
M. Le Moal (Bordeaux, France)
C.L. Masters (Parkville, Vic., Australia)
M. Mattson (Lexington, KY, USA)
B.S. McEwen (New York, NY, USA)
E.G. McGeer (Vancouver, BC, Canada)
R.Y. Moore (Pittsburgh, PA, USA)
P. Morell (Chapel Hill, NC, USA)
W.T. Norton (New York, NY, USA)
J.M. Palacios (Barcelona, Spain)
M. Palkovits (Budapest, Hungary)
R. Quirion (Verdun, Que., Canada)

C.S. Raine (Bronx, NY, USA)
G. Raisman (London, UK)
P. Rakic (New Haven, CT, USA)
H.J. Ralston III (San Francisco, CA, USA)
S.I. Rapoport (Bethesda, MD, USA)
C.E. Ribak (Irvine, CA, USA)
P. Rudomin (Mexico, DF, Mexico)
M. Schachner (Hamburg, Germany)
B.K. Siesjö (Honolulu, HI, USA)
E.J. Simon (New York, NY, USA)
R.S. Sloviter (Tucson, AZ, USA)
S.H. Snyder (Baltimore, MD, USA)
C. Sotelo (Paris, France)
J. Stone (Sydney, NSW, Australia)
D.F. Swaab (Amsterdam, The Netherlands)
L. Swanson (Los Angeles, CA, USA)
L. Terenius (Stockholm, Sweden)
M. Tohyama (Osaka, Japan)
S. Tucek (Prague, Czech Republic)
K. Unsicker (Heidelberg, Germany)
S.G. Waxman (New Haven, CT, USA)
F.G. Wouterlood (Amsterdam, The Netherlands)
R.J. Wurtman (Cambridge, MA, USA)
I.S. Zagon (Hershey, PA, USA)
W. Zieglgänsberger (Munich, Germany)
R.S. Zukin (Bronx, NY, USA)

GUIDELINES FOR THE SUBMISSION OF MANUSCRIPTS

These can be found on the *Brain Research Interactive* Website (<http://www.elsevier.com/locate/bres> or <http://www.elsevier.nl/locate/bres>) as well as in the "front matter" of every first issue of even-numbered volumes of the journal.

The preferred medium of submission is on disk with accompanying manuscript (see "Electronic manuscripts").

Research report

Differential expression of G proteins in the mouse olfactory system

Kennedy S. Wekesa, Robert R.H. Anholt *

Department of Zoology, Box 7617, North Carolina State University, Raleigh, NC 27695-7617, USA

Accepted 11 May 1999

Abstract

Transmembrane signaling events at the dendrites and axons of olfactory receptor neurons mediate distinct functions. Whereas odorant recognition and chemosensory transduction occur at the dendritic membranes of olfactory neurons, signal propagation, axon sorting and target innervation are functions of their axons. The roles of G proteins in transmembrane signaling at the dendrites have been studied extensively, but axonal G proteins have not been investigated in detail. We used immunohistochemistry to visualize expression of α subunits of G_o and G_{i2} in the mouse olfactory system. G_o is expressed ubiquitously on axons of olfactory receptor neurons throughout the olfactory neuroepithelium and in virtually all glomeruli in the main olfactory bulb. In contrast, expression of G_{i2} is restricted to a sub-population of olfactory neurons, along the dorsal septum and the dorsal recess of the nasal cavity, which projects primarily to medial regions of the olfactory bulb, with the exception of glomeruli adjacent to the pathway of the vomeronasal nerve. In contrast to the overlapping expression patterns of G_o and G_{i2} in the main olfactory system, neurons expressing G_o and those expressing G_{i2} in the accessory olfactory bulb are more clearly separated, in agreement with previous studies. Vomeronasal axons terminating in glomeruli in the rostral region of the accessory olfactory bulb express G_{i2} , whereas those projecting to the caudal region express G_o . Characterization of the expression patterns of G_{i2} and G_o in the olfactory projection is essential for future studies aimed at relating transmembrane signaling events to signal propagation, axon sorting and target innervation. © 1999 Elsevier Science B.V. All rights reserved.

Keywords: G protein; Olfaction; Olfactory bulb; Accessory olfactory bulb; Olfactory neuron; Chemotopic projection

1. Introduction

Odor recognition is essential for the survival and procreation of most animals. Chemical information transferred via olfactory neurons to the olfactory bulb is transformed into a chemotopic map [5,10,11,19]. This map is represented by modular neural arrays, glomeruli, which in the mouse number approximately 1800 [31] and each of which represents the convergent projection of neurons of similar chemosensory specificity (see Ref. [16] for review).

The olfactory system contains two interacting components: the main olfactory system is dedicated to general odorant discrimination, whereas the accessory olfactory system primarily processes chemical cues that guide social behaviors (see Ref. [26] for review). In the main olfactory system, odor recognition is mediated by receptors, which belong to the superfamily of G protein coupled receptors and are encoded by as many as 1000 different genes [2,6,22,40–42]. Two distinct families of G protein coupled

receptors have also been identified as putative pheromone receptors in chemosensory neurons of the vomeronasal organ (VNO), the chemosensory organ of the accessory olfactory system [8,15,25,34].

The dendritic and axonal compartments of olfactory neurons fulfill distinct functions for the acquisition of chemosensory information. Whereas dendritic specializations mediate odorant recognition and chemosensory transduction, the axonal compartment regulates signal propagation, axon sorting and target innervation. The roles of G proteins in chemosensory transduction at the dendritic compartments of chemosensory neurons have been studied extensively, but the functions of axonal G proteins have not been investigated in detail.

An important role for axonal G proteins in mammalian chemoreception is implicated by the differential distribution of G_{i2} and G_o in the accessory olfactory system (see Ref. [18] for review). The apical layer of the VNO expresses a distinct family of about 100 putative pheromone receptors (VN1 receptors [8]), whereas VNO neurons in the basal layer express a different family of receptors (VN2 receptors) that resemble metabotropic glutamate re-

* Corresponding author. Fax: +1-919-515-3355; E-mail: anholt@ncsu.edu

ceptors [15,25,34]. Previously, *in situ* hybridization studies in the murine VNO [4] and immunohistochemical studies in opossum, rat and mouse [13,14,18] showed that neurons in the apical layer of the VNO express G_{i2} and project to the rostral region of the accessory olfactory bulb (AOB), whereas neurons in the basal layer express G_o and project to the caudal region of the AOB.

Here we confirm and extend these previous observations. We show that differential expression patterns of G_{i2} and G_o are not unique to the AOB, but also occur in the main olfactory bulb (MOB). Characterization of the expression patterns of G_{i2} and G_o in the main olfactory system is a prerequisite for any future studies aimed at delineating transmembrane signaling events at the axons of olfactory neurons and uncovering their relationships to signal propagation and/or odor coding.

2. Materials and methods

2.1. Animals

CD-1 mice were originally obtained from Charles River Laboratories (Kingston, NY) and maintained in the breeding colony of Dr. J.G. Vandenberg (Department of Zoology, North Carolina State University, Raleigh, NC). Animals were housed in IACUC and USDA inspected and approved facilities and cared for according to the NIH Guide for Care and Use of Laboratory Animals (1997).

2.2. Antibodies

Antibodies against α subunits of G-proteins were obtained from Calbiochem (La Jolla, CA). The antibody against the α subunit of G_{i2} was raised against the C-terminal decapeptide KNNLDCGLF, which is also found in the α subunit of G_{i1} . To distinguish $G_{\alpha_{i2}}$ and $G_{\alpha_{i1}}$ an antibody against a $G_{\alpha_{i1}}$ -specific internal peptide was used. The antibody against the α subunit of G_o was raised against the C-terminal peptide KNNLKECGLY of $G_{\alpha_{i3}}$, which shares the sequence CGLY with G_{α_o} and recognizes the α subunits of both G_o and G_{i3} . To distinguish G_o and G_{i3} an antibody against a $G_{\alpha_{i3}}$ -specific internal peptide was used. Antibodies reactive with $G_{\alpha_{i2}}$ and G_{α_o} did not cross-react. Specificity of the antisera was confirmed by Western blotting.

2.3. Western blotting

Freshly dissected olfactory bulbs were homogenized in ice-cold 0.1 M phosphate buffered saline, pH 7.3 (PBS) with a Teflon homogenizer and membranes were collected by centrifugation, washed once, recentrifuged and resuspended in PBS. Protein was determined according to Lowry et al. [23] using bovine serum albumin as standard, and membranes were subjected to SDS-PAGE, followed by

electrophoretic transfer onto a nitrocellulose membrane [1]. Membrane strips containing approximately 20 μ g protein were incubated with a 1000-fold dilution of rabbit anti-serum against $G_{\alpha_{i2}}$ or G_{α_o} . Bound antibody was visualized with Amersham's chemiluminescent ECL detection system (Amersham, Arlington Heights, IL). Migration distances were calibrated against Kaleidoscope prestained molecular weight markers (BioRad, Richmond, CA).

2.4. Tissue preparation

Mice were given a lethal injection of sodium pentobarbital (50 mg/kg, i.p.) and perfused intracardially with

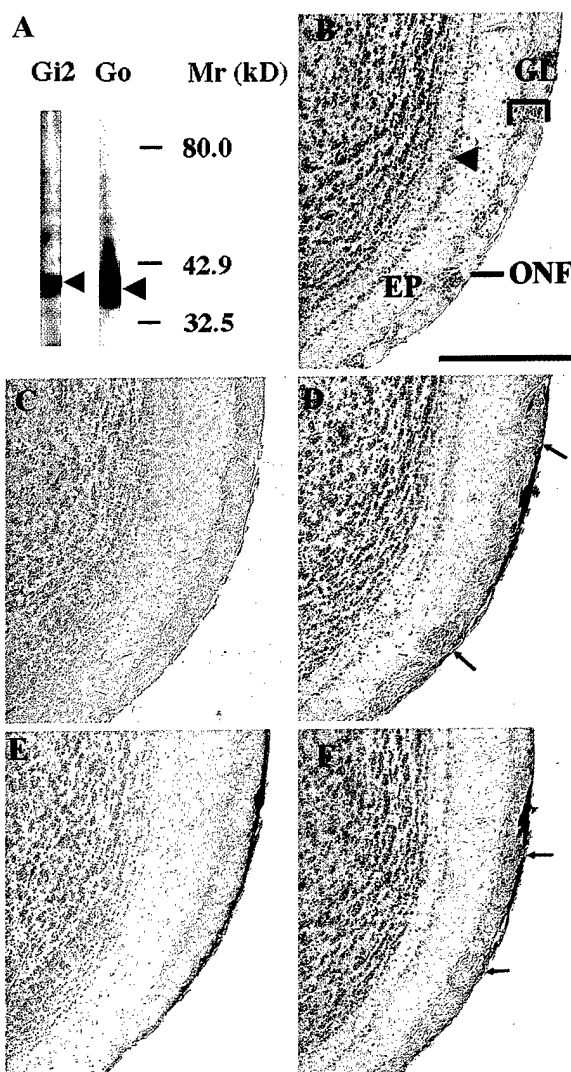


Fig. 1. Specificity of antibodies. (A): Western blot showing immunoreactive bands (arrowheads) with antibodies against $G_{\alpha_{i2}}$ and G_{α_o} in olfactory bulb membranes. (B)–(F): parasagittal sections through mouse olfactory bulbs stained with normal rabbit serum (B) or antisera against α subunits of G_{i1} (C), G_{i2} (D; crossreactive with $G_{\alpha_{i1}}$), G_{i3} (E), and G_o (F; crossreactive with $G_{\alpha_{i3}}$). ONF, olfactory nerve fiber layer; GL, glomerular layer; EP, external plexiform layer; the arrowhead indicates the mitral cell body layer. Note the staining of glomeruli in panels D and F (arrows). The scale bar in B represents 500 μ m and applies to B–F.

PBS, followed by extensive perfusion with 10% buffered neutral formalin. The olfactory bulbs and/or nasal cavities were dissected and fixed overnight in 10% buffered neutral formalin. Decalcification of nasal tissue was performed for 3 days at ambient temperature using the formic acid-sodium citrate method [24].

2.5. Immunohistochemistry

Formalin-fixed and paraffin-embedded, 5 μ thick sections through olfactory bulbs and nasal tissue were deparaffinized in xylene and rehydrated through graded alcohols. The sections were pretreated with 0.1% pepsin (Sigma, St. Louis, MO) in 0.01 M HCl, pH 2.3, for 20 min to facilitate epitope access. Following pepsin treatment, the sections were blocked for 30 min with BEAT blocking solutions A and B (Zymed Laboratories, San Francisco, CA). They were then incubated with a 250-fold dilution of normal rabbit serum or antiserum in PBS, 0.05% Triton X-100 (Boehringer Mannheim, Indianapolis, IN) overnight

at 4°C. Bound antibody was visualized using the Histo-mouse SP kit from Zymed Laboratories. Following incubation with the primary antibody, sections were washed extensively in PBS, 0.05% Triton X-100, and incubated for 10 min at ambient temperature with affinity purified biotinylated goat anti-rabbit antibody. Following 10 min incubation with horseradish peroxidase-conjugated streptavidin, antibody complexes were visualized using 3'-amino-9'-ethylcarbazole as chromogenic substrate. This generates a red deposit at the site of antibody binding. Sections were counterstained with hematoxylin, if desired, and viewed and photographed under a Zeiss Axiophot microscope.

3. Results

3.1. Specificity of antibodies

In pilot experiments, parasagittal sections through olfactory bulbs revealed staining with antisera against α subunits of G proteins (Fig. 1). Before proceeding with a

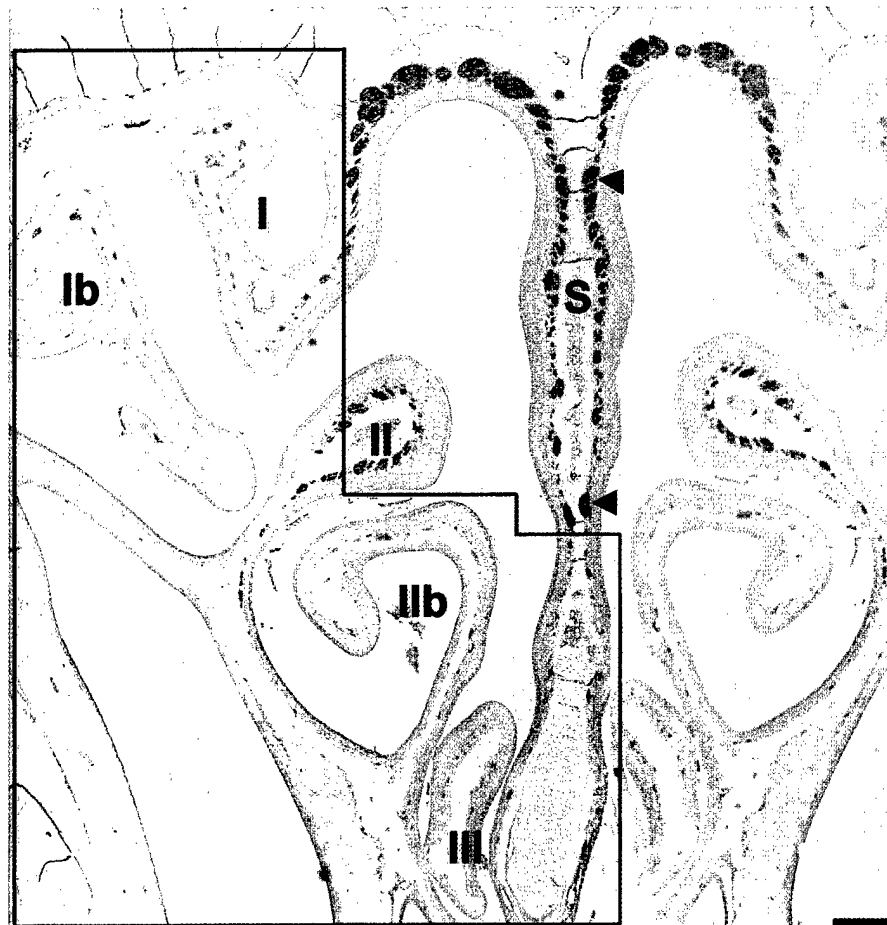


Fig. 2. Immunohistochemical localization of $G\alpha_o$ in a coronal section through the mouse nasal cavity. S designates the septum and the turbinates are indicated with roman numerals. Note that staining with antibodies against $G\alpha_o$ is apparent in all axon bundles in the submucosa (arrowheads). The boxed area delineates the region in which axon bundles stain with antiserum against $G\alpha_o$, but not with antiserum against $G\alpha_{i2}$ (see Fig. 4). The scale bar represents 200 μ m.

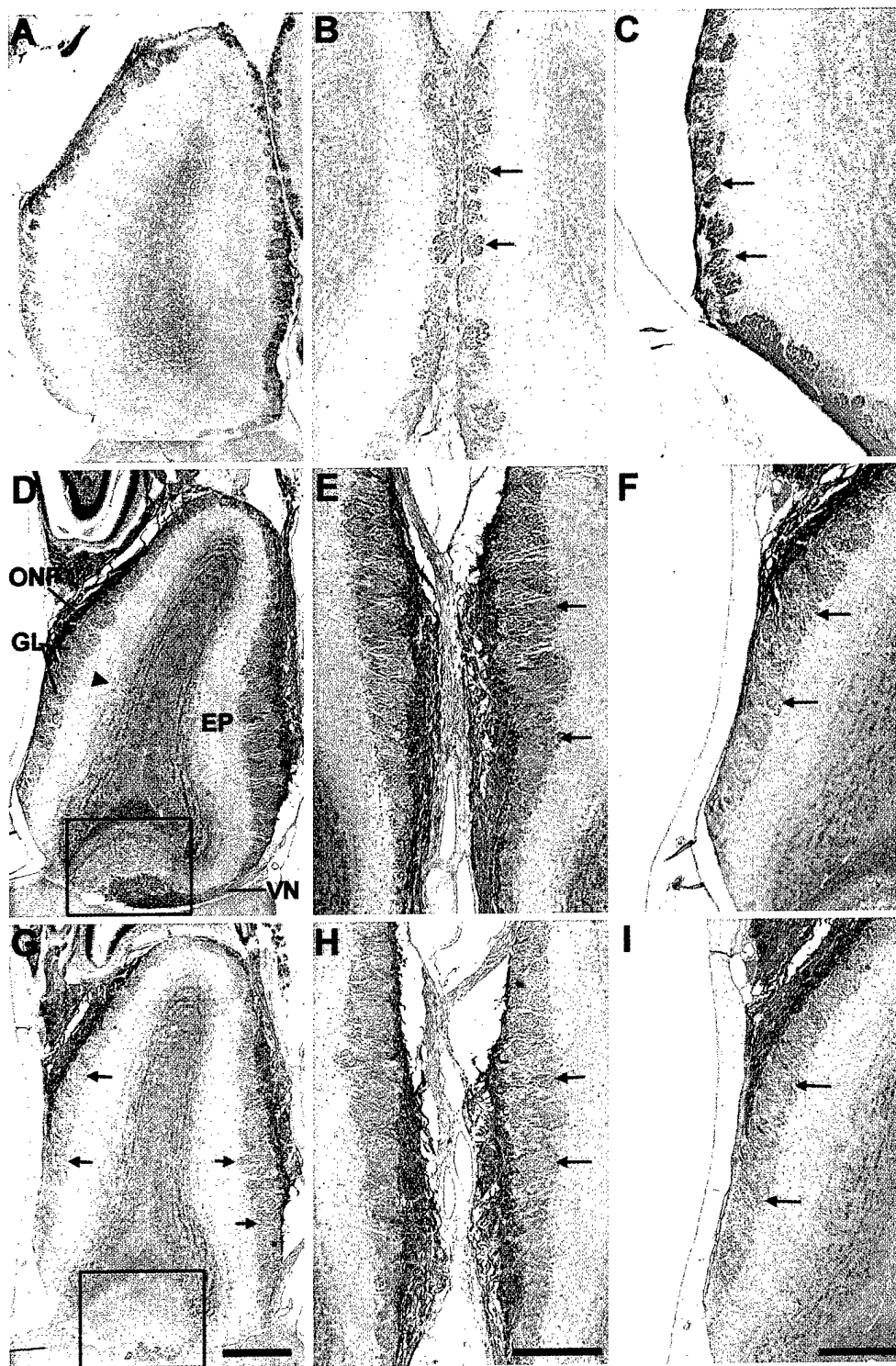


Fig. 3. Immunohistochemical localization of $G\alpha_o$ in horizontal sections through the mouse olfactory bulb. Panels A, D and G show low magnification views of the entire olfactory bulb from a dorsal level (A) to progressively more ventral regions of the bulb (D and G). The scale bar in G represents 500 μm and applies also to panels A and D. Panels B and C show higher magnification views of the medial and lateral region of the olfactory bulb shown in panel A, respectively. Panels E and F show higher magnification views of the medial and lateral region of the olfactory bulb shown in panel D, respectively. Panels H and I show higher magnification views of the medial and lateral region of the olfactory bulb shown in panel G, respectively. The scale bars in panels H and I correspond to 40 μm and apply also to panels B, C, E and F. In panel D, ONF designates the olfactory nerve fiber layer, GL, the glomerular layer, EP, the external plexiform layer, and VN, the vomeronasal nerve. The arrowhead indicates the mitral cell body layer. The boxed areas in panels D and G indicate the AOB. Note the ubiquitous staining of the glomeruli at all three horizontal levels examined, both medially and laterally (arrows).

detailed characterization of staining patterns we assessed the specificity of our antisera. Western blotting with olfactory bulb homogenates reveals a single band with an apparent molecular weight of 41 kDa with the antiserum against $G\alpha_{i2}$ and a single band with an apparent molecular weight of 39 kDa with the antiserum against $G\alpha_o$ (Fig. 1A). There is no evidence for non-specific staining when olfactory bulb sections are incubated with normal rabbit serum (Fig. 1B). To evaluate cross-reactivity of the antiserum against $G\alpha_{i2}$ with $G\alpha_{i1}$, adjacent sagittal sections were stained with antiserum specific for $G\alpha_{i1}$ (Fig. 1C) and with antiserum against $G\alpha_{i2}$ (Fig. 1D). No staining is observed with the $G\alpha_{i1}$ -specific antiserum, whereas staining in glomeruli is evident with the antiserum against $G\alpha_{i2}$. The pattern of glomerular staining in this particular region is not uniform, with some glomeruli staining strongly, whereas others are not stained or show only faint staining (Fig. 1D). Staining within individual glomeruli,

however, is uniform. To determine whether glomerular staining with the antibody against $G\alpha_o$ indeed is due to $G\alpha_o$ rather than $G\alpha_{i3}$ with which this antiserum crossreacts, we stained adjacent parasagittal sections with an antiserum that is specific for $G\alpha_{i3}$ (Fig. 1E) and the antiserum against $G\alpha_o$ (Fig. 1F). Antiserum raised against an internal peptide of $G\alpha_{i3}$ shows staining in the olfactory nerve fiber layer and faint staining in the external plexiform layer of the MOB, but does not stain the glomeruli. In contrast, antiserum against $G\alpha_o$ stains both the olfactory nerve fiber layer and the glomeruli. Although different glomeruli do not stain with equal intensity, staining within individual glomeruli again is uniform (Fig. 1F). Thus, staining detected in MOB glomeruli with the antiserum against $G\alpha_o$ indeed is due to the presence of $G\alpha_o$. The faint staining observed with the $G\alpha_{i3}$ -specific antiserum may reflect the presence of $G\alpha_{i3}$ on glia. These results instill confidence that our antisera against $G\alpha_{i2}$ and $G\alpha_o$

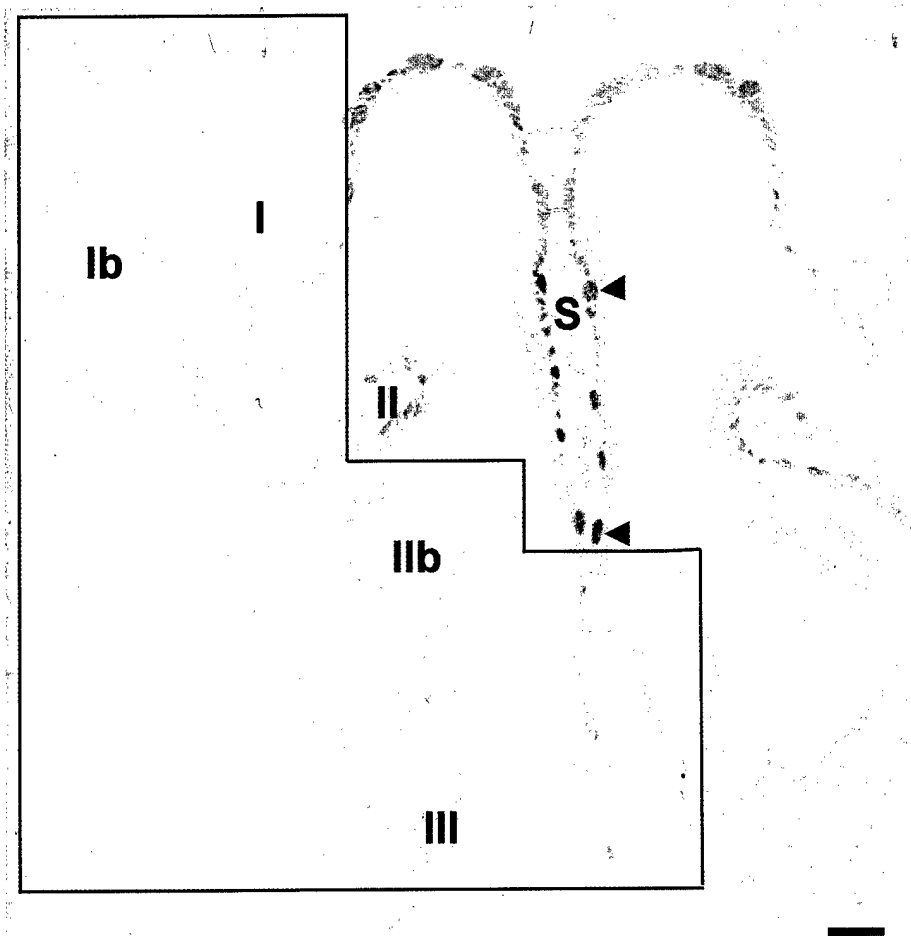


Fig. 4. Immunohistochemical localization of $G\alpha_{i2}$ in a coronal section through the mouse nasal cavity. The section shown in this figure is adjacent to the one shown in Fig. 2. S designates the septum and the turbinates are indicated with roman numerals. Note that staining with antibodies against $G\alpha_{i2}$ is apparent in axon bundles in the submucosa (arrowheads) along the dorsal recess and around the dorsal recess of the nasal cavity. The boxed area delineates the region in which axon bundles do not stain with antiserum against $G\alpha_{i2}$, but stain with antiserum against $G\alpha_o$ (see Fig. 2). The scale bar represents 200 μ m.

specifically recognize the α subunits of G_{i2} and G_o , respectively, in MOB glomeruli.

3.2. Expression of $G\alpha_o$ in the main olfactory projection

Immunohistochemical staining of coronal sections through the murine nasal cavity with an antiserum against $G\alpha_o$ shows extensive staining of axon bundles in the submucosa of the olfactory neuroepithelium (Fig. 2). Virtually all axon bundles along the septum and all five turbinates (I, Ib, II, IIb and III) reveal expression of this G protein.

As predicted from the extensive expression pattern of $G\alpha_o$ in the olfactory neuroepithelium, immunohistochemical localization of this G protein in the olfactory projection to the MOB is widespread. Fig. 3 shows immunohistochemical staining patterns for $G\alpha_o$ at three horizontal levels through the olfactory bulb with views of the entire bulb (A, D and G) and higher magnification views of the medial (B, E and H) and lateral (C, F and I) aspects of the bulb. At all three levels observed, from the most dorsal (A, B and C) to the most ventral (G, H and I), expression of $G\alpha_o$ appears extensive and uniform within the nerve fiber layer and glomeruli. Although staining for $G\alpha_o$ is particularly prominent in the glomeruli, staining is observed in many of the MOB laminae, especially the granular cell layer, with exception of the mitral cell body layer. This is not surprising given the prominence of G_o as one of the major membrane proteins in the central nervous system [17]. Thus, $G\alpha_o$ appears to be universally expressed in olfactory axons that project to the MOB. In contrast, expression of $G\alpha_o$ in glomeruli of the AOB (boxed areas in Fig. 3D and G) is not uniform, but localized to the caudal region of the AOB (see below).

3.3. Expression of $G\alpha_{i2}$ in the main olfactory projection

In contrast to the ubiquitous expression of $G\alpha_o$, immunohistochemical localization of $G\alpha_{i2}$ in coronal sections through the murine nasal cavity shows a more restricted expression pattern (Fig. 4). The expression pattern of $G\alpha_{i2}$ appears nested within the center of the expression pattern of its counterpart, $G\alpha_o$. Whereas virtually all axon bundles stain with antiserum against $G\alpha_{i2}$ in the submu-

cosa along the dorsal septum and around the dorsal recess of the nasal cavity, no expression of this G protein is observed in olfactory neurons originating from turbinates I, Ib, IIb and III and the most ventral region along the septum (Fig. 4). Thus, olfactory neurons in the more lateral regions of the nasal cavity express only $G\alpha_o$, but not $G\alpha_{i2}$, as indicated by the boxed areas in Figs. 2 and 4.

In the MOB, the expression pattern of $G\alpha_{i2}$ contrasts sharply with the uniform pattern of expression of $G\alpha_o$. Fig. 5 shows immunohistochemical staining patterns for $G\alpha_{i2}$ at three horizontal levels through the olfactory bulb with views of the entire bulb (A, D and G) and higher magnification views of the medial (B, E and H) and lateral (C, F and I) aspects of the bulb. At the most dorsal horizontal level examined, only a subset of glomeruli expresses $G\alpha_{i2}$. Whereas different glomeruli stain with different intensity, within a single glomerulus the staining intensity appears uniform. Many glomeruli immunoreactive with antiserum against $G\alpha_{i2}$ are located in the medial region of the MOB, whereas in the lateral region of the bulb more unstained glomeruli are interspersed with those that express $G\alpha_{i2}$ (Fig. 5B and C). Thus, the expression of $G\alpha_{i2}$ appears biased toward the medial aspect of the MOB. This preponderance of the expression pattern of $G\alpha_{i2}$ in the medial rather than the lateral region of the MOB is especially evident in more ventral layers of the bulb (Fig. 5H and I). Interestingly, virtually no expression of $G\alpha_{i2}$ is observed in glomeruli that border the region through which the vomeronasal nerve penetrates toward the AOB (Fig. 5D and E). The vomeronasal nerve stains here prominently and projects to glomeruli in the anterior region of the AOB (Fig. 5D). Thus, the projection of $G\alpha_{i2}$ -expressing olfactory neurons from the dorsomedial region of the nasal cavity fans out across the medial aspect of the MOB, sparing the penetration corridor of the vomeronasal nerve and extending sparsely to scattered glomeruli in the lateral region of the MOB.

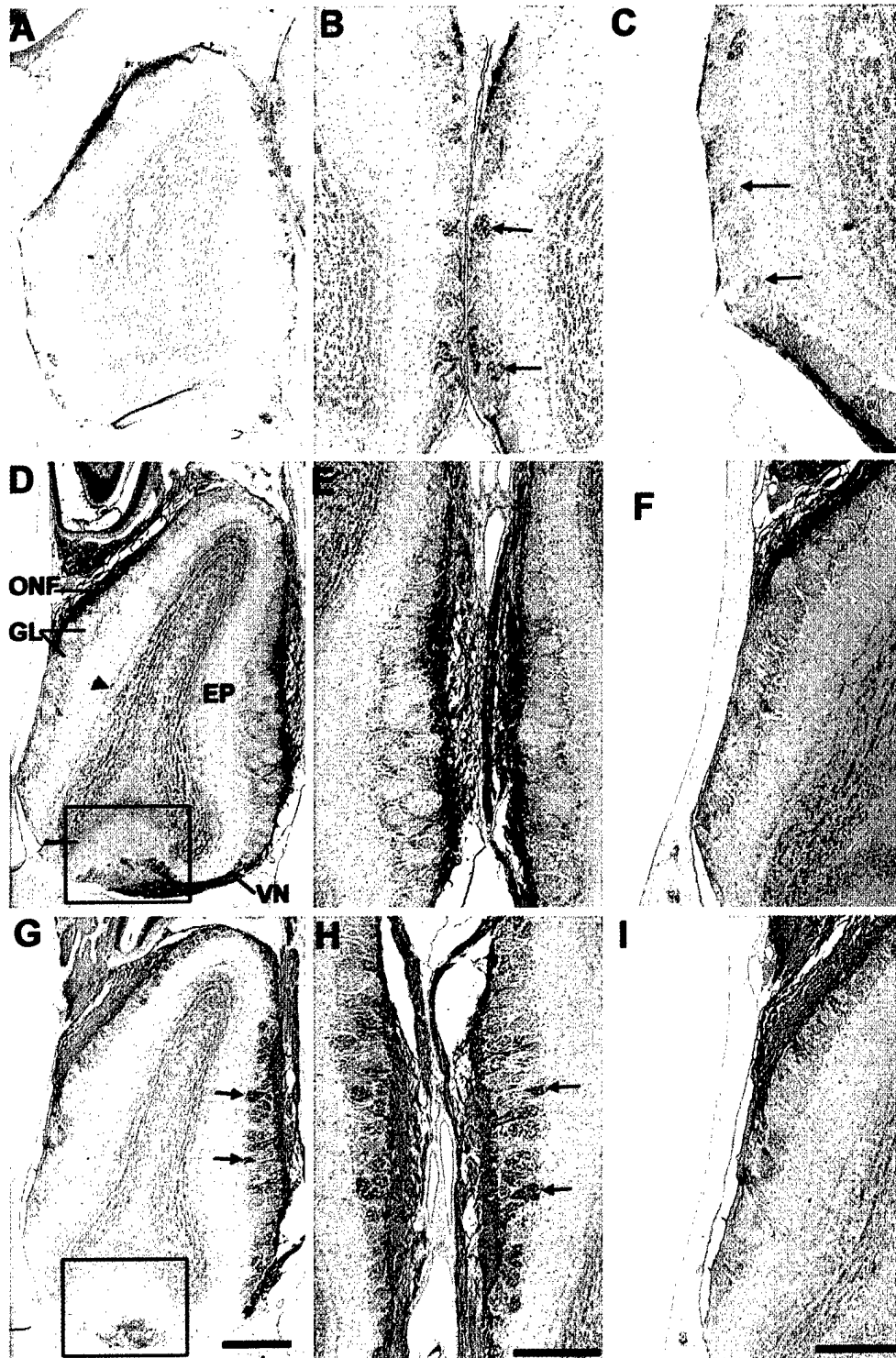
3.4. Expression of $G\alpha_o$ and $G\alpha_{i2}$ in the accessory olfactory projection

Whereas in the MOB the expression of $G\alpha_{i2}$ is more restricted than the distribution of $G\alpha_o$, the reverse pattern is evident in the AOB, where the expression pattern of

Fig. 5. Immunohistochemical localization of $G\alpha_{i2}$ in horizontal sections through the mouse olfactory bulb. Panels A, D and G show low magnification views of the entire olfactory bulb from a dorsal level (A) to progressively more ventral regions of the bulb (D and G). These panels represent sections adjacent to their counterparts shown in Fig. 3. The scale bar in G represents 500 μ m and applies also to panels A and D. Panels B and C show higher magnification views of the medial and lateral region of the olfactory bulb shown in panel A, respectively. Panels E and F show higher magnification views of the medial and lateral region of the olfactory bulb shown in panel D, respectively. Panels H and I show higher magnification views of the medial and lateral region of the olfactory bulb shown in panel G, respectively. The scale bars in panels H and I correspond to 40 μ m and apply also to panels B, C, E and F. In panel D, ONF designates the olfactory nerve fiber layer, GL, the glomerular layer, EP, the external plexiform layer, and VN, the vomeronasal nerve. The arrowhead indicates the mitral cell body layer. The boxed areas in panels D and G indicate the AOB. Note the heterogeneous staining of glomeruli. $G\alpha_{i2}$ -immunoreactivity is mostly found in medial glomeruli of the olfactory bulb (arrows in panels B and H), although some lateral glomeruli in the dorsal region of the bulb also stain (arrows in panel C). Note the virtual absence of expression of $G\alpha_{i2}$ in panels D, E and F where the vomeronasal nerve (VN) travels along the medial aspect of the MOB toward the AOB (boxed area).

$G\alpha_{12}$ appears more extensive than that of $G\alpha_o$. This is especially evident in parasagittal sections through the AOB (Fig. 6A and B). The arrows in panels A and B of Fig. 6 indicate the level of the horizontal sections shown in panels C and D. These horizontal views are higher magnifications of the boxed areas of panels D in Figs. 3 and 5, respectively. The necklace glomeruli, a group of special-

ized glomeruli in the caudal region of the MOB bordering the AOB [37], appear to express $G\alpha_o$, but not $G\alpha_{12}$. Expression patterns in the AOB are similar to those previously observed in opossum, mouse and rat [13,14,18]. Neuronal projections expressing $G\alpha_{12}$ and $G\alpha_o$ are clearly demarcated in the murine AOB, with vomeronasal axons expressing $G\alpha_{12}$ projecting to glomeruli in the rostral



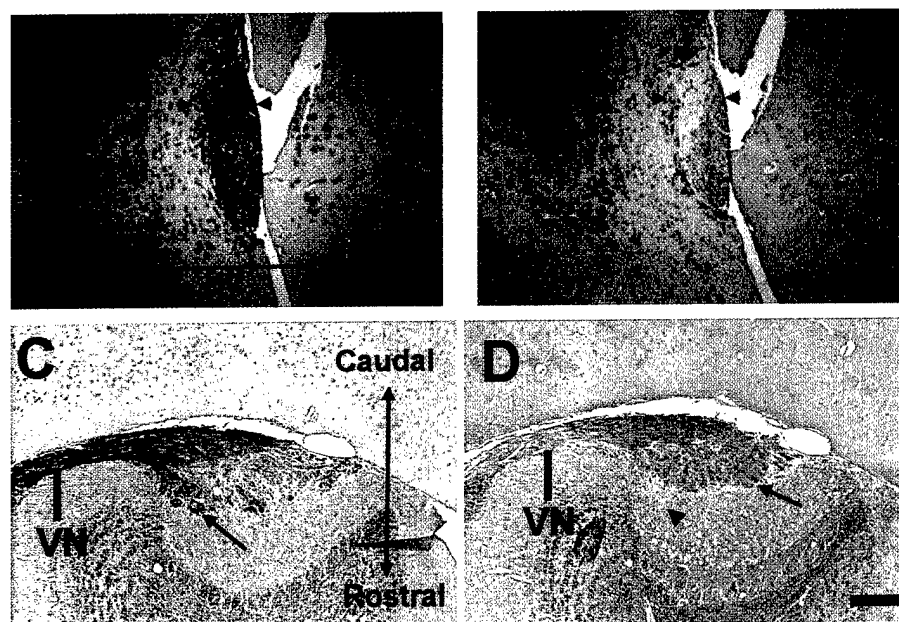


Fig. 6. Immunohistochemical localization of $G\alpha_{12}$ (panels A and C) and $G\alpha_o$ (panels B and D) in the mouse AOB. Panels A and B show parasagittal sections close to the lateral border of the AOB. Panels C and D are high magnification views of the boxed areas of Figs. 3D and 5D and show horizontal views of the projection of the vomeronasal nerve (VN) at the levels indicated by the arrowheads in panels A and B. Note that expression of $G\alpha_{12}$ is mostly confined to the rostral region of the AOB, indicated by the arrow in panel C and the arrowhead in panel D, whereas expression of $G\alpha_o$ is observed in the caudal region of the AOB. The scale bar in panel B represents 25 μm and applies also to panel A. The scale bar in panel D represents 100 μm and applies also to panel C.

region of the AOB and those expressing $G\alpha_o$ being restricted to the caudal region of the AOB (Fig. 6B and D).

4. Discussion

4.1. Differential expression of G proteins in chemosensory projections to the MOB and AOB

We have used immunohistochemistry to visualize the expression patterns of the α subunits of G_o and G_{12} in the mouse olfactory system. G_o is expressed ubiquitously in olfactory receptor neurons throughout the olfactory neuroepithelium and, consequently, is visualized in virtually all glomeruli in the MOB (Figs. 2 and 3). In contrast, the expression of G_{12} is restricted to a subset of olfactory neurons, located along the dorsal septum and around the dorsal recess of the nasal cavity and projecting primarily to medial regions of the MOB, with the exception of glomeruli in the immediate vicinity of the vomeronasal nerve (Figs. 4 and 5).

In contrast to the overlapping expression patterns of G_o and G_{12} in the main olfactory system, the projection fields of neurons expressing G_o and those expressing G_{12} in the AOB are more clearly demarcated, in agreement with previous studies (Fig. 6) (see Ref. [13] for review). In the AOB, vomeronasal axons terminating in glomeruli in the

rostral region of the AOB express G_{12} , whereas axons projecting to the caudal region of the AOB express G_o .

Our results further indicate absence of G_{11} and G_{13} in primary olfactory afferents, although the latter is expressed in the olfactory nerve fiber layer of the MOB (Fig. 1). Previously, we localized $G_{q/11}$ to chemosensory neurons in the porcine VNO, where it is likely involved in regulating inositol-1,4,5-trisphosphate-mediated responses to VNO stimuli [45]. We did, however, not detect $G_{q/11}$ immunoreactivity in the mouse MOB or AOB. An antiserum against G_{12} showed only weak staining in MOB glomeruli and staining patterns observed with this antiserum were inconclusive. Recently, homologous recombinant mice lacking the α subunit of G_{olf} [20] were shown to be anosmic [3]. However, they retained a morphologically intact olfactory neuroepithelium and MOB [3], suggesting that G_{olf} does not play a role in the formation of the olfactory projection.

The prominent presence of G_{12} and G_o in the MOB had been noted previously [38], but differential expression patterns of these G proteins in populations of olfactory neurons throughout the MOB have not been characterized before. Since these G proteins are expressed in different populations of neurons in the VNO and AOB [4,13,14,18], we decided to focus on the characterization of the expression patterns of these two transduction proteins. It should be noted, however, that we cannot exclude that some glomeruli may express different G proteins that have escaped detection in this study.

4.2. What are the functions of G proteins on the axons of olfactory and vomeronasal neurons?

Segregation of lateral and medial olfactory projections has been noted in studies with monoclonal antibodies against surface antigens [12,28,35,36] and N-CAM isoforms [21]. Characterization of segregated populations of neurons expressing different G proteins is especially significant, since these proteins are essential components of signal transduction pathways. Thus, the presence of two distinct G proteins on afferent axons of olfactory neurons raises questions regarding the receptors these proteins are coupled to, the signals they transduce and the effector systems they activate.

G proteins on the axons of olfactory neurons could play a role either in the modulation of signal propagation or in the assembly of convergent axonal projections during the formation and maintenance of the chemotopic map. In the main olfactory system, olfactory neurons expressing the same odorant receptor converge on two glomeruli in the MOB, one medial and one lateral [27,32]. Thus, the olfactory projection forms two chemotopic representations in each olfactory bulb, one lateral map and one medial map. It is tempting to speculate that, whereas G_o may play a role in axonal targeting in all olfactory neurons in the MOB, expression of G_{i2} may direct a subpopulation of neurons to form a dorsomedial projection that may define, at least in part, the medial chemotopic map. Involvement of these G proteins in the formation of chemotopic projections is especially intriguing, since odorant receptors themselves may play a central role in forming convergent glomerular projections [27,44]. As odorant receptors are heptahelical receptors, axonal signaling via these receptors is expected to be mediated via G proteins. Furthermore, in the VNO neurons with VN1 receptors express G_{i2} , whereas neurons with VN2 receptors express G_o [15,25,34]. Thus, it is tempting to speculate that in the main olfactory projection G_{i2} and G_o may be coupled to odorant receptors and play a role in the formation of the glomerular map. This hypothesis implies that odorant receptors and putative pheromone receptors would change their coupling specificity from G_{olf} on olfactory cilia [20] and $G_{q/11}$ on VNO microvilli [45], respectively, to G_{i2} or G_o on olfactory and vomeronasal axons. Such G protein switching appears plausible, since β_2 -adrenergic receptors can switch their G protein specificity upon phosphorylation by cyclic AMP-dependent protein kinase [7]. We are well aware, however, that the hypothesis that axonal odorant receptors may couple to G_o or G_{i2} is at present highly speculative.

Duncan et al. [9] showed that small injections of an anterograde tracer in the frog ventral olfactory epithelium labeled predominantly the lateral portion of the MOB, whereas injections in the dorsal olfactory epithelium generated heavier labeling in the medial region. Mori provided evidence that neighboring glomeruli in the MOB receive inputs from olfactory neurons with related odorant re-

sponse properties [30]. A recent fura-2 calcium imaging study in mouse showed that retrogradely labeled olfactory neurons projecting to defined dorsomedial or dorsolateral glomerular regions respond to different classes of odorants [5]. Dorsolaterally projecting neurons respond to structurally diverse odorants, including carvone, eugenol, cinnamaldehyde and acetophenone, whereas dorsomedially projecting neurons respond preferentially to organic acids [5]. These observations are consistent with earlier electrophysiological studies by Mori et al. [29], which showed that mitral and tufted cells in the dorsomedial region of the rabbit MOB respond preferentially to long chain carboxylic acids, but not to their corresponding alcohols. These findings suggest that the chemotopic glomerular map may comprise dorsolateral and dorsomedial projections of neurons expressing functionally distinct classes of odorant receptors.

As noted above, it is possible that the expression pattern of G_{i2} , nested within the projection of G_o -expressing neurons, is important for the construction of lateral and medial chemosensory projection fields. The widespread expression of G_o on axons of olfactory neurons is perhaps not surprising, since it has long been known that G_o interacts with GAP43 on axonal growth cones and may play a role in linking transduction of extracellular signals to growth cone function [39]. However, homologous recombinant mice deficient in the α subunit of G_o did not show gross behavioral or neurological disorders and their optic nerves were structurally indistinguishable from those of heterozygous litter mates [43]. Similarly, homologous recombinant mice deficient in the α subunit of G_{i2} are viable due to compensatory expression of related G proteins [33]. The functional integrity of the chemotopic maps and the ability of these animals to discriminate odorants or respond to pheromones, however, has not yet been investigated. More detailed studies on these mice could in the future yield important information about the function of these axonal G proteins in the olfactory system.

Acknowledgements

We thank Dr. John G. Vandenberg for providing mice and Monica Mattmuller of the histology laboratory at the NCSU College of Veterinary Medicine for preparation of paraffin sections. This work was supported by grants from the US Army Research Office (DAAH-04-96-I-0096), the North Carolina Biotechnology Center (9605-ARG-0015), the W.M. Keck Foundation and in part by a grant from the National Institutes of Health (DC02485). This is a publication of the W.M. Keck Program for Behavioral Biology at North Carolina State University.

References

- [1] R.R.H. Anholt, S.M. Mumby, D.A. Stoffers, P.R. Girard, J.F. Kuo, S.H. Snyder, Transduction proteins of olfactory receptor cells: iden-

- tification of guanine nucleotide binding proteins and protein kinase C, *Biochemistry* 26 (1987) 788–795.
- [2] R. Axel, The molecular logic of smell, *Scientific American* 273 (1995) 154–159.
 - [3] L. Belluscio, G.H. Gold, A. Nemes, R. Axel, Mice deficient in G_{olf} are anosmic, *Neuron* 20 (1998) 69–81.
 - [4] A. Berghard, L. Buck, Sensory transduction in vomeronasal neurons: evidence for G_o , $G_{\alpha_{12}}$, and adenylyl cyclase II as major components of a pheromone signaling cascade, *J. Neurosci.* 16 (1996) 909–918.
 - [5] T.C. Bozza, J.S. Kauer, Odorant response properties of convergent olfactory receptor neurons, *J. Neurosci.* 18 (1998) 4560–4569.
 - [6] L. Buck, R. Axel, A novel multigene family may encode odorant receptors: a molecular basis for odor recognition, *Cell* 65 (1995) 175–187.
 - [7] Y. Daaka, L.M. Luttrell, R.J. Lefkowitz, Switching of the coupling of the β_2 -adrenergic receptor to different G proteins by protein kinase A, *Nature* 390 (1997) 88–91.
 - [8] C. Dulac, R. Axel, A novel family of genes encoding putative pheromone receptors in mammals, *Cell* 83 (1995) 195–206.
 - [9] H.J. Duncan, W.T. Nickell, M.T. Shipley, R.C. Gesteland, Organization of projections from olfactory epithelium to olfactory bulb in the frog, *Rana pipiens*, *J. Comp. Neurol.* 299 (1990) 299–311.
 - [10] R.W. Friedrich, S.I. Korsching, Combinatorial and chemotopic odorant coding in the zebrafish olfactory bulb visualized by optical imaging, *Neuron* 18 (1997) 737–752.
 - [11] R.W. Friedrich, S.I. Korsching, Chemotopic, combinatorial, and noncombinatorial odorant representations in the olfactory bulb revealed using a voltage-sensitive axon tracer, *J. Neurosci.* 18 (1998) 9977–9988.
 - [12] S.C. Fujita, K. Mori, K. Imamura, K. Obata, Subclasses of olfactory receptor cells and their segregated central projections demonstrated by a monoclonal antibody, *Brain Res.* 326 (1985) 192–196.
 - [13] M. Halpern, C. Jia, L.S. Shapiro, Segregated pathways in the vomeronasal system, *Microsc. Res. Tech.* 41 (1998) 519–529.
 - [14] M. Halpern, L.S. Shapiro, C. Jia, Differential localization of G proteins in the opossum vomeronasal system, *Brain Res.* 677 (1995) 157–161.
 - [15] G. Herrada, C. Dulac, A novel family of putative pheromone receptors in mammals with a topographically organized and sexually dimorphic distribution, *Cell* 90 (1997) 763–773.
 - [16] J.G. Hildebrand, G.M. Shepherd, Mechanisms of olfactory discrimination: converging evidence for common principles across phyla, *Annu. Rev. Neurosci.* 20 (1997) 595–631.
 - [17] R.M. Huff, J.M. Axton, E.J. Neer, Physical and immunological characterization of a guanine nucleotide-binding protein purified from bovine cerebral cortex, *J. Biol. Chem.* 260 (1985) 10864–10871.
 - [18] C. Jia, M. Halpern, Subclasses of vomeronasal receptor neurons: differential expression of G proteins (G_{α_2} and G_{α_0}) and segregated projections to the accessory olfactory bulb, *Brain Res.* 719 (1996) 117–128.
 - [19] J. Joerges, A. Küttner, C.G. Galizia, R. Menzel, Representations of odours and odour mixtures visualized in the honeybee brain, *Nature* 387 (1997) 285–288.
 - [20] D.T. Jones, R.R. Reed, G_{olf} : an olfactory neuron specific-G protein involved in odorant signal transduction, *Science* 244 (1989) 790–795.
 - [21] B. Key, R.A. Akesson, Delineation of olfactory pathways in the frog nervous system by unique glycoconjugates and N-CAM glycoforms, *Neuron* 6 (1991) 381–396.
 - [22] N.S. Levy, H.A. Bakalyar, R.R. Reed, Signal transduction in olfactory neurons, *J. Steroid Biochem. Mol. Biol.* 39 (1991) 633–637.
 - [23] O.H. Lowry, N.J. Rosebrough, A.L. Farr, R.J. Randall, Protein measurement with the Folin phenol reagent, *J. Biol. Chem.* 193 (1951) 265–275.
 - [24] L.G. Luna (Ed.), Preparation of tissues. Manual of Histologic Staining Methods of the Armed Forces Institute of Pathology, McGraw-Hill, New York, 1968, pp. 1–12.
 - [25] H. Matsunami, L. Buck, A multigene family encoding a diverse array of putative pheromone receptors in mammals, *Cell* 90 (1997) 775–784.
 - [26] M. Meredith, Vomeronasal function, *Chem. Senses* 23 (1998) 463–466.
 - [27] P. Mombaerts, F. Wang, C. Dulac, S.K. Chao, A. Nemes, M. Mendelsohn, J. Edmondson, R. Axel, Visualizing an olfactory sensory map, *Cell* 87 (1996) 675–686.
 - [28] K. Mori, S.C. Fujita, K. Imamura, K. Obata, Immunohistochemical study of subclasses of olfactory nerve fibers and their projections to the olfactory bulb in the rabbit, *J. Comp. Neurol.* 242 (1985) 214–229.
 - [29] K. Mori, N. Mataga, K. Imamura, Differential specificities of single mitral cells in rabbit olfactory bulb for a homologous series of fatty acid odor molecules, *J. Neurophysiol.* 67 (1992) 786–789.
 - [30] K. Mori, Relation of chemical structure to specificity of response in olfactory glomeruli, *Curr. Opin. Neurobiol.* 5 (1995) 467–474.
 - [31] S.L. Pomeroy, A.S. Lamantia, D. Purves, Postnatal construction of neural circuitry in the mouse olfactory bulb, *J. Neurosci.* 10 (1990) 1952–1966.
 - [32] K.J. Ressler, S.L. Sullivan, L.B. Buck, A zonal organization of odorant receptor gene expression in the olfactory epithelium, *Cell* 73 (1993) 597–609.
 - [33] U. Rudolph, K. Spicher, L. Birnbaumer, Adenylyl cyclase inhibition and altered G protein subunit expression and ADP-ribosylation patterns in tissues and cells from $G_{12\alpha}^{-/-}$ mice, *Proc. Natl. Acad. Sci. U.S.A.* 93 (1996) 3209–3214.
 - [34] N.J.P. Ryba, R. Tirindelli, A new multigene family of putative pheromone receptors, *Neuron* 19 (1997) 371–379.
 - [35] G.A. Schwarting, J.E. Crandall, Subsets of olfactory and vomeronasal sensory epithelial cells and axons revealed by monoclonal antibodies to carbohydrate antigens, *Brain Res.* 547 (1991) 239–248.
 - [36] J.E. Schwob, D.I. Gottlieb, Purification and characterization of an antigen that is spatially segregated in the primary olfactory projection, *J. Neurosci.* 8 (1988) 3470–3480.
 - [37] K. Shinoda, Y. Shiotani, Y. Osawa, “Necklace olfactory glomeruli” form unique components of the rat primary olfactory system, *J. Comp. Neurol.* 284 (1989) 362–373.
 - [38] H. Shinohara, K. Kato, T. Asano, Differential localization of G proteins, G_i and G_o , in the olfactory epithelium and the main olfactory bulb of the rat, *Acta Anat.* 144 (1992) 167–171.
 - [39] S.M. Strittmatter, D. Valenzuela, T. Vartanian, Y. Sudo, M.X. Zuber, M.C. Fishman, Growth cone transduction: G_o and GAP-43, *J. Cell Sci. Suppl.* 15 (1991) 27–33.
 - [40] J. Strotmann, I. Wanner, T. Helfrich, A. Beck, H. Breer, Rostrocaudal patterning of receptor expressing neurons in the rat nasal cavity, *Cell Tissue Res.* 278 (1994) 11–20.
 - [41] S.L. Sullivan, S. Bohm, K.J. Ressler, L.F. Horowitz, L.B. Buck, Target-independent pattern specification in the olfactory epithelium, *Neuron* 15 (1995) 779–789.
 - [42] S.L. Sullivan, M.C. Adamson, K.J. Ressler, C.A. Kozak, L.B. Buck, The chromosomal distribution of mouse odorant receptor genes, *Proc. Natl. Acad. Sci. U.S.A.* 93 (1996) 884–888.
 - [43] D. Valenzuela, X. Han, U. Mende, C. Fankhauser, H. Mashimo, P. Huang, J. Pfeffer, E.J. Neer, M.C. Fishman, G_{α_o} is necessary for muscarinic regulation of Ca^{2+} channels in mouse heart, *Proc. Natl. Acad. Sci. U.S.A.* 94 (1997) 1727–1732.
 - [44] F. Wang, A. Nemes, M. Mendelsohn, R. Axel, Odorant receptors govern the formation of a precise topographic map, *Cell* 93 (1998) 47–60.
 - [45] K.S. Wekesa, R.R.H. Anholt, Pheromone regulated production of inositol-(1,4,5)-trisphosphate in the mammalian vomeronasal organ, *Endocrinology* 138 (1997) 3497–3504.

Elsevier Science

Fax: (31) (20) 485 2431

Phone: (31) (20) 485 3415

Postal Address:

Brain Research

Elsevier Science

P.O. Box 2759, 1000 CT Amsterdam

The Netherlands

Courier Service Address:

Brain Research

Elsevier Science

Sara Burgerhartstraat 25, 1055 KV Amsterdam

The Netherlands

* * *

If you need information about your accepted manuscript, proof, etc. then phone or FAX us at the above numbers, stating the journal name and article code number. We can FAX this journal's Instructions to Authors to you which can also be found on the World Wide Web: access under <http://www.elsevier.com>

ONLINE ACCESS OF BRAIN RESEARCH ARTICLES on the *Brain Research Interactive* website

As of mid May 1999, online access to the **full text** of articles published in *Brain Research* or any of its sections has been **restricted to those individuals whose library subscribes to the corresponding print journal**. *There is no charge to either the libraries or their authorised users for this service*. Following an initial authorisation check, people logging into this website will be able to access this material simply if their IP domain/host site matches that of a subscribing library

Note: There are NO such subscription-related restrictions for accessing:

- the *Contents lists* of the print issues
- the *Abstracts* of articles published in the print journals
- the **interactive area** of the website, namely:
 - *Brain Research Interactive Reports* and linked Commentaries
 - *Brain Research Interactive Symposia* material: abstracts, papers, discussion fora
 - the general Discussion Forum

While the above information is accessible completely free of charge, users of this site must have registered once and log in in order to access the *Interactive Reports*.

Brain Research Interactive:

www.elsevier.com/locate/bres

www.elsevier.nl/locate/bres

www.elsevier.jp/locate/bres

SUBSCRIPTION AND PUBLICATION DATA 1999

Brain Research (including **Molecular Brain Research**, **Developmental Brain Research**, **Cognitive Brain Research**, **Brain Research Protocols** and **Brain Research Reviews**) will appear weekly and be contained in 61 volumes (129 issues): **Brain Research**, Volumes 815–850 (36 volumes in 72 issues), **Molecular Brain Research**, Volumes 62–73 (12 volumes in 24 issues), **Developmental Brain Research**, Volumes 112–118 (7 volumes in 14 issues), **Cognitive Brain Research**, Volume 7 (1 volume in 4 issues), **Brain Research Protocols**, Volumes 3 and 4 (2 volumes in 6 issues) and **Brain Research Reviews**, Volumes 29–31 (3 volumes in 9 issues). Please note that **Volume 62** (Issues no. 1 and 2) and **63** (Issue no. 1) of **Molecular Brain Research**, **Volume 7** (Issues no. 1 and 2) of **Cognitive Brain Research** and **Volume 3** (Issues no. 1 and 2) of **Brain Research Protocols** were published ahead of schedule in 1998, in order to reduce publication time. The volumes remain part of the 1999 subscription year.

Separate subscriptions: **Molecular Brain Research**, Vols. 62–73, **Developmental Brain Research**, Vols. 112–118, **Cognitive Brain Research**, Vol. 7, **Brain Research Protocols**, Vols. 3 and 4 and **Brain Research Reviews**, Vols. 29–31, may also be ordered separately. Subscription prices are available upon request from the Publisher or from the Regional Sales Office nearest you or from this journal's website (<http://www.elsevier.nl/locate/xxxxx>). Further information is available on this journal and other Elsevier Science products through Elsevier's website (<http://www.elsevier.nl>). Subscriptions are accepted on a prepaid basis only and are entered on a calendar year basis. Issues are sent by standard mail (surface within Europe, air delivery outside Europe). Priority rates are available upon request. Claims for missing issues should be made within six months of the date of dispatch.

Claims for missing issues must be made within six months of our publication (mailing) date, otherwise such claims cannot be honoured free of charge.

Orders, claims, and product enquiries: please contact the Customer Support Department at the Regional Sales Office nearest you: **New York:** Elsevier Science, P.O. Box 945, New York, NY 10159-0945, USA; phone: (+1) (212) 633 3730, [toll free number for North American customers: 1-888-4ES-INFO (437-4636)]; fax: (+1) (212) 633 3680; e-mail: usinfo-f@elsevier.com. **Amsterdam:** Elsevier Science, P.O. Box 211, 1000 AE Amsterdam, The Netherlands; phone: (+31) 20 4853757; fax: (+31) 20 4853432; e-mail: nlinfo-f@elsevier.nl. **Tokyo:** Elsevier Science, 9-15 Higashi-Azabu 1-chome, Minato-ku, Tokyo 106-0044, Japan; phone: (+81) (3) 5561 5033; fax: (+81) (3) 5561 5047; e-mail: info@elsevier.co.jp. **Singapore:** Elsevier Science, No. 1 Temasek Avenue, #17-01 Millenia Tower, Singapore 039192; phone: (+65) 434 3727; fax: (+65) 337 2230; e-mail: asiainfo@elsevier.com.sg. **Rio de Janeiro:** Elsevier Science, Rua Sete de Setembro 111/16 Andar, 20050-002 Centro, Rio de Janeiro - RJ, Brazil; phone: (+55) (21) 509 5340; fax: (+55) (21) 507 1991; e-mail: elsevier@campus.com.br [Note (Latin America): for orders, claims and help desk information, please contact the Regional Sales Office in New York as listed above].

Advertising information. Advertising orders and enquiries can be sent to: **USA, Canada and South America:** Mr Tino de Carlo, The Advertising Department, Elsevier Science Inc., 655 Avenue of the Americas, New York, NY 10010-5107, USA; phone: (+1) (212) 633 3815; fax: (+1) (212) 633 3820; e-mail: t.decarlo@elsevier.com. **Japan:** The Advertising Department, Elsevier Science K.K., 9-15 Higashi-Azabu 1-chome, Minato-ku, Tokyo 106-0044, Japan; phone: (+81) (3) 5561 5033; fax: (+81) (3) 5561 5047. **Europe and ROW:** Rachel Gresle-Farthing, The Advertising Department, Elsevier Science Ltd., The Boulevard, Langford Lane, Kidlington, Oxford OX5 1GB, UK; phone: (+44) (1865) 843565; fax: (+44) (1865) 843976; e-mail: r.gresle-farthing@elsevier.co.uk.

ADONIS Identifier. This Journal is in the ADONIS Service, whereby copies of individual articles can be printed out from CD-ROM on request. An explanatory leaflet can be obtained by writing to ADONIS B.V., P.O. Box 17005, 1001 JA Amsterdam, The Netherlands.

Legends to Figures

Figure 1: Diagrammatic representation of the “dipstick” assay for measurements of olfactory avoidance responses. After a 15s recovery period, the number of flies in the compartment away from the odor source is counted at 5s intervals and the average of 10 consecutive measurements is recorded as the avoidance score. The example shows a typical wild-type avoidance response. Details of the assay are described in the text.

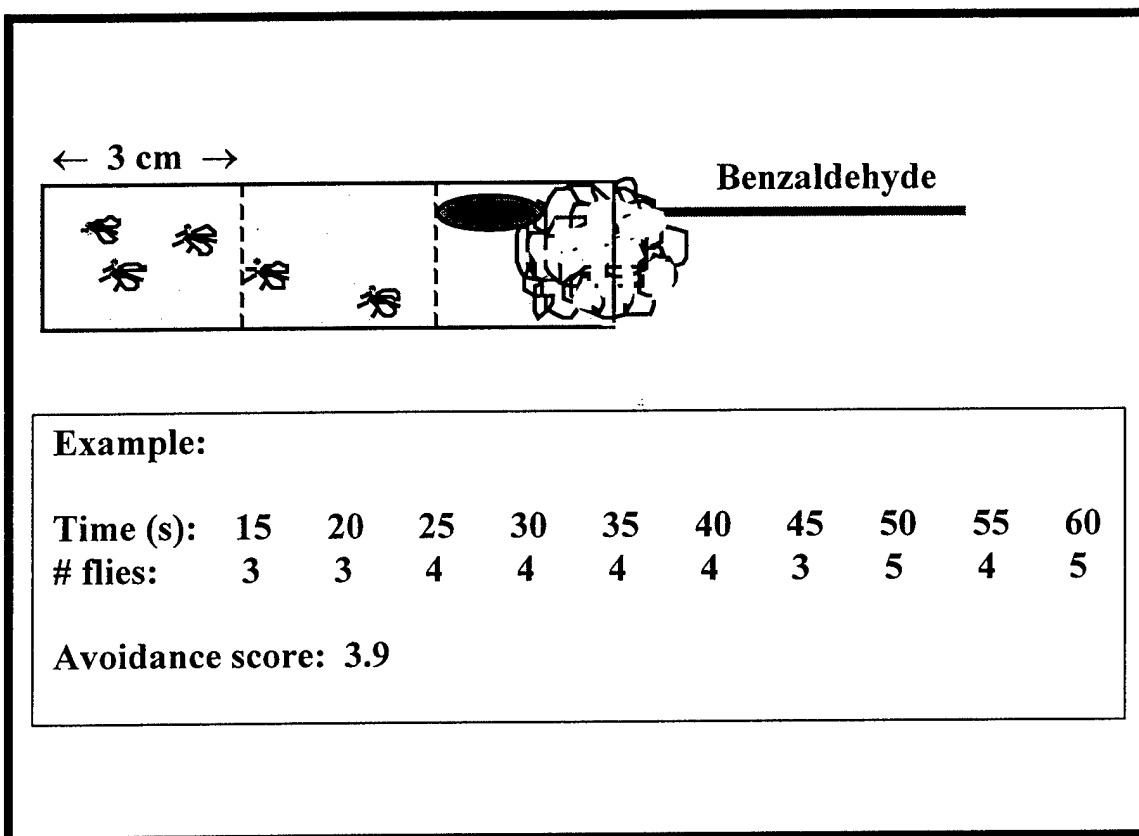
Figure 2: Variation for avoidance response to benzaldehyde among isogenic chromosome 1 (X; left panel) and chromosome 3 (right panel) substitution lines of *Drosophila melanogaster*. The male and female avoidance scores of each line are connected. Adapted from Mackay *et al.*, 1996.

Figure 3: Interaction diagram of *smi* loci. The dotted and uninterrupted lines indicate epistatic effects that enhance and suppress the homozygous mutant phenotype, respectively. Two loci, *smi60E* and *smi61A*, form an independent pair with a positive epistatic effect (not shown). Adapted from Fedorowicz *et al.*, 1998.

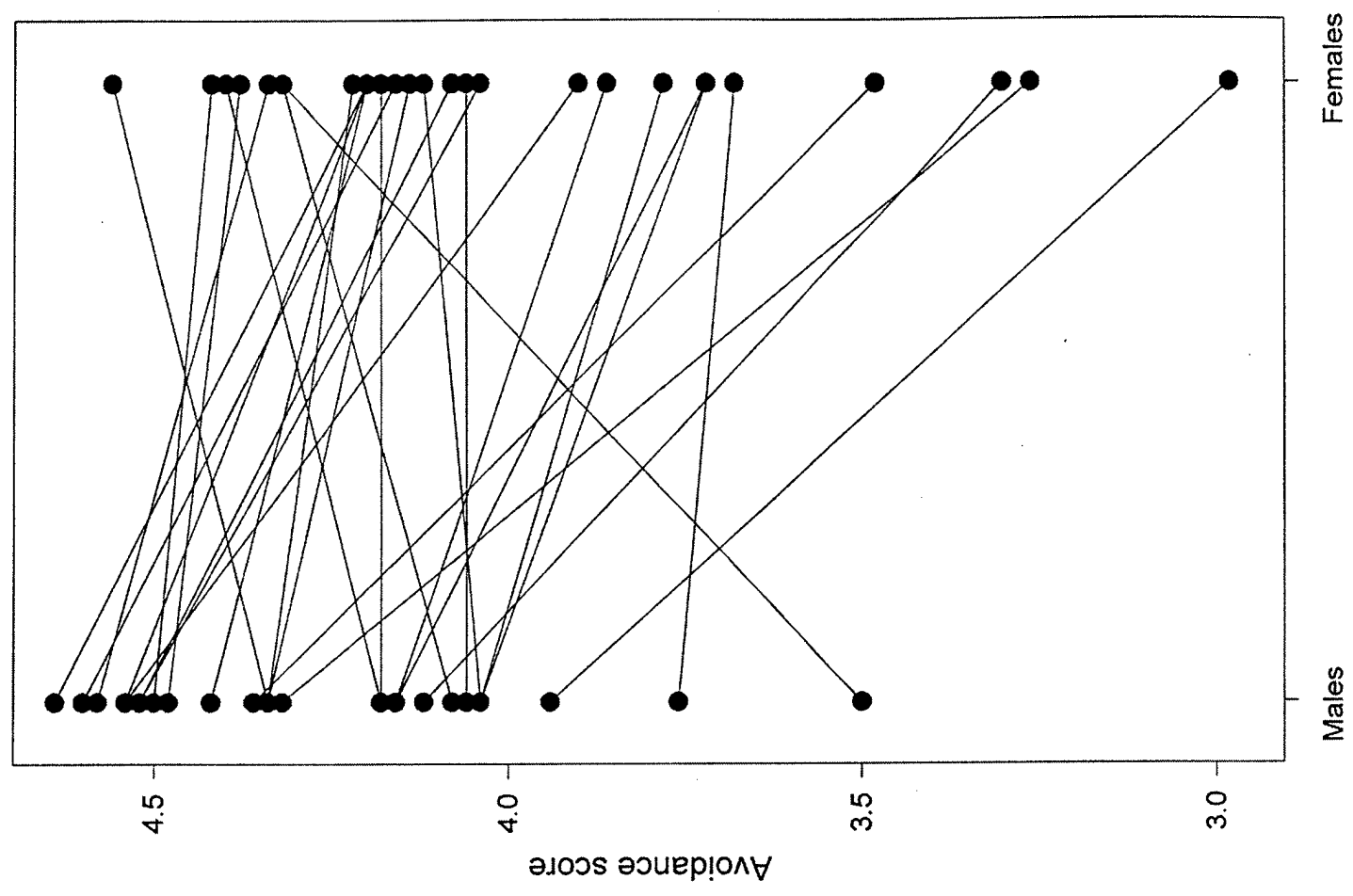
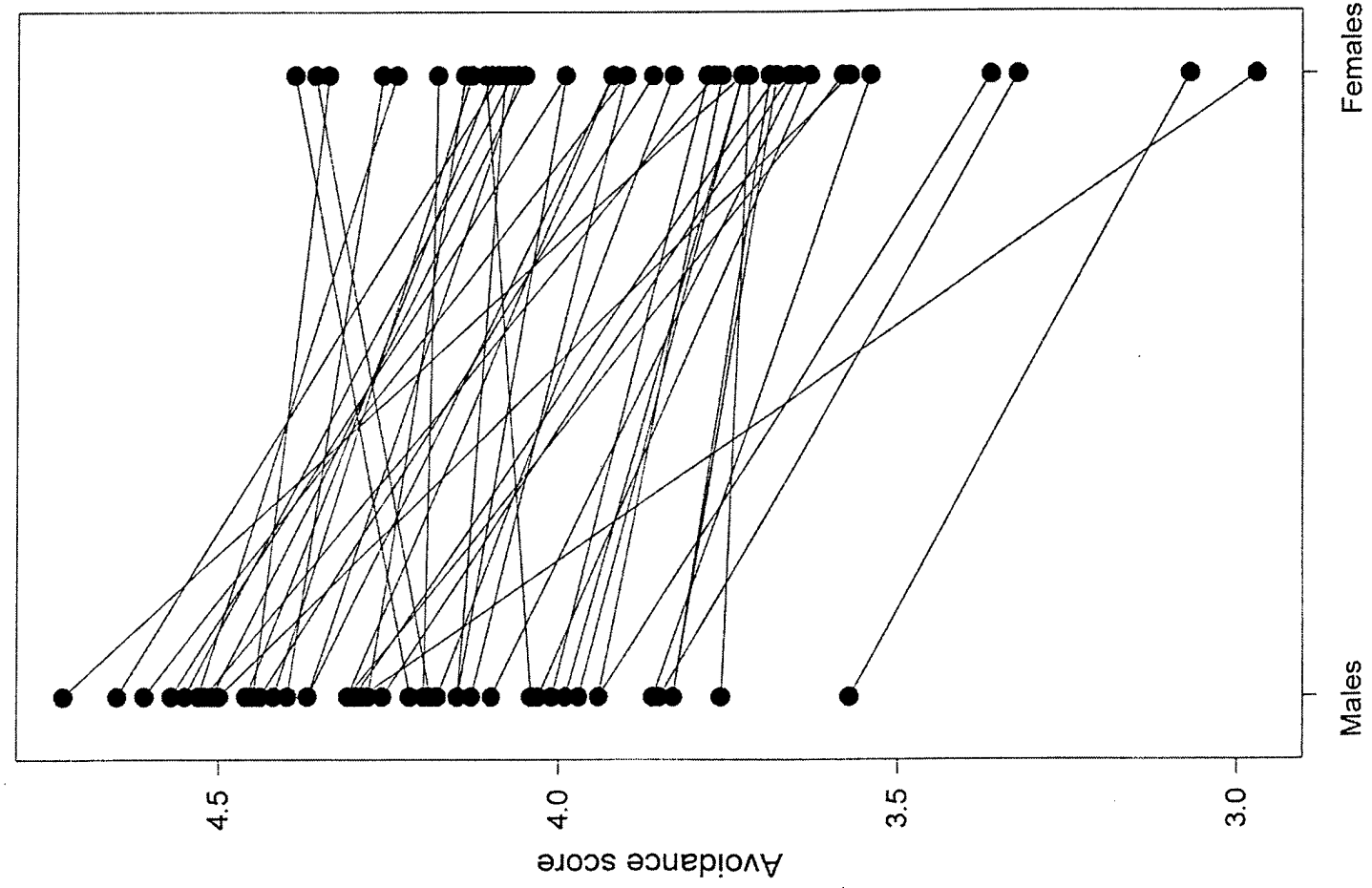
Figure 4: Unrooted neighbor-joining trees of 18 olfactomedin-related proteins (A) and their olfactomedin homology domains (B). The bootstrap values are coded such that a closed circle refers to a value of 95 - 100% and an open circle refers to values between 70 and 94%. GenBank accession numbers for these protein sequences are as follows:

CL2BA_Rat	gi 3695129 gb AAC62657.1;
CL3_Rat	gi 3695143 gb AAC62664.1;
KIAA0821_Human	gi 4240128 dbj BAA74844.1;
Latrophilin1_Cow	gi 4185802 gb AAD09191.1;
Latrophilin1-precursor	gi 2213659 gb AAC98700.1;
Latrophilin2_Human	gi 4034486 emb CAA10458.1;
Latrophilin3_Cow	gi 4164059 gb AAD05324.1;
Olf_Frog	gi 585611 sp Q07081;
Olf1_Worm	gi 1947128 gb AAB52933.1;
Olf2_Worm	gi 3875750 emb CAB04088.1;
OlfA_Human	gi 3024228 sp Q99784;
OlfA_Mouse	gi 2599125 gb AAB84058.1;
OlfA_Rat	gi 3024210 sp Q62609;
OlfB_Human	gi 2159929 gb AA447264.1;
OlfC_Human	gi 4406679 gb AAD20056.1;
OlfD_Human	gi 1349928 gb W53028.1;
TIGR/myocilin_Human	gi 3024209 sp Q99972;
Pancortin3_Mouse	gi 3218528 dbj BAA28767.1

Figure 5: Tissue-specific expression of olfactomedin-related gene products. Non-crosshybridizing radiolabeled oligonucleotide probes were hybridized to a Northern blot containing samples of human heart (H), brain (B), placenta (Pl), lung (Lu), liver (Li), skeletal muscle (M), kidney (K), pancreas (Pa), spleen (S), thyroid (Th), prostate gland (P), testis (Ts), ovary (O), small intestine (Si), colon (C), and peripheral blood leukocyte (Pb). Two blots were hybridized sequentially to different probes and complete removal of the previous probe was verified between hybridizations. A faint band of hybridization is detected in pancreas with the TIGR/myocilin probe. This band is not an artifact due to incomplete erasure of the hOlfB probe, since hybridization with TIGR/myocilin was preceded by hybridization with hOlfA to this blot.



Chromosome 3



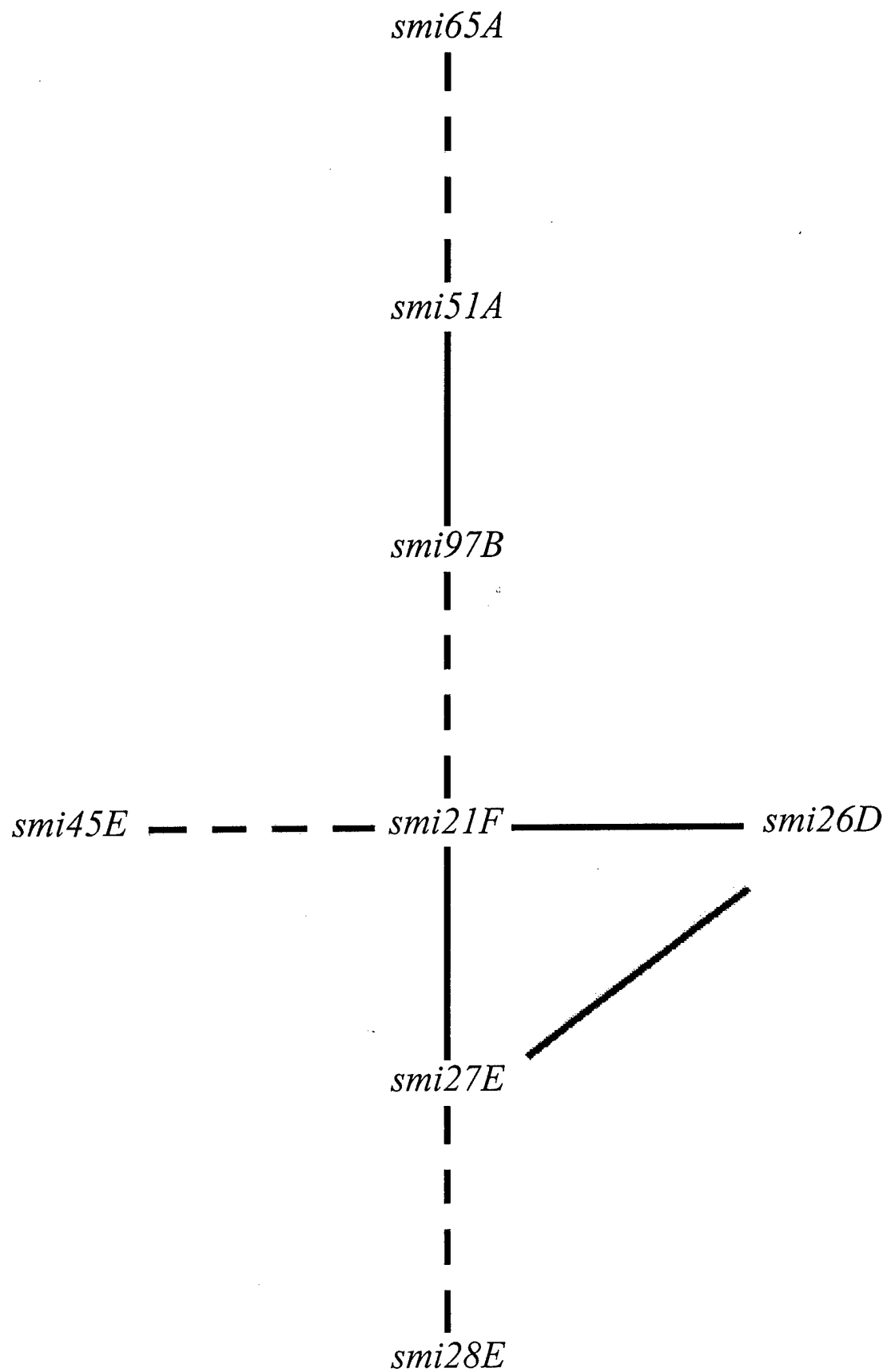


Fig 4

A

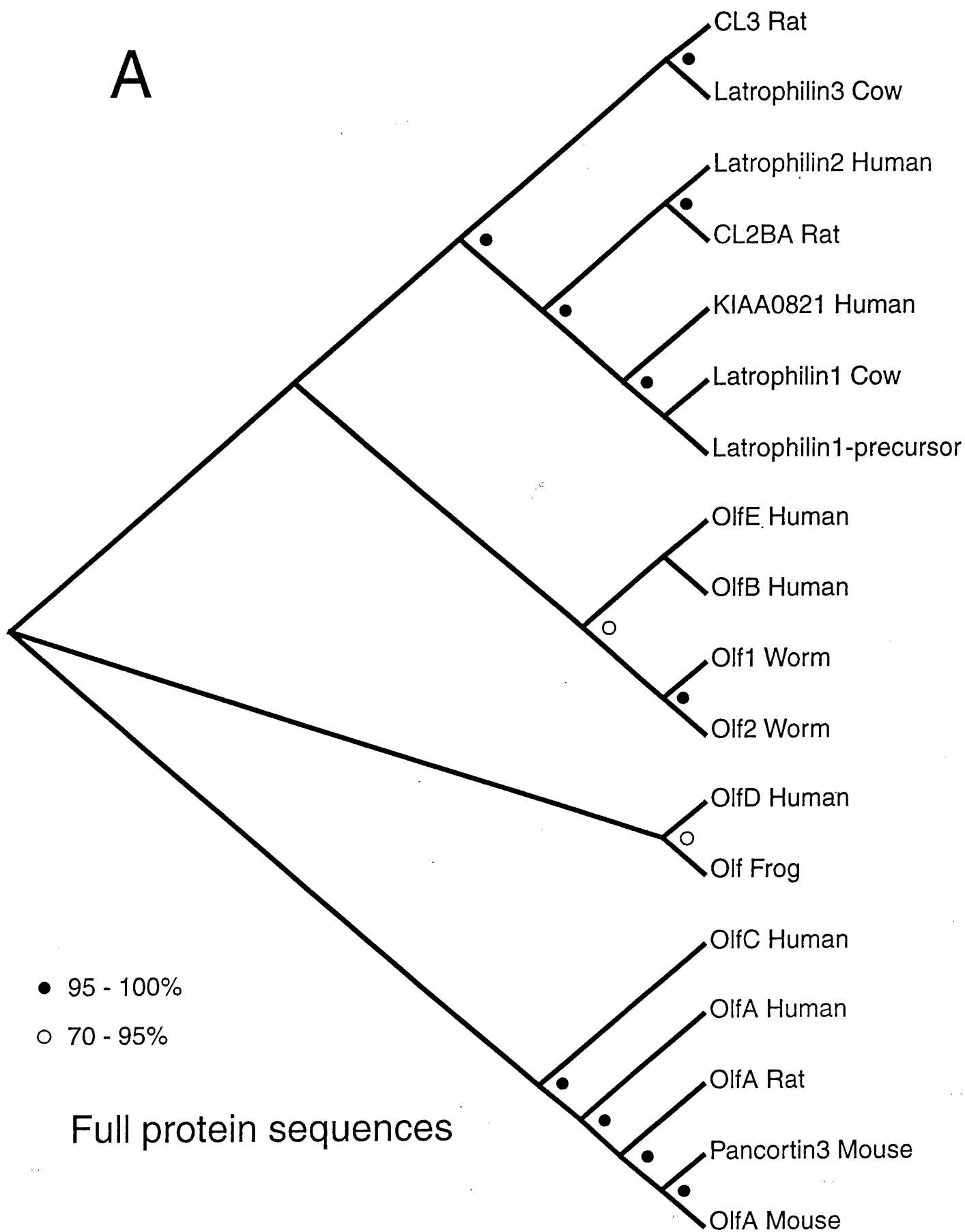


FIG 4

B

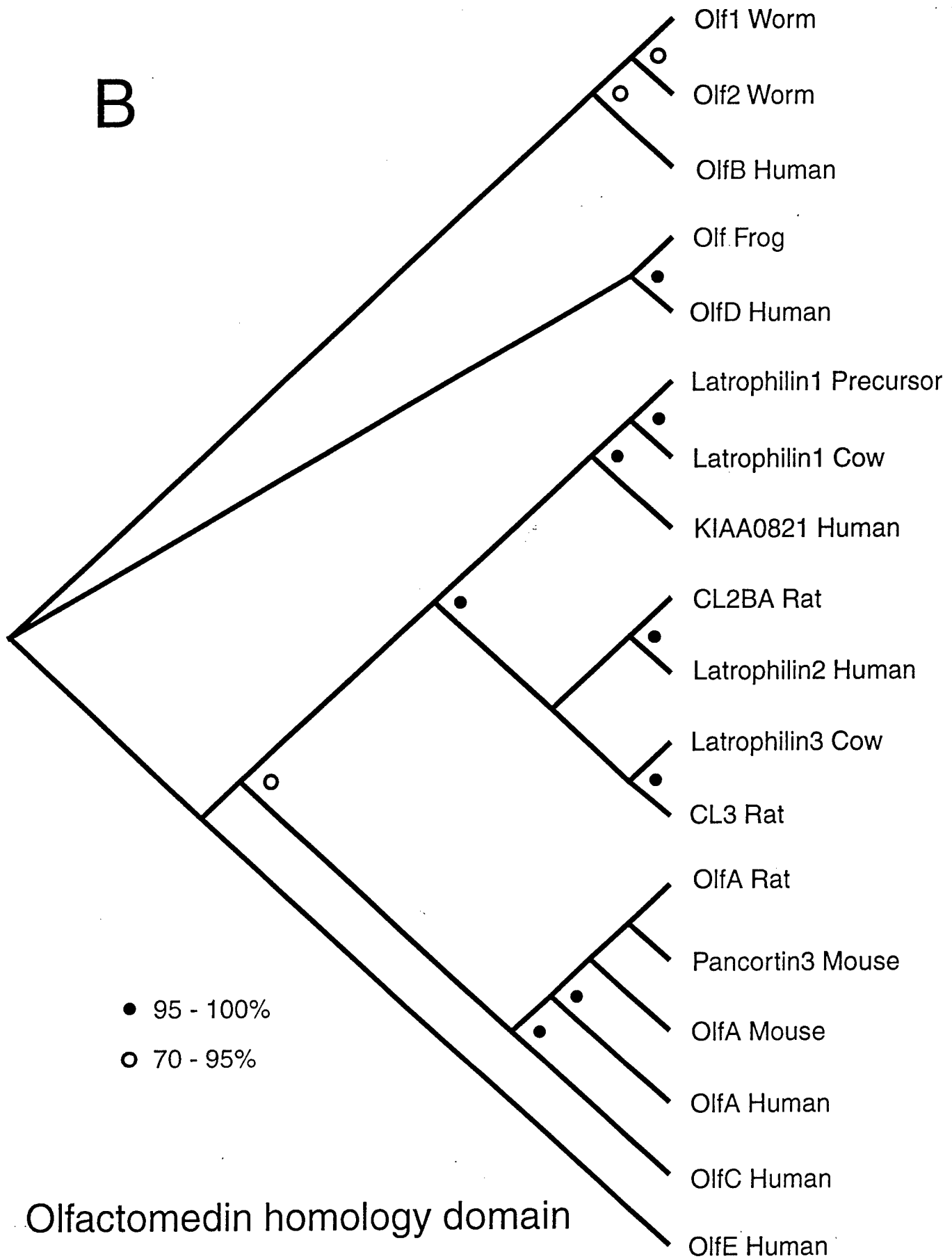


FIG 5

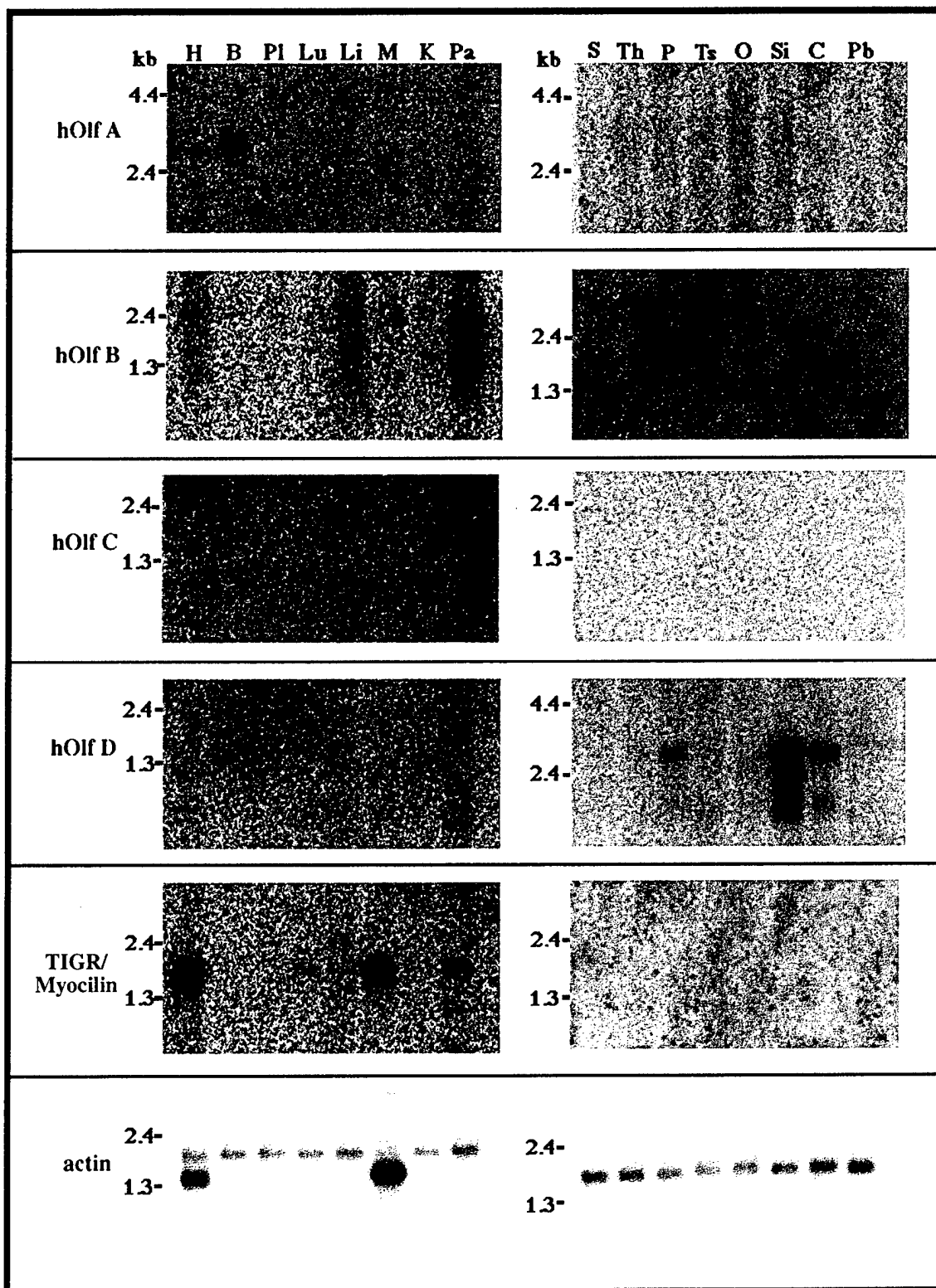


Table 1: Transposon insertion sites and candidate *smi* genes *

<i>P</i> -element insertion	candidate genes at the cytological location
<i>smi21F</i>	CG5397 (carboxyl esterase); CG4523 (cell adhesion protein); <i>Acap</i> (adenyl cyclase - associated protein); CG4887 and CG4896 (RNA binding proteins); CG5001 (heat shock protein); CG5080 (cytoskeletal protein); CG5105 (phospholipase A2 activating protein); up to 18 unknown gene products, including a putative odorant binding protein .
<i>smi26D</i>	CG9493 (protein phosphatase); CG9499 and CG9501 (putative ion channels); CG9507 and CG9505 (endopeptidases); CG9500 (structural protein); <i>Tig</i> (Tiggrin; extracellular matrix protein); CG9527 (acyl coenzyme A oxidase homologue); CG9508 (neprilysin); <i>Cpr</i> (cytochrome P450 reductase); CG9490, CG11573 and CG9488 (protein kinases); CG9491(cAMP-dependent Rap1 guanine nucleotide exchange factor); up to 16 unknown gene products.
<i>smi27E</i>	CG4496 (zinc finger transcription factor); CG4675 (transport protein); <i>Wnt4</i> (Wnt oncogene analog 4; up to 12 unknown gene products.
<i>smi28E</i>	CG7219 (serpin); CG7221 (putative dehydrogenase enzyme); CG7367 (lipase homologue); CG7392 (calmodulin binding protein homologue); CG7424 (ribosomal protein); CG7466 (cell adhesion protein); CG7227 (lysosome membrane protein homologue); CG7356 (γ -glutamyl transferase); <i>Calo</i> (calmodulin binding protein); <i>poe</i> (transmembrane protein); CG7586 α_2 -macroglobulin homologue); <i>Trf</i> (RNA polymerase II transcription factor); CG8668 and CG8673 (putative galactosyl transferase); up to 17 unknown gene products (including <i>gel</i> and <i>belt</i>).
<i>smi35A</i>	This is the alcohol dehydrogenase (<i>Adh</i>) region, which has been extensively annotated by Ashburner <i>et al.</i> (1999). The <i>P[ArB]</i> insertion site is near <i>wb</i> (laminin) and <i>l(2)34Fa</i> (dyrk2 kinase homologue).
<i>smi45E</i>	<i>Wnt2</i> (Wnt oncogene analog 2); <i>cro</i> (<i>croaker</i> , a courtship impaired and slow mating mutant); CG1931 (cytoskeletal protein); <i>rdgG</i> (<i>retinal degeneration G</i> ; unknown gene product); up to 5 unknown gene products, including an olfactory receptor .
<i>smi51A</i>	CG8151 (RNA polymerase II transcription factor); CG8422 (G protein-coupled receptor); CG10104 (endopeptidase); CG17385 and CG17390 (zinc finger transcription factors); <i>phyl</i> (<i>phyllopod</i> ; nuclear protein); <i>cpsf</i> (component of the cleavage and adenylation specificity factor complex); <i>Asx</i> (<i>Additional sex combs</i> ; chromatin binding protein); <i>itv</i> (glucuronyl N-acetylglucosaminyl transferase homologue); CG10110 (RNA binding protein); up to 23 unknown gene products (including the <i>oho51</i> , <i>auk</i> , <i>L</i> , and <i>xen</i> loci).
<i>smi60E</i>	<i>gsb</i> and <i>gsb-n</i> (<i>gooseberry</i> ; RNA polymerase II transcription factor); <i>uzip</i> (integral membrane axon guidance protein); <i>gol</i> (<i>goliath</i>) and <i>Tkr</i> (zinc finger transcription factors); CG2803 (troponin homologue); BcDNA:GH04753 (glutathione-S-transferase homologue); CG12850 (transcription factor); CG2811 and CG9358 (putative ligand carrier proteins); <i>RpL19</i> (ribosomal protein); CG10142, CG9047 and <i>ESTS:17F2S</i> (peptidases); <i>emp</i> (epithelial membrane protein); <i>zip</i> (non-muscle myosin); <i>ETH</i> (ecdysis triggering hormone); <i>NaCP60E</i> (sodium channel protein) ; up to 20 unknown gene products.
<i>smi61A</i>	CG1201, BcDNA:GH04978 and <i>Pk61C</i> (protein kinases); CG1216 and <i>Gyk</i> (glycerol kinase); CG11869 (putative microtubule-associated protein); CG13406 (G protein-coupled receptor); <i>miple2</i> (midline/pleiotrophin family protein); Lsp1 γ (larval serum protein 1 γ -subunit); CG1212 (putative signal transduction protein); CG7051 (dynein-like motor protein); CG7036 (putative transcription factor); <i>Mtch</i> (mitochondrial carrier protein); <i>NitFlit</i> (nitrilase and fragile histidine triad fusion protein); CG17142 (cytoskeletal structural protein); <i>Kaz1</i> (serine protease inhibitor); up to 16 unknown gene products (including <i>fwd</i>).
<i>smi65A</i>	CG10541(cytoskeletal structural protein); CG10546 (ligand carrier binding protein); CG17498 (cell cycle regulator); CG5537 (uracil phosphoribosyl transferase); <i>S6k</i> (ribosomal protein S-p70-protein kinase); <i>vn</i> (neuregulin-like protein); <i>Bj1</i> (chromatin binding protein); <i>33-13</i> and <i>Ets65A</i> (DNA binding proteins); CG10486, CG5592, CG6600 and CG10226 (transport proteins); CG10487 (receptor guanylate cyclase); CG10489 (DNA replication

	protein); CG13287, CG13296, CG10274 and CG7386 (transcription factors); CG10467 (aldose 1-epimerase homologue); CG10469, CG10472, CG10475, CG10477, CG6457, CG6462, CG6467, CG6483, CG6480, and CG6592 (endopeptidases); CG10163 (phospholipase A1 homologue); <i>l(3)mbn</i> (lethal(3) malignant blood neoplasm membrane protein); CG10533, CG10461, CG10529, and CG12330 (structural proteins); <i>Lcp20</i> , <i>Lcp11</i> , <i>Lcp65Aa</i> , <i>Lcp65Ac</i> , <i>Lcp65Ad</i> , <i>Lcp6</i> , <i>Lcp65Ab1</i> , <i>Lcp65Ab2</i> , <i>Lcp65Ae</i> , <i>Lcp65Af</i> , and <i>Lcp65Ag3</i> (larval cuticle proteins); <i>Acp65Aa</i> (adult cuticle protein); CG13289 (cell adhesion protein); CG6062 and CG6619 (putative signal transduction proteins); CG6610, <i>l(3)02094</i> and CG13298 (RNA binding proteins); <i>Snap25</i> (synaptosome-associated protein 25kD); CG10160 (lactate dehydrogenase); CG10173 (peptidase); <i>D19A</i> and <i>D19B</i> (nuclear zinc finger proteins); <i>lanA</i> (laminin A); <i>Mdr65</i> (multiple drug transporter); <i>Tm</i> (transportin); up to 41 unknown gene products (including <i>Jon65A</i> , <i>tantalus</i> and <i>prdI</i>).
<i>smi79E</i>	<i>Aats-ile</i> and CG11471 (isoleucyl tRNA synthetase); CG7495 (dopamine β -monooxygenase homologue); CG9085 (protein kinase); <i>Csp</i> (cysteine string protein); <i>Ddx1</i> (ATP-dependent helicase); <i>Hem</i> (plasma membrane protein); <i>Ten-m</i> (tenascin); up to 15 unknown gene products (including <i>exb</i>).
<i>smi97B</i>	CG6036 (protein phosphatase); CG6162 (transporter protein); <i>ird15</i> (<i>immune response deficient</i>); CG14239 (putative ion channel); <i>scrib</i> (<i>scribbled</i>; an adhesion protein with multiple leucine-rich repeats and PDZ domains) ; CG5443 (hexokinase); <i>Pdf</i> (pigment dispersing factor, neuropeptide hormone); <i>dei</i> (RNA polymerase II transcription factor); CG5432 (aldolase homologue); CG6490 (cell adhesion protein); up to 6 unknown gene products.
<i>smi98B</i>	CG4849 and CG4980 (RNA binding proteins); CG5540 (olfactory receptor); CG4963 (mitochondrial carrier protein homologue); CG12260, CG12261, and CG4976 (transcription factors); CG5017 and CG5520 (chaperones); CG5527 (endopeptidase); <i>Acp98AB</i> (accessory gland specific peptide); <i>Ets98B</i> (DNA binding protein); <i>RpL1</i> (ribosomal protein); up to 16 unknown gene products.

* Candidate genes likely to account for smell-impairments induced by *P*-element insertions, as evident from preliminary unpublished experiments, are shown in bold print. Note the large number of predicted transcription units of unknown function, which may harbor genes that contribute to odor-guided behavior. Data were compiled from the *Drosophila* genomic sequence as accessed via Flybase. (<http://flybase.bio.indiana.edu/>). For *smi35A* only the two most likely candidate genes have been indicated. This region has been annotated extensively by Ashburner *et al.* (1999). The *P*[*lArB*] element in *smi79E* has inserted next to a *hoppel* transposon, complicating efforts to identify the affected *smi* gene.